1    **Validation of models of the distribution of structure-forming invertebrates in**

2    **the eastern Bering Sea using an underwater stereo camera**

3

4    Chris Rooper. Mike Sigler, Pam Goddard, Pat Malecha, Rick Towler, Kresimir Williams, and

5    Rachel Wilborn

6

7    **Abstract**

8    In summer 2014 we conducted a survey of the eastern Bering Sea slope and outer shelf using an

9    underwater stereo camera at 250 randomly selected transects. The objective of this survey was to

10   verify distribution models of coral, sponge, and sea whips that were based on bottom trawl

11   survey data that had been presented to the North Pacific Fishery Management Council in June

12   2013. Additionally, we collected data on invertebrate density, height, and fish associations and

13   documented the presence of fishing gear and damage to invertebrates.  Presence or absence

14   models of coral, sponge and sea whips were also constructed from the camera survey data and

15   were compared to previous coral, sponge, and sea whip models constructed from bottom trawl

16   survey data. The model of coral presence or absence based on bottom trawl survey data was

17   generally accurate in predicting coral presence or absence in the camera survey. The bottom

18   trawl survey models were also accurate in predicting sponge and sea whip presence or absence,

19   but to a lesser degree than for coral. Corals were found at 32 of 250 transects, most of which

20   were located in Pribilof Canyon and the slope area to the northwest. Overall, the densities of

21   corals were low, averaging 0.005 individuals$*$m$^{-2}$ and ranging from 0 to 0.28 individuals$*$m$^{-2}$.

22   The low densities were consistent with the absence of hard substrates for coral attachment in

23   most areas of the eastern Bering Sea. Densities of corals were generally highest in Pribilof

24     Canyon and corals were largest in the slope area to the northwest of Pribilof Canyon. For

25     sponges, densities and heights were highest surrounding Pribilof Canyon, north of Bering

26     Canyon, and in some locations in Zhemchug Canyon. Sea whip densities and heights were

27     highest on the outer shelf between Pribilof and Zhemchug Canyon and in an area to the south of

28     Pribilof Canyon. There were significant positive relationships between fish density and the

29     presence of coral and sponge for some rockfish species and king crabs. There were significant

30     negative relationships for grenadiers and *Chionoecetes* crabs. Direct evidence of fishing gear

31     occurred at 12.8% of transects. Individual demosponges (0.3%), Isididae corals (2.9%) and sea

32     whips (9.0%) were observed to be damaged. Vulnerability of benthic invertebrates was estimated

33     from the field data on invertebrate density and height and was modeled for the entire eastern

34     Bering Sea outer shelf and slope. Based on height and density, the areas that appeared to be most

35     vulnerable for coral occurred in narrow areas of the two arms of Pribilof Canyon and in deeper

36     areas to the northwest along the slope. For sponge and sea whips, the most vulnerable areas were

37     centered around the shelf break and extended from Pribilof Canyon to the north for sponge and

38     from Bering Canyon to the north for sea whips. Although combining the bottom trawl survey

39     models and the camera survey models only exhibited some improvement over bottom trawl

40     survey data-based models alone, the combined models were able to integrate both bottom trawl

41     and camera data into a single map of the probability of invertebrate presence and from this a

42     prediction of density of invertebrates for the eastern Bering Sea slope and outer shelf.

43

44     **1. Introduction**

45          The fish and crab resources of the eastern Bering Sea slope and outer shelf are widely

46     utilized by commercial fisheries in Alaska. The eastern Bering Sea slope and outer shelf is a

47   region of enhanced primary and secondary productivity (the "Bering Sea Greenbelt") that attracts

48   large numbers of fish, seabirds, and marine mammals; productivity is enhanced because of

49   physical processes at the shelf break including intensive tidal mixing and transverse circulation

50   and eddies in the Bering Slope Current which bring nutrients into the photic zone (Springer et al.

51   1996). About 40% of U.S. commercial fisheries catch originates from the eastern Bering Sea;

52   some of these fisheries concentrate on the slope and outer shelf. The eastern Bering Sea slope

53   contains 5 major canyons that incise the outer shelf (Figure 1). In 2012, the North Pacific Fishery

54   Management Council (NPFMC) received testimony from environmental organizations

55   suggesting management measures to provide Essential Fish Habitat (EFH) protection to coral,

56   sponge and other benthic habitat of fish and crab species for two of the five major eastern Bering

57   Sea canyons (Pribilof and Zhemchug).

58        Based on this testimony, the NPFMC requested that the Alaska Fisheries Science Center

59   (AFSC) conduct an analysis to determine whether Bering Sea canyons were unique habitats and

60   whether there were fish and invertebrate assemblages within the canyons vulnerable to the

61   effects of commercial fishing, such as coral and sponge communities. An analysis of existing

62   data was conducted and presented to the NPFMC in 2013 (Sigler et al. 2013, Sigler et al. 2015).

63   Their conclusions were that although there were some physical characteristics that distinguished

64   the canyons from the surrounding slope and shelf areas, there were no unique faunal features that

65   distinguished Pribilof or Zhemchug Canyons from the surrounding slope areas. The major

66   variables structuring the biological communities on the eastern Bering Sea slope and outer shelf

67   instead are depth and latitude (Sigler et al. 2015, Hoff in review).

68        As a part of the analysis by Sigler et al. (2013), models of the distribution of structure-

69   forming invertebrates (deep-sea corals, sponges, and sea whips) were developed based on bottom

70   trawl survey data. A key outcome of this distribution modeling was the finding that about 1/3 of

71   the predicted coral habitat for the eastern Bering Sea slope occurs in Pribilof Canyon, an area

72   that comprises only about 10% of the total slope area (Figure 2). Much of the remaining

73   predicted coral habitat was found in the inter-canyon slope area to the northwest of Pribilof

74   Canyon. This finding resulted in a request from the NPFMC for the AFSC to conduct further

75   field research in 2014 using a stereo drop camera to survey the eastern Bering Sea slope and

76   outer shelf.

77   The primary objective of this research was to validate the predictions of coral distribution

78   by testing the predictions of coral presence or absence using a randomized stereo camera survey.

79   The secondary objectives were to 1) validate the sponge and sea whip model predictions, 2)

80   measure heights and densities of structure-forming invertebrates where they occurred, 3)

81   examine any associations of structure-forming invertebrates and fish species, 4) document any

82   observations of fishing gear effects on the coral and sponge habitats, 5) collect data useful to

83   estimate an index of vulnerability of structure-forming invertebrates to commercial fishing, and

84   6) improve or refine the predictions of coral distribution if possible.

85

86   **2. Materials and Methods**

87

88   *Study area*

89   The eastern Bering Sea is dominated by a broad shallow continental shelf that stretches

90   east to west from the Alaska mainland to the shelf break roughly 700 km away (Figure 1). The

91   eastern Bering Sea shelf is commonly divided into three domains based on bathymetry and

92   oceanographic fronts, the inner shelf (0 to 50 m), the middle shelf (50 to 100 m) and the outer

93    shelf (100 to 180 m) (Coachman 1986). The shelf break is typically at 180 to 200 m depth,

94    except at the northern edge of Bering Canyon, where the shelf break is at 500 m (Sigler et al.

95    2015). The eastern Bering Sea slope is made up of 5 major canyons (Bering, Pribilof, Zhemchug,

96    Pervenets and Navarin canyons) with an inter-canyon area between each (Figure 1). There are

97    also multiple smaller canyons along the shelf break, but none incise the shelf to the degree of the

98    5 largest (Karl et al. 1996). The focus of this study is 10 regions, which includes the 9 regions

99    (canyon and intercanyon) along the continental slope as well as the outer region of the eastern

100   Bering Sea shelf.

101

102   *Survey design and field sampling*

103        A total of 300 station locations were randomly selected for sampling from August 8-

104   September 6, 2014. This sample size was chosen based on a simulation of the effect of sample

105   size on the performance of the coral presence/absence model as measured by the AUC-value, a

106   test statistic used for evaluating model performance (Hosmer and Lemeshow 2005). Based on the

107   bottom trawl survey model and data (Sigler et al. 2015), an AUC-value of 0.78 could be

108   achieved with sample size of 300, about 85% of the value achieved for sample sizes of 1,000-

109   2,000. Since AUC values of > 0.70 are considered acceptable and AUC values > 0.80 are

110   considered excellent (Hosmer and Lemeshow 2005); a sample size of approximately 300 stereo

111   camera drops was predicted to result in a model with acceptable to excellent predictive power.

112   Stations were chosen from a regular-spaced grid overlaid on the eastern Bering Sea outer shelf

113   and slope with each grid cell having 100 m by 100 m sides. Random stations were chosen in two

114   stages. For the first set of stations, 10 stations were chosen randomly from each of the 9

115   individual canyon and intercanyon areas (n = 90) to ensure that there was some spatial coverage

116   of each area. The large size of the eastern Bering Sea outer shelf area and potential for isolated

117   stations located far from other stations prevented us from choosing 10 at-random stations in this

118   area. For the second stage of sample site selection, we randomly chose 210 stations throughout

119   the nine slope areas and the outer shelf based on the probability of coral presence from the

120   bottom-trawl model of coral distribution (Sigler et al. 2015). Thus, areas with a higher

121   probability of coral presence (such as Pribilof Canyon, the adjacent intercanyon area to the

122   northwest and the outer shelf near Pribilof Canyon and to the north and south) received

123   proportionally more allocated stations (Figure 1). Due to poor weather and time constraints 250

124   of the 300 stations were occupied during field sampling (Table 1). The majority of the

125   unsampled stations were north of Zhemchug Canyon (Figure 1). The northernmost canyon,

126   Navarin Canyon, and the inter-canyon area between Navarin and Pervenets canyons, were not

127   sampled. As a result, a total of 8 of the 10 regions were sampled.

128         The primary sampling tools for this study were two stereo drop camera systems

129   (Williams et al. 2010). The camera systems were deployed from a chartered fishing vessel, the

130   FV *Vesteraalen*, during August 10 – September 5, 2014.  Each stereo drop camera is designed to

131   be towed or drifted continuously along a linear transect at or near the seafloor, rather than a

132   camera that is lowered to the seafloor at one position and then brought immediately to the

133   surface or lowered to the seafloor and anchored during an observation period. The electronic

134   components of the drop cameras were protected from physical damage by a cage constructed

135   from aluminum tubing. Two machine-vision cameras spaced approximately 30 cm apart in

136   underwater housings were connected via ethernet cables to a computer also in an underwater

137   housing. On the first drop camera system, one of the paired cameras recorded monochromatic

138   still images sized at 1.45 megapixels (JAI, CM-140GE), while the other camera collected 1.73

139    megapixel color still images (JAI, AB-201GE). On the second drop camera system, one of the

140    paired cameras recorded monochromatic still images sized at 1.45 megapixels (JAI, CM-

141    140GE), while the other camera collected 2.82 megapixel color still images (Prosilica GX

142    1920C). Lighting was provided by four strobe lights constructed of four Bridgelux® BXRA LED

143    arrays capable of producing 1,300 lumens at 10.4 W.  The computer, cameras, and lights were

144    powered by a 28 V NiMH battery pack. Synchronous images were collected from each of the

145    cameras at a frequency of one image per second and written to a computer hard drive.

146    Additionally, images from the monochrome camera were viewed in real time at a rate of four

147    images per second on a monitor at the surface aboard the vessel. This allowed the height of the

148    camera to be actively controlled to keep it just above the seafloor using a quick response electric

149    winch. A 1/4 inch diameter coaxial cable provided the connection from the drop camera system

150    to the winch at the surface and allowed image viewing in real time.

151         At each occupied station, the camera was deployed at the center of the grid cell and

152    lowered to the seafloor. Once seafloor contact was made, the drop camera was drifted along the

153    bottom for 15 minutes. During each deployment, the drop camera system was drifted or lightly

154    towed through the water column in the direction of the prevailing current at a speed of 0.48 to

155    3.34 km*hr-1 (0.26 to 1.8 knots) approximately 1 to 2 m above the substrate with the cameras

156    pointed slightly downward at an angle of approximately 35° off parallel to the seafloor. The

157    research vessel GPS was used to determine the position of the camera throughout the

158    deployment. The deployment cable was held as near vertical as possible to improve positional

159    accuracy, given weather and wind conditions. The distances traveled during deployments ranged

160    from 27 m to 839 m (mean = 362 m, SE = 8.8). Only 4 tows were less than 100 m in total length

161    and these were the result of equipment failure (such as dying batteries) and over 85% of the

162    deployments had distances between 200 and 600 m

163

164    *Image analysis*

165        A post-cruise image analysis was conducted to determine substrate types, species

166    abundance, and composition and size. Image pairs collected during each deployment were

167    viewed using stereo image processing software developed in the Python programming language

168    (Kresimir Williams, AFSC-RACE Division, unpublished software). To compute range and size

169    information for simultaneously captured image pairs, the cameras were calibrated following

170    methods described in Williams et al. (2010). The calibration procedure corrects for image

171    distortion due to the lens and viewport optics, and solves for the epipolar geometry between the

172    two cameras. The image analysis software incorporates the camera calibrations and determines

173    the three-dimensional coordinates for any corresponding point that is identified in the stereo-

174    image pair using a stereo-triangulation function.

175        The substrate observed in the underwater video transects was classified by a commonly

176    used seafloor substratum classification scheme (Stein et al. 1992, Yoklavich et al. 2000).  The

177    classification consists of a two-letter coding of substratum type denoting a primary substratum

178    with > 50% coverage of the seafloor bottom and a secondary substratum with 20% - 49%

179    coverage of the seafloor.  There were eight identified substratum types: mud (M), sand (S),

180    gravel-pebble (G, diameter < 6.5 cm), mixed course material (MC), cobble (C, 6.5 < diameter <

181    25.5 cm), boulder (B, diameter > 25.5 cm), exposed low relief bedrock (R), and exposed high

182    relief bedrock and rock ridges (K).  By this classification, a section of seafloor covered primarily

183    in cobble, but with boulders over more than 20% of the surface, would receive the substratum

184     code cobble-boulder (Cb) with the secondary substratum indicated by the lower-case letter. The

185     primary substratum code was only changed if a substratum encompassed more than 10 images.

186     The size of each substrate was estimated from the viewing path width or by direct measurement.

187          All fishes and commercially important crabs were identified to the lowest taxonomic

188     level possible and counted for each image pair. Structure-forming invertebrates (corals, sponges

189     and sea whips) were also identified to the lowest possible taxonomic level (typically genus for

190     corals and sea whips and order for sponges) and counted for each image pair. Careful

191     examination and accounting of individual targets in adjacent frames was used to ensure that

192     objects were counted only once. Species identifications for sponges and corals were based on

193     Stone et al. (2011), Stone (2014) and Stone (personal communication). Demosponges on four

194     transects were too numerous to individually count. In this case 135 image pairs were randomly

195     subsampled and all of the individual sponges in these frames counted. The counts from this

196     subsample of frames were then expanded to the un-sampled frames.  Sponges less than 10 cm in

197     height were difficult to discern from other small white- or yellow-colored items on the seafloor,

198     so these were not included in the counts or analyses.

199          Densities of individual taxa were calculated by dividing counts by the area swept

200     (distance observed*path width observed). The image analysis software provided a range (in cm)

201     from the camera to each individual target that was identified in an image pair. The path width

202     was estimated from the median of this range for each transect. The median range of all objects

203     counted on a transect was assumed to be the distance from the camera where 100% of fishes and

204     invertebrates were detected for that transect. The viewing angle for each camera is known (and

205     fixed by the camera lens). Using the median range and the known viewing angle, a horizontal

206     line in front of the camera can be calculated using formulae for sizing triangle components. Since

207    we have an angle (viewing angle) and the adjacent side of a triangle (range) for each camera, the

208    length of the opposite side can be calculated. This opposite side is the viewing path width at the

209    median range for each transect.  This width was calculated for each transect and used as the path

210    width in density estimation. The mean path width across all transects was 3.08 m (SE = 0.05),

211    with a minimum of 1.55 m and a maximum of 5.51 m for any individual transect.

212         Fish lengths and invertebrate heights were obtained by identifying the pixel coordinates

213    of corresponding points (such as a fish snout or tail) seen in the left and right camera frames.

214    These points were used to calculate three-dimensional coordinates in the images by triangulation

215    using the calibration-derived parameters. All fish where the snout and tail were visible in both

216    cameras were measured for length using stereo techniques, with the exception of fish whose

217    body position was too curved to obtain an accurate length. Heights of all corals where the base

218    and tip could be observed were also measured. Heights were measured for all sea whips for

219    transects with less than ~500 individual sea whips. For transects with more than ~500 individual

220    sea whips or sponges, a random subsample of 135 paired images were selected to obtain ~200

221    individual heights for each taxonomic grouping. Curved sea whips were measured to their

222    highest point above the seafloor. Except where noted, the height and length data from each

223    transect presented here were weighted by the density of the taxa for that transect.

224         The data resulting from image analysis include densities of fishes, crabs, and structure-

225    forming invertebrates (no.$*m^{-2}$); fish lengths for each species; heights of structure-forming

226    invertebrates; and the proportions of each type of substrate for the 250 transects.

227

228    **2.1 Validation of presence/absence models based on bottom trawl data**

229

230    In the time between the original presentation of the coral, sponge and sea whip models

231    (June 2013) and the camera survey (August 2014), some improvements were made to the

232    distribution models based on bottom trawl survey data. The grid size of the original bottom trawl

233    survey models (Sigler et al. 2015) was reduced from 1 $km^2$ to 1 hectare (100 m by 100 m grid

234    size). Improved bathymetry layers became available in early 2014 (M. Zimmermann and M.

235    Prescott, AFSC-RACE Division, unpublished data) and were incorporated into the new model.

236    An additional environmental variable, tidal current speed, was also incorporated into the new

237    model and the position of the net behind the trawl survey vessel was corrected for using the

238    depth and wire out measured at the time of the trawl. The revised models fit slightly better and

239    had higher resolution, but did not change the overall picture of the distribution of corals,

240    sponges, and sea whips (Figure 2), as most areas of predicted presence remained in Pribilof

241    Canyon and to the northwest of Pribilof Canyon, similar to the June 2013 model. Hereafter, the

242    models used for validation are the improved versions of the Sigler et al. (2015) distribution

243    models.

244    Model validation was conducted by comparing the predictions of probability of structure-

245    forming invertebrate presence or absence from the models based on bottom trawl survey data to

246    the observations of structure-forming invertebrate presence or absence from the camera survey.

247    Since model predictions were made on a map, the camera survey transects were overlaid on each

248    of the prediction maps and the underlying predictions were extracted. Because each camera

249    transect may have viewed multiple grid cells on the prediction map, the maximum probability

250    value underlying each camera survey drop was extracted and then compared to the observation

251    of presence or absence from image analysis at that site.

252    The area under the receiver operating curve (AUC) was used to evaluate the fit of the

253    trawl survey model to the camera drop observations. The AUC is a measure of rank-correlation

254    and can range from zero to one. It compares the probability associated with randomly selected

255    presence sites to randomly selected absence sites and determines if the probability is higher at

256    random sites with observed presence than random sites with observed absence. A value of 0.5

257    indicates model predictions are only as good as a random guess. A high AUC value indicates the

258    model better fits the observations. The correlation between the observations and predictions was

259    also calculated.

260    As a secondary test of the model fit, a threshold probability was calculated where the rate

261    of false positives (prediction of presence where absence was observed) was equal to the rate of

262    false negatives (prediction of absence where presence was observed). This threshold probability

263    was applied to all the camera survey sites to produce a matrix indicating the percent correctly

264    predicted. A Cohen's Kappa was also computed using the threshold value, which is another

265    statistic used to measure goodness-of-fit for presence-absence models.

266    Various plots of model accuracy are also included for reference. All of the model

267    evaluations were carried out on the three taxonomic groups of structure-forming invertebrates

268    (corals, sponges and sea whips). All the analyses, modeling and mapping were carried out using

269    R software (R Core Development Team 2013).

270

271    **2.2 Model improvements and model averaging**

272

273    Using only the camera survey data, a new model was developed for presence or absence

274    of structure-forming invertebrates. A generalized additive modeling framework (GAM; Wood

275    2006) was used with some of the same explanatory variables (latitude, depth, bottom

276    temperature, slope, mean current speed, mean tidal current speed, ocean color, grain size and

277    sediment sorting) as the bottom trawl survey model, to predict presence or absence of the camera

278    survey data. Longitude was not included in the camera survey model, as based on previous

279    results (Sigler et al. 2015, Hoff in review), latitude and depth were expected to be the most

280    important variables driving community patterns on the eastern Bering Sea slope. Removing

281    longitude also minimized the number of model parameters that had to be used in the smaller

282    camera survey data set.

283         The camera survey model was evaluated using the same methods as were used for

284    evaluating the bottom trawl survey model. AUC and correlation were calculated, a threshold

285    probability was estimated that balanced the false positive and false negative error rates, the

286    percent classified correctly and the Cohen's Kappa were also computed. These same diagnostics

287    were computed comparing the bottom trawl survey observations to the camera survey model.

288    These camera survey models were developed independently for coral, sponges, and sea whips.

289         The camera model predictions were combined with the bottom trawl model predictions

290    using model prediction averaging. The predictions of the two models were averaged for each

291    grid cell on the raster maps and weighted by the inverse of the standard error of the prediction for

292    each grid cell of each model. This resulted in a map of predictions where values for each

293    particular grid cell reflected the average predicted probability for the two models, as well as the

294    confidence of each models prediction (i.e. grid cells where the bottom trawl based model had a

295    high prediction error were down-weighted relative to the camera based model if its prediction

296    error was low). Since the camera survey extended only to a depth of 808 m depth, whereas the

297    trawl survey extended to 1200 m in depth, the average model was only extended to a depth of

298    825 m where both models were supported by observations. The resulting average model was

299    tested against the observations from the two surveys (bottom trawl and camera) using the

300    standard set of diagnostics (AUC, correlation, percent correct and Cohen's Kappa).

301

302    **2.3 Density and height distribution of structure-forming invertebrates**

303

304    The densities of structure-forming invertebrates (corals, sponges, and sea whips) were

305    compared among the eight eastern Bering Sea slope and outer shelf regions sampled during the

306    camera survey. Height frequencies were also compared among the regions using frequency plots

307    and mean values. These heights were weighted by the density of the structure-forming

308    invertebrates to account for differences in abundance among transects. Densities and mean

309    heights were compared among regions using analysis of variance (ANOVA) to test for

310    significant differences at $p = 0.05$. When significant differences were found, Tukey's post-hoc

311    tests for multiple comparisons were conducted to determine pairwise significant differences.

312    Finally, hurdle models (Cragg 1971, Potts and Elith 2006) predicting spatial distribution

313    of density and height using the camera survey data were produced for each structure-forming

314    invertebrate taxonomic grouping. Hurdle models predict the spatial distribution of abundance (or

315    in this case abundance and height) in three stages: 1) probability of presence is predicted from

316    presence-absence data;  2) a threshold presence probability is determined; 3) a separate model is

317    constructed that predicts abundance (or height). In the first step, we used the average models for

318    each taxonomic group developed in Section 2.2. In the second step, we used the optimum

319    thresholds determined by the camera data from Table 4 (since the density and height data were

320    derived from the camera survey). In the third step, we modeled the density and height data from

321    the camera survey. In this third step, the density models and height models used only data from

322    the camera survey because density and height information were not available from the bottom

323    trawl survey data. For each taxonomic grouping, the density or height of the species was

324    predicted by a GAM model utilizing latitude, depth, bottom temperature, ocean color, current

325    speed, sediment size and tidal current speed. In the GAM model estimation, only transects where

326    non-zero values were included. Density data was fourth-root transformed to meet the assumption

327    of normality, height was untransformed. Models of density and height were evaluated against

328    observations using the deviance explained and correlations between observations and

329    predictions.

330

331    **2.4 Fish and structure-forming invertebrate associations**

332

333        Associations between fish and structure-forming invertebrates were examined through

334    analysis of covariance (ANCOVA) to test whether the presence of structure-forming

335    invertebrates at a transect had a significant positive or negative effect on fish densities for that

336    transect. For these analyses, fish and crabs were placed into one of the following groupings:

337    rockfishes (all *Sebastes* sp.), sculpins, grenadiers, flatfishes, C*hionoecetes* crabs, king crabs, and

338    skates and analyzed separately. In addition, the individual species of Pacific ocean perch,

339    shortraker rockfish, shortspine thornyhead, Pacific cod, pollock, northern rockfish, sablefish, and

340    rougheye/blackspotted rockfish were also analyzed independently. Fish density was fourth root

341    transformed and used as the dependent variable. The independent variables were presence or

342    absence of corals, presence or absence of sponges, or presence or absence of sea whips and

343    depth. All covariate-invertebrate group interactions were included and stations were used as

344    replicates. Statistical significance was judged at p = 0.05.

345

346    **2.5 Observations of fishing gear and damage to structure-forming invertebrates**

347

348         Direct evidence of fishing (e.g., lost gear) was documented during the underwater camera

349    survey. Fishing evidence was classified as lost longline or crab gear, lost trawl net, or trawl

350    tracks. We computed the proportion of affected transects and mapped their locations.

351         Damage to structure-forming invertebrates also was documented during the underwater

352    camera survey. Damage may be due to natural causes (e.g., nudibranch predation of sea whip

353    soft tissue) or fishing (e.g., moving fishing gear that knocks down sea whips). While we were

354    able to identify damaged structure-forming invertebrates, we were unable to identify the cause of

355    this damage (i.e., the proportion damaged by fishing is unknown). During image analysis, we

356    recorded individual sponges and corals that were observed to be broken or broken off and lying

357    on the seafloor. For sea whips, damage was difficult to discern, but individuals with tissue

358    damage (abrasions or exposed axial rods) or individual sea whips that were lying horizontal on

359    the seafloor either dead (axial rod exposed) or possibly alive (apparently fleshy and otherwise

360    undamaged) were recorded as dead or damaged. We computed the proportion of transects with

361    damaged taxa and mapped their locations. We also computed the overall proportion of damaged

362    coral, sponge, and sea whips relative to their total numbers and compared their locations and

363    depths to all coral, sponge, and sea whips.

364

365    **2.6 Framework for estimating vulnerability of structure-forming invertebrates**

366

367     In its simplest form, vulnerability of structure-forming invertebrates to fishing gear and

368     other anthropogenic activities should reflect 1) the abundance of the organism, 2) the size of the

369     organism, 3) the rate of the impact and 4) the amount of time it will take the population to

370     recover to the existing state post-impact. The data collected during the camera survey can be

371     used to address the first two items. We did not examine vulnerability of structure-forming

372     invertebrates directly, but instead we examined the areas with the highest densities and largest

373     sizes of each taxonomic group of structure-forming invertebrates based on the model results

374     from section 2.3 above. Quantiles of density were computed for the grid cells of the best-fitting

375     density models. The two upper quartiles of density were then plotted for each taxonomic group.

376     This was repeated for the height models and the two resulting upper quartile plots were

377     combined; grid cells where either the density or height was in the upper quartile and the other

378     measure (density or height) was in the upper two quartiles were plotted for each taxa. It is

379     important to note that the thresholds (in our case quantile divisions) are rather arbitrary and could

380     be set to alternative values.

381

382     **3. Results**

383

384     The 250 successfully occupied stations sampled much of the area of the eastern Bering

385     Sea outer shelf and slope (Figure 1). Stations were occupied from Bering Canyon in the south to

386     Pervenets Canyon in the north (Table 1). The depths sampled ranged from 91 m to 808 m, with a

387     median depth of 276 m. The area viewed on each transect averaged 1,131 m$^2$ (SE = 34) and

388     ranged from 84 m$^2$ to 3,441 m$^2$. Sand was the dominant substrate observed (Figure 3). Over 97%

389    of the images of the seafloor were classified as containing only unconsolidated substrates (mud,

390    sand, gravel, pebble or mixed coarse material). The remaining 2.8% of images contained some

391    type of rocky substrate (cobble, boulder or exposed bedrock), however, only 0.8% of the images

392    had rocky substrates as the primary substrate type (Figure 3). Some amount of rocky substrate

393    occurred at 45 transects (18%), while the remaining transects lacked rocky substrates.

394        Over 7,000 fishes and crabs were counted from roughly 52 different species or taxonomic

395    groupings (Table 2). Eelpouts and *Chionoecetes* crabs dominated (~57% of the total

396    observations). However, grenadiers and rockfishes (especially Pacific ocean perch) were also

397    common. The abundant species mostly were small benthic dwelling fishes such as eelpouts,

398    snailfishes, sculpins, and poachers. Over 70,000 structure-forming invertebrates were observed

399    (Table 3). Most were demosponges (55%), predominantly from two individual transects, and sea

400    whips (40%). Few were corals (2%, < 1500 individuals).

401        Corals occurred on 32 of the 250 survey transects (Table 1). They were classified into 5

402    taxonomic groups including three families (Primnoidae, Plexauridae, and Isididae) and two

403    genera (*Plumarella* sp. and *Swiftia* sp.). The most common corals were *Plumarella* sp., which are

404    members of the Primnoidae family, and *Swiftia* sp., which are members of the Plexauridae

405    family. The median depth at which coral occurred was 451 m (range = 201 – 770 m), much

406    deeper than the median depth of all transects (276 m). Coral did not occur in Bering Canyon,

407    Pervenets Canyon, or the regions between Bering and Pribilof canyons or between Zhemchug

408    and Pervenets canyons. Coral occurred at 50% of transects in Pribilof Canyon and about 18% of

409    transects in the inter-canyon area between Pribilof and Zhemchug Canyons. Coral was present at

410    one station on the outer shelf and one station in Zhemchug Canyon (Figure 4).

411     Sponges occurred on 113 of the 250 survey transects (Table 1). They were classified into

412     three orders; hexactinellids, demosponges, and calcareous sponges. The vast majority of sponges

413     were hexactinellids. The median depth at which sponges occurred was 311 m, and they covered

414     almost the entire depth range of sampling from 111 m to 781 m. Sponges were widely distributed

415     and occurred in all of the sampled regions (Figure 4), ranging from a low of 17% of the stations

416     in Pervenets Canyon to a high of 73% of stations in the inter-canyon region between Zhemchug

417     and Pervenets canyons.

418     Sea whips were also widely distributed both in terms of depth and region. They occurred

419     at depths from 91 m to 760 m (median = 266 m) at 105 of the 250 stations surveyed (Table 1). At

420     least two different species of sea whip were observed, *Halipteris willemoesi* and an unidentified

421     *Halipteris* species.  Sea whips occurred in all regions, occurring at a low of 25% of the stations

422     in Pribilof Canyon to a high of 53% of stations in the inter-canyon region between Bering and

423     Pribilof Canyons (Figure 4).

424

425     **3.1 Validation of presence/absence models based on bottom trawl data**

426

427     The model based on bottom trawl survey data predicted the distribution of presence or

428     absence of coral in the camera survey data very well. The AUC was 0.73 (standard deviation =

429     0.05) and the correlation was highly significant (r = 0.28, p < 0.0001) indicating model

430     predictions were well correlated to observations (Table 4). The observations of coral presence (n

431     = 32) occurred mostly in Pribilof Canyon and the area to the northwest of Pribilof Canyon,

432     which corresponded well with the predictions from the bottom trawl survey model (Figure 4).

433     The AUC diagnostics indicated that through most of the data, as the probability of occurrence

434    was predicted to increase, the observations of occurrence also increased (Figure 5). At the higher

435    probabilities of occurrence (> 0.60), there appeared to be a drop off in model performance at 11

436    stations where coral didn't occur but was predicted to be present. The prediction error for these

437    11 stations was about twice (0.19) the overall average (0.09). Six of these stations were located

438    in Pervenets Canyon, and the remaining five were scattered in the region between Pribilof

439    Canyon and Zhemchug Canyon. A threshold probability of 0.19 best balanced the false positive

440    and false negative error rates for coral prediction. Applying this threshold resulted in a Cohen's

441    Kappa of 0.26 (standard deviation = 0.06) and a percentage of stations with presence predicted

442    correctly of 72% (standard deviation = 0.03).

443        The model based on bottom trawl survey data predicted the distribution of presence or

444    absence of sponge in the camera survey data less well. The AUC was 0.63 (standard deviation =

445    0.04), although the correlation was highly significant (r = 0.21, p = 0.0006) indicating model

446    predictions were well correlated to observations (Table 4). The observations of sponge presence

447    (n = 113) occurred throughout all areas and depths (Figure 4). The AUC diagnostics indicated

448    that through most of the data, as the probability of occurrence was predicted to increase, the

449    observations of occurrence also increased (Figure 5). A threshold probability of 0.70 best

450    balanced the false positive and false negative error rates for sponge prediction. Applying this

451    threshold resulted in a Cohen's Kappa of 0.17 (standard deviation = 0.06) and a 59% of stations

452    with presence predicted correctly (standard deviation = 0.03).

453        The bottom trawl survey model predicted the distribution of sea whips in the camera

454    survey data fairly well. The AUC was 0.69 (standard deviation = 0.03), although the correlation

455    was highly significant (r = 0.30, p < 0.0001) indicating model predictions were well correlated to

456    observations (Table 4). The observations of sea whip presence (n = 105) occurred throughout all

457     areas and depths (Figure 4). The AUC diagnostics indicated that through most of the data, as the

458     probability of occurrence was predicted to increase, the observations of occurrence also

459     increased (Figure 5). In contrast to the coral model, the sea whip model was almost always

460     correct in predicting presence at high probabilities. A threshold probability of 0.06 best balanced

461     the false positive and false negative error rates for sponge prediction. Applying this threshold

462     resulted in a Cohen's Kappa of 0.29 (standard deviation = 0.06) and a percentage of stations with

463     presence predicted correctly of 65% (standard deviation = 0.03).

464

465     **3.2 Model improvements and model averaging**

466

467         The best-fitting model of coral presence or absence based on the camera survey data

468     contained four significant terms, with depth and latitude being the most important (Table 5).

469     Probability of coral presence increased sharply with increasing depth to about 300 m and then

470     leveled off with further increase in probability of presence below 600 m (Figure 6).

471     Unsurprisingly, the model predicted higher probabilities of presence in the middle latitudes of

472     the eastern Bering Sea slope. Probability of presence of coral increased slightly with increasing

473     tidal currents and increased sediment sorting (Figure 6). The model explained about 51% of the

474     deviance in the camera observations, the AUC of the camera survey model was 0.95 (SD = 0.01)

475     and the correlation was 0.67. A threshold probability of 0.21 best balanced error rates resulting in

476     a Cohen's Kappa of 0.57. The model predicted 87% of the stations correctly. The predictions

477     from the camera-based model (Figure 7) were similar to the predictions of the trawl survey-based

478     model (Figure 2).

479     When the camera survey model was used to predict the observations of coral presence or

480     absence in the bottom trawl survey data, the results were very good (Table 4). The AUC was

481     0.73 (SD = 0.04) and the correlation was 0.27. Using a threshold of 0.01, the Cohen's Kappa was

482     0.19 (SD = 0.03) and 78% of the bottom trawl survey observations were predicted correctly by

483     the camera survey model. Most of the mismatches were in the northern portion of the eastern

484     Bering Sea slope and outer shelf, where no camera stations were occupied, but there was bottom

485     trawl survey data.

486     The average model (combining both the predictions from the bottom trawl survey model

487     and the camera survey model) exhibited a similar pattern to the individual models, with most

488     areas of high probability of coral occurrence found in Pribilof Canyon and the area to the

489     northwest (Figure 8). This model also performed well at predicting the observations from both

490     the bottom trawl survey (AUC = 0.85, SD = 0.03) and the camera survey (AUC = 0.90, SD =

491     0.02) (Table 4). Using a combined threshold of 0.02, resulted in correctly predicting 81% of the

492     100 observations of coral (n = 68 for the bottom trawl survey and n = 32 for the camera survey)

493     correctly.

494     The best-fitting model of sponge presence or absence based on the camera survey data

495     contained seven significant terms (Table 5). Probability of sponge presence increased to a peak

496     at a depth of ~300 m and then decreased at deeper depths (Figure 10). Probability of sponge

497     presence decreased with increasing long-term average temperature and was highest at the large

498     and small extremes of sediment sorting. There were increases in sponge probability of presence

499     related to slope and sediment size and there was a dome-shaped relationship between sponge

500     presence and ocean productivity (Figure 10). The model explained only about 16% of the

501     deviance in the camera observations of sponge presence or absence. The AUC of the camera

502    survey model was 0.80 (SD = 0.03) and the correlation was 0.52 (Table 4). A threshold

503    probability of 0.44 best balanced error rates resulting in a Cohen's Kappa of 0.45 (SD = 0.06).

504    The model predicted 73% of the stations correctly. The predictions from the camera-based model

505    (Figure 7) were similar to the predictions of the trawl survey-based model (Figure 2), although

506    the bottom trawl survey model predicted a wider range of high probability sponge areas along

507    the outer shelf, and the camera based model predicted a higher probability of presence in the

508    northeastern outer shelf. The camera based predictions on the northeastern outer shelf were

509    undoubtedly spurious, as no camera sampling was conducted here. The camera and trawl survey

510    models did agree that sponge occurs in most areas of the outer shelf and slope.

511         When the camera survey model was used to predict the observations of presence or

512    absence of sponge in the bottom trawl survey data, the results were not very good (Table 4). The

513    AUC was 0.54 and the correlation was negative. Using a threshold of 0.56, only 50% (i.e., only

514    equal to chance) of the bottom trawl survey observations were predicted correctly by the camera

515    survey model. Most of the mismatches were in the northern and northeastern portion of the

516    eastern Bering Sea slope and outer shelf, where no camera stations were occupied and the

517    camera model predicted a high probability of sponge presence, but sponge catches in the bottom

518    trawl survey were generally minimal.

519         The average sponge model (combining both the predictions from the bottom trawl survey

520    model and the camera survey model) combined the best features of the individual models, with

521    most areas of high probability of sponge occurrence found in Bering Canyon, Pribilof Canyon

522    and the area to the northwest, Zhemchug Canyon and in areas of the outer shelf (Figure 8). This

523    model performed well at predicting the observations from both the bottom trawl survey (AUC =

524    0.71, SD = 0.01) and the camera survey (AUC = 0.76, SD = 0.03) (Table 4). Using a combined

525     threshold of 0.59 resulted in correctly predicting 70% of the 724 observations of sponge presence

526     (n = 611 for the bottom trawl survey and n = 113 for the camera survey) correctly.

527          The best-fitting model of sea whip presence or absence based on the camera survey data

528     contained seven significant terms, with sediment grain size being the most important (Table 5).

529     Probability of sea whip presence increased sharply with increasing grain size to a value of ~4

530     (which corresponds to very fine sand) and then decreased (Figure 11). The model predicted

531     higher probabilities of presence in the middle latitudes of the eastern Bering Sea slope.

532     Probability of presence of sea whips had a dome-shaped relationship with depth, peaking at

533     about 450 m. There was generally a nonlinear increase in sea whip probability of presence with

534     increasing temperature, slope and tidal currents and a linear increase in probability of presence

535     with current speed. The model explained only about 26% of the deviance in the camera

536     observations; the AUC of the camera survey model was 0.83 (SD = 0.03) and the correlation was

537     0.56 (Table 4). A threshold probability of 0.44 best balanced error rates resulting in a Cohen's

538     Kappa of 0.51 (SD = 0.05). The model predicted 76% of the stations correctly. The predictions

539     from the camera-based model (Figure 7) were different from the predictions of the trawl survey-

540     based model (Figure 2), in that the camera model predicted a much wider depth range for sea

541     whips and a much broader distribution on the outer shelf. Similar to the case for the sponges, the

542     high probability of presence in the northeastern outer shelf and also in the southeastern outer

543     shelf were outside the area of sampling for the camera survey and should be viewed with some

544     caution.

545          When the camera survey model was used to predict the observations of presence or

546     absence of sea whips in the bottom trawl survey data, the results were mixed (Table 4). The

547     AUC was relatively low at 0.57 (SD = 0.02) and the correlation between predictions and

548    observations was 0.12. Using a threshold of 0.72, only 55% of the bottom trawl survey

549    observations were explained by the camera survey model (only slightly better than chance). Most

550    of the mismatches were at deeper depths where bottom trawl survey catches of sea whips were

551    not common and in the previously mentioned northern areas and northeastern outer shelf where

552    there were no camera observations.

553        The average model (combining both the predictions from the bottom trawl survey model

554    and the camera survey model) performed better with extensive predictions of presence of sea

555    whips along the outer shelf and some in deeper waters (Figure 8). This model also performed

556    well at predicting the observations from both the bottom trawl survey (AUC = 0.82, SD = 0.02)

557    and the camera survey (AUC = 0.74, SD = 0.03). Using a combined threshold of 0.31 resulted in

558    correctly predicting 67% of the 250 observations of sea whip presence (n = 145 for the bottom

559    trawl survey and n = 105 for the camera survey) correctly (Table 4).

560

561    **3.3 Density and height distribution of structure-forming invertebrates**

562

563        The densities of coral found at transects were very low (mean = 0.005, SE = 0.002) and

564    ranged from 0 to 0.28 individuals/m$^2$. Of the 32 transects with coral, 11 had less than 5

565    individuals occurring on them. The highest densities of corals were observed in Pribilof Canyon

566    and the area to the northwest (Figure 12). The best-fitting GAM model predicting coral density

567    included only bottom depth and slope as significant factors (Table 5). The model explained 70%

568    of the variability in the coral density data and generally, density increased with increasing depth

569    and decreased with increasing slope (Figure 13). Density of coral predicted by the GAM model

570    was highest in Pribilof Canyon and to the northwest of Pribilof Canyon in deeper waters (Figure

571    14).

572           The densities of sponge found at transects averaged 0.11 individuals/m$^2$ (SE = 0.06) and

573    ranged from 0 to a high of 13.1 individuals/m$^2$. The density of hexactinellid sponges was 0.006

574    (SE = 0.002) and the density of demosponges was 0.11 (SE = 0.06). Four of the transects had

575    densities of sponges in excess of 0.5 individuals/m$^2$ (one in Pribilof Canyon, one in Zhemchug

576    Canyon, one in the intercanyon area near Zhemchug Canyon, and one on the outer shelf

577    northwest of Pribilof Canyon; Figure 12). The best-fitting GAM model predicting sponge density

578    included latitude, current speed, and grain size as significant factors. The GAM model explained

579    only 20% of the variability in the sponge densities, which were highest at the middle latitudes of

580    the eastern Bering Sea outer shelf and slope (Table 5).  Density decreased with decreasing

581    current speed, and sponge density was highest at the smallest grain sizes and at phi of ~4.5.

582    However, this relationship may have reflected low sample sizes at some of the middle values of

583    phi (Figure 15). Density of sponge predicted by the GAM model was highest in Pribilof Canyon

584    and on the surrounding outer shelf, to the northwest of Pribilof Canyon in deeper waters, and in

585    Zhemchug Canyon and to the north (Figure 14).  Two large areas of predicted high density of

586    sponge on the outer shelf northeast of Zhemchug Canyon and southeast of Pervenets Canyon

587    were not sampled during the camera survey and may be spurious.

588           The densities of sea whips found at transects averaged 0.11 individuals/m$^2$ (SE = 0.04)

589    and ranged from 0 to a high of 8.4 individuals/m$^2$. Ten of the transects had densities of sea whips

590    in excess of 0.5 individuals/m$^2$ (one in Bering Canyon, one in the area between Bering Canyon

591    and Pribilof Canyon, three in the intercanyon area between Pribilof Canyon and Zhemchug

592    Canyon, and five on the outer shelf; Figure 12). The best-fitting GAM model predicting sea whip

593     density included only bottom depth and slope as significant factors. The same as for the coral

594     GAM model (Table 5). The sea whip GAM model explained 33% of the variability in the sea

595     whip density data. Unlike the model of coral density, sea whip density decreased with increasing

596     depth, except for an uptick in density at the deepest depths below 600 m (Figure 16). Density

597     decreased with increasing slope. Density of sea whips predicted by the GAM model was

598     relatively uniform (and high) throughout the outer shelf and slope (Figure 14).

599          The size of corals varied by taxonomic group (Table 6). On average, individuals from the

600     family Isididae were the largest, ranging from 10 cm to 116 cm tall. The *Swiftia* sp. were the

601     smallest corals observed ranging from 2 cm to 24 cm, but most of the other taxonomic groups of

602     coral averaged less than 20 cm in height (Figure 17).  Observed average coral heights were

603     highest on the slope northwest of Pribilof Canyon (Figure 18). Sponges from all groups averaged

604     about 17 cm in height, similar to the height distribution of corals (Figure 17). However, sponges

605     less than 10 cm in height were not measured or counted. Of the sponge groups, hexactinellid

606     sponges tended to be the largest, with one specimen having a height of greater than 2 m (Table

607     6). Sponges were tallest at or near the shelf break around Bering Canyon, Pribilof Canyon, and to

608     the northwest of Pribilof Canyon (Figure 18). Sea whips exhibited a bimodal height frequency

609     (Figure 17) with many individuals smaller than 40 cm tall, but also with another peak in height at

610     about 110 cm. This is reflected in the overall average height of sea whips of 62 cm (Table 6). On

611     a few occasions sea whip heights were estimated at > 2 m as well. The largest sea whips were

612     observed between Pribilof Canyon and Zhemchug Canyon at or near the shelf break (Figure 20).

613          The best-fitting GAM model predicting coral height included latitude, tidal current speed,

614     slope, sediment grain size, temperature, and average current speed as significant factors (Table

615     5). The model explained 93% of the variability in observed coral heights data and generally,

616    heights  increased with increasing slope and were highest at the latitudes around Pribilof Canyon

617    and to the northwest (Figure 19). Interestingly, heights of coral increased with increasing average

618    current speed, but decreased strongly with increasing tidal current speed.  Corals were predicted

619    by the GAM model to be tallest in the deeper waters between Pribilof Canyon and Zhemchug

620    Canyon (Figure 20).

621            The best-fitting GAM model predicting sponge height included temperature, slope, and

622    sediment grain size as significant factors (Table 5). The model explained 41% of the variability

623    in observed sponge heights data and generally, heights increased with increasing slope and

624    temperature and peaked at a phi of about 3.5 (corresponding to fine sand to very fine sand)

625    (Figure 21). Sponges were predicted to be tallest in Bering Canyon and on the outer shelf area to

626    the north and around Pribilof Canyon and deeper waters to the northwest (Figure 20).

627            The best-fitting GAM model predicting sea whip height included depth, temperature,

628    latitude, average current speed, and sediment grain size as significant factors (Table 5). The

629    model explained 60% of the variability in observed sea whip  height. Sea whip height decreased

630    with increasing depth, temperature, and sediment size (Figure 22). Sea whip height also

631    decreased from south to north. Current speed was the only factor that had a positive effect on sea

632    whip height as it increased.  Sea whips were tallest in the outer shelf region between Pribilof and

633    Zhemchug Canyons (Figure 20).

634

635    **3.4 Fish and structure-forming invertebrate associations**

636

637            Most of the fish and crab species and taxa groupings examined from the camera survey

638    had strong associations with depth (Table 7). Of the 15 groups examined, the presence of coral

639 had a positive effect on the density of shortraker rockfish, combined king crabs, and rougheye-

640 blackspotted rockfish. Sponge presence had a significantly positive effect on density of

641 combined rockfishes, Pacific ocean perch, and combined king crabs. Sea whip presence had a

642 positive effect on flatfish species and a negative effect on shortspine thornyhead, Pacific cod, and

643 grenadier. Grenadier was interesting in that they were the only group where the presence of

644 either corals, sponges, or sea whips negatively affected their densities. The density of

645 *Chionoecetes* crabs was lower where sponge or coral were present; but the presence of sea whips

646 had no effect. The density of combined rockfishes was higher where sponges were present and

647 lower where corals were present. The densities of pollock, sculpins, skates, northern rockfish,

648 and sablefish were not related to the presence of structure-forming invertebrates (Table 7).

649

650 **3.5 Observations of fishing gear and damage to structure-forming invertebrates**

651

652     At least one damaged coral, sponge, or sea whip was identified on 0-24% of transects,

653 depending on taxa (Table 8). Only the taxa Isididae (0.8% of transects), demosponge (2.8%), and

654 *Halipteris* sp. (24%) were identified as damaged. The other observed taxa were Gorgonacea,

655 *Plumarella aleutiana*, *Plumarella* sp., Primnoidae, Porifera, Calcarea, and Hexactinellid, but

656 none were identified as damaged. Damaged taxa were found on 27.2% of transects, with only

657 one transect with two taxa damaged (both Demosponge and *Halipteris* sp. were found damaged

658 on one transect). Damaged *Halipteris* sp. were widespread, whereas damaged Isididae were

659 limited to Pribilof Canyon and westward and damaged demosponge were limited to Pribilof

660 Canyon and westward as well as Pervenets Canyon (Figure 23).

661       Of the three taxa identified as damaged, demosponge was the most common (present on

662     42.4% of transects), followed by *Halipteris* sp. (42.0%) and Isididae (2.8%) (Table 9). On

663     transects where they occurred, damage of *Halipteris* sp. was most common (one or more

664     damaged *Halipteris* sp. was identified on 57.1% of transects where *Halipteris* sp. was observed),

665     followed by Isididae (28.6%) and demosponge (6.6%). The remaining coral and sponge taxa

666     were found on 0.4% (Gorgonacea) to 22.4% (Hexactinellid) of transects, but none were

667     identified as damaged. Undamaged and damaged *Halipteris* sp. were widely distributed. Isididae

668     were limited to Pribilof Canyon and westward as were damaged Isididae. In contrast,

669     demosponges were widespread but damaged demosponges were limited to Pribilof Canyon and

670     westward as well as Pervenets Canyon. While transects with damaged *Halipteris* sp. were

671     common (present on 24% of transects), the proportion of damaged individuals was much smaller

672     (9% of *Halipteris* sp. were damaged) (Table 10). Similarly, only 2.9% of individual Isididae and

673     0.3% of individual demosponges were identified as damaged. *Halipteris* sp. were found over a

674     wide depth range (91-760 m) and were concentrated at 100-150 m; damaged *Halipteris* sp. also

675     were found over a wide range (91-719 m) and were concentrated at 100-150 m (Figure 24).

676     Demosponges also were found over a wide depth range (110-770 m), but damaged demosponges

677     were found within a narrower depth range (206-412 m). Isididae were found from 349-760 m

678     and damaged Isididae were found over a narrower depth range (455-760 m).

679       Evidence of fishing was found on 0.8-7.6% of transects, depending on the type of

680     evidence (Table 8). Evidence of fishing included trawl net (0.8% of transects), longline or crab

681     gear (4.4%), and trawl tracks (7.6%). Evidence of fishing was found on 12.8% of transects, each

682     with only one type of fishing evidence. Evidence of longline or crab gear occurred from Pribilof

683     Canyon northward to Pervenets Canyon, whereas evidence of trawl gear (either gear itself or

684   trawl tracks) occurred primarily from Pribilof Canyon southward to Bering Canyon, except for

685   trawl tracks at the north edge of Zhemchug Canyon and at Pervenets Canyon (Figure 25).

686   Evidence of longline or crab fishing was found over a depth range of 241-748 m. Evidence of

687   trawl fishing was found from 111-394 m and was somewhat concentrated at 100-150 m.

688         Damaged taxa and/or evidence of fishing were found on 36.8% of transects (Table 8).

689   Both damaged taxa and evidence of fishing occurred on 3.2% of transects (8 of 250). Of these 8

690   transects, 7 had damaged *Halipteris* sp. and 1 had damaged demosponge. Damaged *Halipteris*

691   sp. were observed on 5 transects with trawl tracks, one transect with trawl net, and one transect

692   with either longline or crab gear. The damaged demosponge was observed on a transect with

693   derelict longline or crab gear. Damaged taxa and/or evidence of fishing was most common from

694   Pribilof Canyon and northward to Pervenets Canyon (Figure 26).

695         The depth distributions of undamaged and damaged taxa nearly completely overlapped,

696   except for *Halipteris* sp., which was the only taxa found at <100 m (minimum depth of 91 m).

697   The depth distributions of the undamaged taxa were 695 m (Gorgonacea), 455-759 m

698   (Plexauridae), 349-761 m (*Plumarella aleutiana*), 201-761 m (*Plumarella* sp.), 212-760 m

699   (Primnoidae), 264-770 m (*Swiftia* sp.), 150-761 m (Porifera), 215-532 m (Calcarea), and 110-

700   770 m (Hexactinellid).The depth distributions of the damaged taxa were 349-760 m (Isididae),

701   91-760 m (*Halipteris* sp.), and 110-770 m (demosponge). The two most commonly observed

702   sponge taxa (Hexactinellid and demosponge) were observed within the same depth range (110-

703   770 m). However, only demosponges were identified as damaged.

704

705   **3.6 Vulnerability of structure-forming invertebrates**

706

707        The upper quartiles of coral density occurred in the two arms of Pribilof Canyon, to the

708    northwest of Pribilof Canyon and in spots along the eastern Bering Sea slope in deeper waters

709    from Pribilof Canyon to Zhemchug Canyon (Figure 27). For sponge, the upper quartiles of

710    density occurred on the northern edge of Pribilof Canyon and to the northwest of Pribilof

711    Canyon along the slope (Figure 27). There were also significant areas of sponge abundance in

712    Zhemchug Canyon and north of Zhemchug Canyon. Two large areas on the outer shelf were

713    unsampled by the camera survey, so they should be viewed with caution. The upper quartiles of

714    sea whip density were scattered all along the outer shelf between Bering Canyon and Pervenets

715    Canyon in a fairly distinct band along the shelf break with some gaps above Pribilof Canyon and

716    Zhemchug Canyon (Figure 27).

717        The upper quartiles of coral height occurred predominantly in deeper waters off to the

718    north of Pribilof Canyon and in a small area in the southeastern arms of Pribilof Canyon and

719    Zhemchug Canyon (Figure 28). The upper quartiles of sponge height occurred predominantly in

720    deeper waters from Bering Canyon through Pribilof Canyon and to the northwest of Pribilof

721    Canyon and then in Zhemchug Canyon and to the north (Figure 28). Sea whip heights were

722    predicted to be highest on the inner portion of the outer shelf to the north and east of Zhemchug

723    canyon; however these areas were not sampled using the camera so are likely spurious. The more

724    likely areas for tall sea whips are in a band along the outer shelf between Pribilof Canyon and

725    Zhemchug Canyon (Figure 28).

726        The combined density-height quartiles indicated only very small areas where high density

727    and greater heights both occurred for corals, such as in the two arms of Pribilof Canyon and in

728    deeper waters scattered along the slope (Figure 29). There was also a patch in the southern

729    portion of Zhemchug Canyon. The intersection of the upper quartiles of height and density for

730    sponge occurred for the northern section of Pribilof Canyon and to the northwest along the slope

731    and sections of Zhemchug Canyon. Taller and more dense sea whips were found mostly at the

732    shelf break in a fairly narrow band (Figure 29) and in unsampled sections of the outer shelf

733    where the potential for spurious results mean these should be viewed with caution. .

734

735    **4. Discussion**

736

737        The 2014 camera survey indicated that coral is mostly limited to Pribilof Canyon and

738    northwest of Pribilof Canyon, whereas sponge and sea whips are more widespread. The depth

739    distributions of the different types of coral overlapped to a large degree, but all were located

740    below 200 m in depth. *Plumarella* sp. and *Swiftia* sp. were the most commonly observed corals,

741    and they generally occurred in highest densities at depths between 200 and 525 m (8 of the top

742    10 highest coral densities) and in Pribilof Canyon (8 of the top 10 coral densities). *Isididae*

743    species were somewhat deeper, with all but a single occurrence below 435 m and less than half

744    (3 of 7) of the transects with *Isididae* sp. were found in Pribilof Canyon. Because of the relative

745    size differences among these groups (with Isididae being the tallest corals observed), the tallest

746    corals tended to be observed in deep water on the slope between Pribilof and Zhemchug canyons.

747        This area was also where the largest sponges were observed, with some of the largest

748    hexactinellid species observed in the deeper waters. However, the most dense aggregations of

749    sponge tended to occur in shallower waters on the outer shelf and shelf break. These shallow

750    sponges were a mixture of predominantly demosponges with some hexactinellids and calcareous

751    sponges mixed in at lower densities.

752    The most dense areas of sea whips occurred in both shallow areas (at the shelf break) and

753    on a couple of deep transects. These two distributions probably represented two different species

754    of sea whips (*Halipteris willoemesi* and *Halipteris* sp.; Robert Stone, AFSC-ABL, personal

755    communication), especially as the shallow species tended to be much larger than the deeper

756    group.  The size distribution of sea whips within a transect was sometimes variable  and

757    sometimes uniform, i.e., the sizes could be a mixture of very small and very large individuals in

758    some places or either uniformly tall or uniformly short in others, with no obvious cause for these

759    differences.

760

761    **4.1 Validation of presence/absence models based on bottom trawl data**

762

763    The results of the camera survey supported the presence-absence coral model that was

764    developed from bottom trawl survey data. Both the model diagnostics and the observed coral

765    presence overlaid on maps of predictions of probability of coral presence indicated that the

766    bottom trawl survey model was accurate in predicting coral distribution. The bottom trawl survey

767    model for sponge did less well at predicting the camera observations for sponge, although the

768    results were still better than chance. The bottom trawl survey model for sea whips also predicted

769    the sea whip data from the camera observations fairly well. The most likely reason for the

770    different accuracy in model predictions from the three invertebrate groupings was that the

771    allocation of stations was designed to test the predictions of coral presence or absence based on

772    the bottom trawl survey model. Since the bottom trawl survey model predicted a higher

773    probability of coral in and around Pribilof Canyon, more stations were allocated to these areas.

774    If, for example, we had allocated stations to validate the bottom trawl survey sponge model, the

775    distribution of stations would have been different, probably with more stations on the outer shelf

776    around Pribilof Canyon and fewer stations within Pribilof Canyon. This may have resulted in the

777    data better resolving the full distribution of sponge on the outer shelf. However, allocating

778    stations in this way would have resulted in a correspondingly worse dataset for evaluating the

779    coral model since Pribilof Canyon would have received fewer stations. Model estimates likely

780    were degraded by the sometimes poor bathymetry near the shelf break, which was observed

781    during the camera survey.

782        Independent surveys to validate distribution models are rarely undertaken. In most cases,

783    model validation is performed by re-substitution (Kumar and Stohlgren 2009, Krigsman et al.

784    2012) or splitting the data set at random into training and testing data sets (Bryan and Metaxis

785    2007, Franklin et al. 2013, Sagarese et al. 2014). Using newly collected data that is independent

786    of the original data set is less common, but usually utilizes data collected in additional years or

787    additional areas (Eskildsen et al. 2013, Rooper et al. 2014). Using an independent data set

788    collected with an entirely different survey design and data collection method is very rare, but it

789    can provide the most insight into model performance (Elith et al. 2006).

790        The type of validation technique utilized can influence the perception of the model's

791    predictive ability. In general, the more independent the cross-validation, the higher the chances

792    that the cross-validation can indicate problems in the original model. Because the GAM

793    methodology used here can represent very complex relationships between organisms and their

794    environment, the GAMs are prone to over-fitting the data. We limited the number of inflection

795    points ("knots") in the functional relationships in the GAMs, but this alone cannot entirely

796    prevent model overfitting. The support of the independent camera survey observations for the

797     bottom trawl survey coral model provides confidence in the model predictions and an additional

798     measure of the uncertainty around those predictions (Guisan et al. 2013).

799

800     **4.2 Model improvements and model averaging**

801

802         The coral model that blended both the bottom trawl survey model and the camera survey

803     model best matched both data sets. Each individual data set best fit to its individual model, as

804     expected. For example, the AUC for the bottom trawl model predicting bottom trawl catches of

805     coral was 0.92 and the AUC for the camera model predicting the camera data was 0.95, whereas

806     the cross-predictions yielded AUCs of 0.73 in both cases (bottom trawl model predicted camera

807     observations and vice versa). The combined model fit resulted in AUCs of 0.85 and 0.90 for the

808     bottom trawl data, and camera data respectively, which is better than the cross-predictions for the

809     individual models. For coral, the combined model best matched both data sets, with a little better

810     fit to the camera data than the bottom trawl data. The favorable matching of both data sets likely

811     occurred because both individual coral models (bottom trawl and underwater camera) showed

812     almost exactly the same spatial pattern of coral distribution.

813         This is in contrast to the sponge model, where the two independent models and data

814     sources did not agree very well (e.g., the bottom trawl model for sponge was negatively

815     correlated with the camera data observations). In this case, the combined model fit both the

816     camera and trawl survey observations reasonably well (AUCs of 0.76 and 0.71), but not as well

817     as for the coral model. This lack of coherence for the sponge models may have been due to the

818     fact that the camera observations did not cover shallow areas of the outer shelf where there was

819     trawl survey data. This implies that the sponge model is inadequate for extrapolating outside the

820     camera survey area. Much of the disagreement between the camera and bottom trawl models was

821     on the northeast outer shelf where the camera model predicted a high probability of sponge

822     occurrence. Because the probability of sponge presence increased with latitude (Figure 10) and

823     camera sampling in the high latitude shallow areas was lacking, these predictions represent

824     extrapolation outside the camera survey area and thus are probably inaccurate. The same

825     phenomenon was also apparent with the sea whip predictions in the same area (northeastern

826     outer shelf). These predictions should be viewed with caution.

827         Catchability for sponges may be higher in the bottom trawl survey compared to the

828     camera survey. Only sponges that exceeded 10 cm height were counted in the image analysis,

829     since smaller specimens could not be identified from other other white- or yellow-colored items

830     on the seafloor., However, some fraction of these smaller sponges are caught by the trawl survey,

831     thus contributing to the mismatch between the bottom trawl and camera based models. The

832     opposite effect likely occurs for sea whips. All sea whips were easily observed and counted in

833     the camera survey, but their trawl catchability likely is lower because of their flexibility and low

834     profile, thus contributing to the mismatch between the camera and bottom trawl sea whip

835     models.

836

837     **4.3 Density and height distribution of structure-forming invertebrates**

838

839         The densities of corals and sponges observed on the eastern Bering Sea slope and outer

840     shelf in this study were low (mean = 0.005 individuals*m$^{-2}$, SE = 0.002) compared with other

841     areas of Alaska where similar studies have been conducted. In 2012 a randomized stereo camera

842     survey was conducted in the eastern and central Aleutian Islands (n = 93 transects) and Bowers

843    Bank (n = 19 transects) using the same methodology and covering a similar depth range (C.

844    Rooper, AFSC-RACE Division, unpublished data) as the eastern Bering Sea study. The Aleutian

845    Islands study found that coral densities (predominantly gorgonian species) averaged 0.11

846    individuals*m$^{-2}$ (SE = 0.03) and ranged as high as 1.3 individuals *m$^{-2}$ (Figure 30). On Bowers

847    Bank, coral densities ranged as high as 1.67 individuals*m$^{-2}$ and averaged 0.21 individuals*m$^{-2}$

848    (SE = 0.11), although the Bowers Bank corals were predominantly small hydrocorals

849    (Stylasteridae) from two very dense transects. Hydrocorals were not observed in the Bering Sea.

850    A randomized survey conducted in 2010 at two areas closed to fishing (to protect coral) in the

851    Gulf of Alaska estimated average density of corals at 0.10 individuals*m$^{-2}$ (SE = 0.04) and a

852    maximum density of 1.2 individuals*m$^{-2}$ (C. Rooper, AFSC-RACE Division, unpublished data).

853    The survey design differed somewhat  from the eastern Bering Sea and Aleutian Islands surveys

854    in that the transects were shorter and the depths examined ranged only from 78-359 m.

855    Additionally, this study was conducted in an area that had been closed to protect presumed coral

856    habitat, so the densities probably do not reflect the overall Gulf of Alaska average.

857        Other published density estimates for coral are available for Pribilof and Zhemchug

858    canyons from a study conducted in 2007. The densities of gorgonian corals found in Pribilof

859    Canyon was 0.73 individuals*m$^{-2}$ (SE = 0.4) and Zhemchug Canyon densities were 0.13

860    individuals*m$^{-2}$ (SE = 0.1), while maximum densities were 2.41 individuals*m$^{-2}$ (Miller et al.

861    2012). These density estimates are higher than the densities we found, likely due to differences

862    in sampling design. In the Miller et al. (2012) study, the transects were placed systematically

863    rather than randomly as in our study, and their sample size was low (16 transects). Transects

864    sometimes were clustered so that fewer distinct geographic locations were sampled; 5 distinct

865    geographic locations were sampled within or near Zhemchug Canyon and 4 distinct geographic

866    locations were sampled within or near Pribilof Canyon (Miller et al., 2012). In contrast, we

867    sampled 25 locations within Zhemchug Canyon and 36 locations within Pribilof Canyon. In

868    addition, the Miller et al. (2012) densities were calculated treating each frame as an independent

869    sample rather than each transect (adjacent frames are correlated). In other areas of Alaska, a

870    study in the central Aleutian Islands yielded an average coral density of 1.23 individuals$*$m$^{-2}$ and

871    a maximum density of 3.85 individuals$*$m$^{-2}$ (Stone 2006). For the Gulf of Alaska, a study of

872    Primnoa thickets yielded densities of red tree coral of 0.52 individuals$*$m$^{-2}$ (Stone 2014).

873    Coral densities differ among the three regions of Alaska because of differences in the

874    amount of appropriate substrates available for colonization. In the studies above that performed

875    random camera surveys in the Aleutian Islands, Bowers Bank, and Gulf of Alaska (C. Rooper,

876    AFSC-RACE Division, unpublished data), the percentage of transects with rocky habitat

877    somewhere present on the transect was 63%, 42% and 58%, respectively, compared to 18% for

878    the current study. A linear relationship of the percentage of transects with some rocky habitats

879    and the overall density of coral in the four regions (0.106, 0.015, 0.100 and 0.005 individuals$*$m$^{-}$

880    $^2$) explains most (~82%) of the variability in average density among the areas. In addition, the

881    percentage of individual frames that were dominated by rocky substrates was 23% in the

882    Aleutian Islands, 8% at Bowers Bank and only 0.8% in the eastern Bering Sea. These substrate

883    differences also heavily influenced the overall distribution of corals as well. Since corals require

884    hard substrate for attachment, most were found in areas with more exposed substrate, such as the

885    areas in Pribilof Canyon and to the northwest along the slope. These tended to be the only areas

886    where rocky substrate occurred deep enough to support coral attachment. One shallow rocky

887    outcrop was sampled in the middle of the outer shelf. Although this area supported the densest

888    observed aggregation of sponges, coral was absent. According to the coral model, this location

889    was too shallow but otherwise was suitable coral habitat.

890         Sponge densities were highly variable in the eastern Bering Sea, ranging from 0 to 13

891    individuals*m$^{-2}$, averaging 0.11 individuals*m$^{-2}$. In the Aleutian Islands camera survey, sponge

892    densities averaged 0.50 individuals*m$^{-2}$ (SE = 0.18). In the Bowers Bank area, the density of

893    sponge was 0.22 individuals*m$^{-2}$ (SE = 0.09) and in the Gulf of Alaska closed areas, sponge

894    density averaged 0.07 individuals*m$^{-2}$ (SE = 0.02). Bowers Bank and the Aleutian Islands both

895    had substantially higher densities of sponge than the eastern Bering Sea, while the densities in

896    the Gulf of Alaska closed areas were slightly lower. Another study  in Alaska conducted by

897    Stone et al. (2014) found densities of 2.51individuals*m$^{-2}$ . The study of Pribilof and Zhemchug

898    canyons by Miller et al. (2012) reported densities of hexactinellid sponges of 0.40 and 0.02,

899    respectively, and for other sponges (likely demosponges) 0.24 and 0.001 individuals*m$^{-2}$. The

900    overall density of sponges, as well as the individual groups reported by Miller et al. (2012) was

901    higher than we found, although as mentioned previously, this is probably a factor of sampling

902    design differences.

903         Sea whip densities were higher on average in the eastern Bering Sea than in the Aleutian

904    Islands, Gulf of Alaska, or Bowers Bank. In the eastern Bering Sea, sea whip densities were

905    more than twice as high (0.11 individuals*m$^{-2}$) than in the Aleutian Islands (0.04 individuals*m$^{-2}$

906    ) and were orders of magnitude higher than at Bowers Bank (0.004 individuals*m$^{-2}$). No sea

907    whips were observed in the closed areas in the Gulf of Alaska. The differences between the

908    regions are probably also related to the amount of sandy habitat available near the shelf break.

909    Overall sea whip densities reported in Miller et al. (2012) were generally higher than we found in

910    Pribilof Canyon (0.24 individuals*m$^{-2}$), and lower in Zhemchug Canyon (0.05 individuals*m$^{-2}$).

911    Brodeur (2001) reported densities in a grove of sea whips near Pribilof Canyon of 0.25

912    individuals*m$^{-2}$. In other studies in Alaska, especially in the Gulf of Alaska some areas of dense

913    sea whips have also been observed, such as the sea whip grove in southeastern Alaska studied by

914    Malecha and Stone (2009), which had densities of ~0.5 individuals*m$^{-2}$, and the maximum

915    densities of *Protoptilum* sp. and *H. willemoesi* near Kodiak found by Stone et al. (2005) of 16

916    and 6 individuals*m$^{-2}$.

917        Coral heights averaged 20 cm or less for most taxonomic groups. The exception was the

918    bamboo corals, Isididae. These corals occurred in deeper water on the slope to the north of

919    Pribilof Canyon. Primnoa corals, such as the red tree corals (*Primnoa resedaeformis*) can grow

920    to very large sizes, exceeding 1 m tall in areas of southeast Alaska (Andrews et al. 2002). In the

921    Aleutian Islands survey mentioned above, the average gorgonian coral size was 33 cm (SE =

922    0.45). The species composition was much richer in the Aleutian Islands than was found for the

923    eastern Bering Sea, but when only the common groups were compared,  *Plumarella* sp. (mean =

924    0.36, SE = 0.92), *Swiftia* sp. (mean = 26, SE = 2.07) and Plexauridae (mean = 25.6, SE = 1.43)

925    were all about twice as tall in the Aleutian Islands as in the eastern Bering Sea. The only

926    exception was for Isididae, which were about 48 cm tall (SE = 5.1) in the eastern Bering Sea on

927    average and were about 44 cm tall in the Aleutian Islands (SE = 9.8).  Growth rates for Isididae

928    indicate that large specimens of these species (>70 cm) are likely in excess of 50 years old

929    (Andrews et al. 2009). A single specimen from the Gulf of Alaska with a height of 120 cm

930    (similar to the maximum height found during this study) was estimated to be 116 years of age.

931    There have been no aging studies for the other species of corals observed during this study, but

932    the large red tree corals (~2 m)  found in southeastern Alaska have been aged to be over 100

933    years old (Andrews et al. 2002).

934        In the eastern Bering Sea, sponge height differed by group, as the hexactinellid sponges

935    tended to be taller than the demosponges. In the Aleutian Islands, demosponges were on average

936    about 10 cm taller than in the eastern Bering Sea. However in the Aleutian Islands, demosponges

937    < 20 cm were not measured (as opposed to the Bering Sea where sponges < 10 cm were not

938    measured). This implies that sponge sizes between the two regions were roughly the same. This

939    is supported by the average height for hexactinellid sponges, which averaged 24 cm (SE = 1.59)

940    in the Aleutian Islands and 25 cm (SE = 0.78) in the eastern Bering Sea.

941        Sea whips were also found to be very similar in size between the Aleutian Islands and the

942    eastern Bering Sea. In the Aleutian Islands survey, sea whip heights averaged 68 cm, although

943    they were also highly variable (SE = 21.69) as very few were measured. In the eastern Bering

944    Sea, the average sea whip height was 62 cm (SE = 0.92).  In an ageing study of sea whips,

945    Wilson et al. (2002) estimated a linear growth rate of 7.42 cm*yr$^{-1}$ for the interval between small

946    (~27 cm) and medium (~100 cm) sea whips. Based on these growth rates, the average sea whip

947    from the eastern Bering Sea or Aleutian Islands (62-68 cm tall) would be between ~ 12-14 years

948    of age.

949

950    **4.4 Fish and structure-forming invertebrate associations**

951

952        Fish associations were similar to findings from other studies in Alaska. Rockfish species

953    tended to be associated with corals and sponges, in particular, Pacific ocean perch, shortraker

954    rockfish and rougheye-blackspotted rockfishes. Similar associations were found by Miller et al.

955    (2012) in their study of Pribilof and Zhemchug canyons. Similar patterns were found in analyses

956    of trawl survey catches (Malecha et al. 2005, Heifetz 2002, Rooper and Boldt 2005, Laman et al.

957    2015). Pacific ocean perch were strongly associated with sea whip forests near Pribilof Canyon

958    during the night-time when these fish were resting (Brodeur 2001) and a similar relationship

959    between sponge and northern rockfish was observed near Zhemchug Canyon (Rooper et al.

960    2010). We did not perform nighttime camera survey operations, so our data would not have

961    detected these types of associations. The association of king crabs with corals and sponges has

962    also been observed in previous studies. Most of the king crabs that we observed during the

963    camera survey were juvenile king crabs. In previous laboratory and field studies, juvenile king

964    crab were found to seek out complex structure (Sundberg and Clausen 1977, Loher and

965    Armstrong 2000, Stoner 2009, Pirtle and Stoner 2010). Two taxonomic groups that have

966    negative associations with coral and sponge were *Chionoecetes* crabs and grenadiers, which

967    likely reflects differences in habitat preferences.

968

969    **4.5 Observations of fishing gear and damage to structure-forming invertebrates**

970

971    Quantifying anthropogenic damage to deepwater benthic organisms, such as sponge and

972    coral, is challenging. Many species have irregular and sometimes amorphous body shapes that

973    make simple identifications difficult. In fact, determining sponge species often requires

974    examining spicules under magnification because the same species may exist in various shapes

975    and sizes. These growth form variations make distinguishing damage problematic because

976    damage may not be obvious within the spectrum of body shapes for some species. Additionally,

977    the variability of response to damage of the individual taxa may bias observations because it may

978    be easier to identify damage among some species. For instance, sea whips and bamboo corals

979    have bright white internal skeletons that, when exposed (i.e., denuded of their overlying soft

980    tissues) are very conspicuous especially when lying on the seafloor. Depending on sedimentation

981    rates, the skeletons of these species may remain conspicuous for long periods of time since they

982    are made of durable materials. Conversely, other species such as *Fanellia* sp. and *Calcigorgia* sp.

983    have dark internal skeletons that are less conspicuous when exposed and damage is more

984    difficult to detect among these species whether they are upright or prone.

985         Direct evidence of fishing (mostly trawl tracks, but also some lost trawl net, crab pot and

986    longline gear) occurred at 32 (12.8%) transects. The proportion of observed damage for coral

987    (2.9%) and sponge (0.3%) was low. About 9% of individual sea whips observed were classified

988    as either being somehow damaged, dead, or lying horizontal on the seafloor. In most cases, it

989    was difficult to determine if the damage was human-induced (e.g., fishing or other activity) or

990    natural (e.g., brittle star or nudibranch predation, ocean currents).  Few transects showed both

991    clear evidence of fishing activity (e.g., trawl tracks or fishing gear) and damaged coral, sponges,

992    or sea whips. This occurred in just 3.2% of our transects (8 of 250). We observed effects of

993    fishing slightly less frequently than a previous study of Pribilof and Zhemchug canyons, which

994    observed effects on 3 of 16 transects (Miller et al. 2012); this difference may simply be due to

995    chance and their much smaller sample size. This difference also may be due to sampled depths;

996    ours covered a wider depth range and differences in fishing effort with depth is a confounding

997    factor in comparing the two studies.

998         *Halipteris* sp. were the most common taxa observed and the largest taxa observed, as well

999    as the most common taxa damaged. *Halipteris* sp. differ from the remaining coral taxa and the

1000   sponge taxa by largely occurring on the continental shelf, where softer sediments occur, and not

1001   on the continental slope. Damaged *Halipteris* sp. occurred on 24% of transects, but a relatively

1002   low proportion of damaged individuals (9%) was observed. *Halipteris* sp. were concentrated at

1003    depths 100-150 m, as was evidence of damaged *Halipteris* sp. (Figure 5). Damaged *Halipteris*

1004    sp. on an individual basis were more frequent at depths 100-150 m (12.9%) than for all depths

1005    (9%). Effects of fishing on *Halipteris* sp. also were observed in previous studies at Pribilof

1006    Canyon (Brodeur et al. 2001, Miller et al. 2012), but the proportions affected were not stated.

1007    Two sponge taxa occurred over the same depth ranges (Figure 9) yet only one taxa was identified

1008    as damaged (demosponge, 6.6% of transects) and the other taxa was not (Hexactinellid, 0% of

1009    transects). Both taxa were found over a wide depth range (110-770 m) and frequently co-

1010    occurred (19.6% of transects). The lack of identified co-occurrent damage of Hexactinellid and

1011    demosponge may simply be due to chance; damaged demosponge was infrequent (only 7 of 250

1012    transects) and Hexactinellid only co-occurred on three of these transects.

1013

1014    **4.6 Vulnerability of structure-forming invertebrates**

1015

1016    Vulnerability of invertebrates to fishing impacts is a function of several processes. Data

1017    was collected during this research that addresses two aspects of vulnerability, density, and

1018    height. We provided an example based on the modeled distribution of height and density of areas

1019    where each taxa may be most vulnerable. However, the thresholds in terms of density and height

1020    that we set (the upper quartiles) may not be equally appropriate for all groups. The sensitivity

1021    and vulnerability of deepwater coral and sponge varies greatly between taxa. For this reason, an

1022    equal level of disturbance may present a wide range of observed damage responses. Factors that

1023    influence vulnerability include flexibility and height above the seafloor. Flexible species are less

1024    vulnerable than rigid ones, as they are able to bend and rebound from impact. Likewise, low

1025    lying and encrusting species are less vulnerable than upright species that extend into the water

1026    column since their exposure to passing fishing gear is reduced. Some species, such as *Farrea*

1027    *occa*, are fragile and may break apart with light disturbance. Evidence of damage to a species

1028    such as this may be ephemeral, as fragments of the damaged individuals are quickly dispersed.

1029    Lacking lasting evidence, their damage rate appears low.

1030

1031    **5. Conclusions**

1032

1033        We attempted to address six objectives during the 2014 eastern Bering Sea slope and

1034    outer shelf survey. Based on the data collected on the survey we conclude that:

1035    ● The model of coral presence or absence based on bottom trawl survey data only was

1036        generally accurate in predicting presence or absence in the camera survey. The bottom

1037        trawl survey models were also accurate in predicting sponge and sea whip presence or

1038        absence, but to a lesser degree than for coral.

1039    ● The combined distribution models based on the bottom trawl survey models and models

1040        derived from the camera survey data also performed well. These combined models

1041        predicted the distribution of corals, sponges, and sea whips with better accuracy than the

1042        individual models did during cross-validation. For example, the combined sponge model

1043        performed better at predicting the camera observations of sponge than the bottom trawl

1044        survey sponge model data did at predicting the camera survey observations.

1045    ● Densities and heights of corals were generally highest in Pribilof Canyon and to the

1046        northwest of Pribilof Canyon along the slope. For sponges, densities and heights were

1047        highest surrounding Pribilof Canyon, north of Bering Canyon and in some locations in

1048        Zhemchug Canyon. Sea whip densities and heights were highest on the outer shelf

1049        between Pribilof and Zhemchug Canyon and in an area to the south of Pribilof Canyon.

1050    ●   There were significant positive relationships between fish density and the presence of

1051        coral and sponge for some rockfish species and king crabs. There were significant

1052        negative relationships for grenadiers and *Chionoecetes* crabs.

1053    ●   Evidence of fishing gear or damage to benthic invertebrates occurred at 37% of transects.

1054        Individual demosponges (0.3%), Isididae corals (2.9%) and sea whips (9.0%) were

1055        observed to be damaged.

1056    ●   Two pieces of data important for estimating vulnerability of benthic invertebrates

1057        (density and height) were estimated from the field research and modeled for the entire

1058        eastern Bering Sea outer shelf and slope.

1059    ●   Combining the bottom trawl survey models and models based on the camera survey

1060        showed improvement over bottom trawl survey-based models alone.

1061

1062   **6. Acknowledgements**

1063

1071 updated bathymetry layers for the eastern Bering Sea slope and outer shelf and Al Hermann

1072 provided ROMS model outputs for current speed and direction.

1073

1074 **7. Literature cited**

1075 Andrews, A.H., Cordes, E.E., Mahoney, M.M., Munk, K., Coale, K.H., Cailliet, G.M., Heifetz,

1076 J., 2002. Age, growth and radiometric age validation of a deep-sea, habitat-forming

1077 gorgonian (*Primnoa resedaeformis*) from the Gulf of Alaska. Hydrobiologia 471:101-

1078 110.

1079 Andrews, A.H., Stone, R.P., Lundstrom, C.C., DeVogelaere, A.P., 2009. Growth rate and age

1080 determination of bamboo corals from the northeastern Pacific Ocean using refined $^{210}$Pb

1081 dating. Mar. Ecol. Prog. Ser. 397:173–185.

1082 Brodeur, R.D., 2001. Habitat-specific distribution of Pacific ocean perch (*Sebastes alutus*) in

1083 Pribilof Canyon, Bering Sea. Cont. Shelf Res. 21:207-224.

1084 Bryan T.L, Metaxas A. 2007. Predicting suitable habitat for deep-water gorgonian corals on the

1085 Atlantic and Pacific Continental margins of North America. Mar. Ecol. Prog. Ser.

1086 330:113-126.

1087 Coachman, L.K., 1986. Circulation, water masses and fluxes on the southeastern Bering Sea

1088 shelf. Cont. Shelf Res. 5:23-108.

1089 Cragg, J.G. 1971. Some statistical models for limited dependent variables with application to the

1090 demand for durable goods. Econometrica 39:829-844.

1091 Elith, J., Graham, C. H., Anderson, R. P., Dudı´k, M., Ferrier, S., Guisan, A., Hijmans, R. J.,

1092 Huettmann, F., Leathwick, J. R., Lehmann, A., Li, J., Lohmann, L. G., Loiselle, B. A.,

1093 Manion, G.,Moritz, C., Nakamura, M., Nakazawa, Y., Overton, J. McC., Peterson, A. T.,

1094    Phillips, S. J.,Richardson, K. S., Scachetti-Pereira, R., Schapire, R. E., Sobero´n, J.,

1095    Williams, S., Wisz, M. S., Zimmermann, N. E. 2006. Novel methods improve prediction

1096    of species' distributions from occurrence data. Ecography 29:129-151.

1097    Eskildsen, A., le Roux, P.C., , Heikkinen, R.K., Høye, T.T., Kissling, W.D., Pöyry, J., Wisz,

1098    M.S.,  Luoto, M. 2013. Testing species distribution models across space and time: high

1099    latitude butterflies and recent warming. Global Ecol. Biogeogr 22:1293-1303.

1100    Franklin E.C., Jokiel P.L., Donahu M.J.. 2013. Predictive modeling of coral distribution and

1101    abundance in the Hawaiian Islands. Mar. Ecol. Prog. Ser. 481:121-132.

1102    Guisan A., Tingley R., Baumgartner J.B., Naujokaitis-Lewis I., Sutcliffe P.R., et al. 2013.

1103    Predicting species distributions for conservation decisions. Ecol. Lett. 16:1424–1435.

1104    Heifetz, J. 2002. Coral in Alaska: distribution, abundance, and species associations.

1105    Hydrobiol. 471:19-28.

1106    Hoff, G.R.  in review. Biodiversity along the Eastern Bering Sea Slope from Trawl Survey Data.

1107    Submitted to Marine Biodiversity

1108    Hosmer, D.W., Lemeshow, S., 2005. Multiple logistic regression. Applied logistic regression,

1109    Second Edition, John Wiley & Sons, Hoboken NJ.

1110    Karl, H.A., Carlson, P.R., Gardner, J.V., 1996. Aleutian Basin of the Bering Sea: Styles of

1111    sedimentation and canyon development. In Gardner JF, Field ME, Twichell DC. Geology

1112    of the United States seafloor: the view from GLORIA. Press Syndicate of the University

1113    of Chicago, Chicago IL.

1114    Krigsman, L.M., Yoklavich, M.M., Dick, E.J., Cochrane, G.R. 2012. Models and maps:

1115    predicting the distribution of corals and other macro-invertebrates in shelf habitats.

1116    Ecosphere 3:1-16.

1117    Kumar, S., Stohlgren, T. J. 2009. Maxent modeling for predicting suitable habitat for threatened

1118         and endangered tree *Canacomyrica monticola* in New Caledonia. J. Ecol. Nat. Environ.

1119         1:94-98.

1120    Laman, N., Kotwicki, S., Rooper, C.N.. 2015. Sponge and coral morphology influences the

1121         distribution of Pacific ocean perch life stages. Fish Bull. 113:270-289.

1122    Loher, T., Armstrong, D.A. 2000. Effects of habitat complexity and relative larval supply on the

1123         establishment of early benthic phase red king crab (*Paralithodes camtschaticus* Tilesius

1124         1815) populations in Auke Bay, Alaska. J. Exp. Mar. Biol. Ecol. 245:83–109.

1125    Malecha, P.W., Stone, R.P., Heifetz, J., 2005. Living substrate in Alaska: Distribution,

1126         abundance, and species associations. Am. Fish. Soc. Symp. 41, Bethesda, Maryland.

1127    Malecha, P.W., Stone, R.P.. 2009. Response of the sea whip *Halipteris willemoesi* to simulated

1128         trawl disturbance and its vulnerability to subsequent predation. Mar. Ecol. Prog. Ser.

1129         388:197-206.

1130    Miller, R.J., Hocevar, J., Stone, R.P., Fedorov, D.V., 2012. Structure-forming corals and sponges

1131         and their use as fish habitat in Bering Sea submarine canyons. PLoS ONE 7(3),

1132         e33885.doi:10.1371/journal.pone.0033885.

1133    Pirtle, J.L., Eckert, G.L., Stoner, A.W. 2010. Red king crab (*Paralithodes camtschaticus*) early

1134         post-settlement habitat choice: Structure, food, and ontogeny. J. Exp. Mar. Biol. Ecol.

1135         393:130-137.

1136    Potts J., Elith, J. 2006. Comparing species abundance models. Ecol. Model. 199: 153-163.

1137    R Core Development Team, 2013. R: A language and environment for statistical computing. R

1138         Foundation for Statistical Computing, Vienna, Austria. ISBN 3-900051-07-0, URL

1139         http://www.R-project.org/.

1140    Rooper, C.N., Boldt, J.L., 2005. Distribution of juvenile Pacific ocean perch *Sebastes*

1141        *alutus* in the Aleutian Islands in relation to benthic habitat. Alaska Fish.

1142        Res. Bull., 11:102-112.

1143    Rooper, C.N., Hoff, G.R., De Robertis A., 2010. Assessing habitat utilization and rockfish

1144        (*Sebastes* sp.) biomass in an isolated rocky ridge using acoustics and stereo image

1145        analysis. Can. J. Fish. Aquat. Sci. 67:1658-1670.

1146    Rooper, C.N., M. Zimmermann, M. Prescott, A. Hermann. 2014. Predictive models of coral and

1147        sponge distribution, abundance and diversity in bottom trawl surveys of the

1148        Aleutian Islands, Alaska. Mar. Ecol. Prog. Ser. 503: 157-176.

1149    Sagarese, S.R., Frisk, M.G., Cerrato, R.M., Sosebee, K.A., Musick, J.A., Rago, P.J. 2014.

1150        Application of generalized additive models to examine ontogenetic and seasonal

1151        distributions of spiny dogfish (*Squalus acanthias*) in the Northeast (US) shelf large

1152        marine ecosystem. Can. J. Fish. Aquat. Sci. 71:847-877.

1153    Sigler, M.F., Rooper, C.N., Hoff, G.R., Stone, R.P., McConnaughey, R.A., Wilderbuer, T.K..

1154        2013. Are Bering Sea canyons unique habitats within the eastern Bering Sea? Report to

1155        North Pacific Fishery Management Council. Available at http://www.npfmc.org/wp-

1156        content/PDFdocuments/conservation_issues/BSHC/BeringSeaCanyons_a_513.pdf

1157    Sigler, M.F., Rooper, C.N., Hoff, G.R., Stone, R.P., McConnaughey, R.A., Wilderbuer, T.K.

1158        2015. Faunal features of submarine canyons on the eastern Bering Sea slope. Mar. Ecol.

1159        Prog. Ser. 526:21-40.

1160    Springer, A.M., McRoy, C.P., Flint, M.V. 1996. The Bering Sea Green Belt: shelf-edge

1161        processes and ecosystem production. Fish. Oceanogr., 5:205–223.

1162    Stein, D.L.,Tissot, B.N., Hixon, M.A., Barss, W. 1992.  Fish-habitat associations on a deep reef

1163         at the edge of the Oregon continental shelf.  Fish. Bull. 90:540-551.

1164    Stone, R. P., H. Lehnert, and H. Reiswig. 2011. A guide to the deepwater sponges of the

1165         Aleutian Island Archipelago. U.S. Dep. Commer., NOAA Prof. Paper, NMFS 12,

1166    Stone, R.P. 2006. Coral habitat in the Aleutian Islands of Alaska: depth distribution, fine-scale

1167         species associations, and fisheries interactions. Coral Reefs 25:229-238.

1168    Stone, R.P. 2014. The ecology of deep-sea coral and sponge habitats of the central Aleutian

1169         Islands of Alaska. U.S. Dep. Commer., NOAA Prof. Paper NMFS 16, 52 p.

1170    Stone, R.P., M. M. Masuda, and P. W. Malecha. 2005. Effects of bottom trawling on soft-

1171         sediment epibenthic communities in the Gulf of Alaska. p. 461-475. In P.W. Barnes and

1172         J.P. Thomas (editors), Benthic Habitats and the Effects of Fishing. Am. Fish. Soc. Symp.

1173         41, Bethesda, Maryland.

1174    Stone, R.P., Masuda, M.M., Karinen, J.F. 2015. Assessing the ecological importance of red tree

1175         coral thickets in the eastern Gulf of Alaska. ICES J. Mar. Sci. 72:900-915.

1176    Stoner, A.W., 2009. Habitat-mediated survival of newly settled red king crab in the presence of a

1177         predatory fish: role of habitat complexity and heterogeneity. J. Exp. Mar. Biol. Ecol. 382,

1178         54–60.

1179    Sundberg, K.A., Clausen, D. 1977. Post-larval king crab (*Paralithodes camtschatica*)

1180         distribution and abundance in Kachemak Bay Lower Cook Inlet, Alaska. In: Trasky, L.L.,

1181         Flagg, L.B., Burbank, D.C. (Eds.), Environmental Studies of Kachemak Bay and Lower

1182         Cook Inlet, Vol. 5. Alaska Department of Fish and Game, Anchorage, pp. 1–36.

1183   Williams, K., Rooper, C.N., Towler, R. 2010. Use of stereo camera systems for assessment of

1184       rockfish abundance in untrawlable areas and for recording pollock behavior during

1185       midwater trawls. Fish. Bull. 108:352-362.

1186   Wilson, M.T., Andrews, A.H., Brown, A.L., Cordes E.E. 2002. Axial rod growth and age

1187       estimation of the sea pen, *Halipteris willemoesi* Kölliker. Hydrobiol. 471:133-142.

1188   Wood, S.N., 2006. Generalized additive models: an introduction with R. Chapman & Hall, Boca

1189       Raton FL.

1190   Yoklavich, M.M., Greene, H G., Cailliet, G.M.,Sullivan, D.E., Lea, R.N., Love, M.S. 2000.

1191       Habitat associations of deep-water rockfishes in a submarine canyon: an example of a

1192       natural refuge. Fish. Bull., U.S. 98:625-641.

**8. Tables**

Table 1. Summary of stations occupied in each area of the eastern Bering Sea slope and outer slope. The total number of station with each taxonomic group of structure-forming invertebrates is also given for each area.

| Area | Stations sampled | Stations with coral present | Stations with sponge present | Stations with sea whips present |
|---|---|---|---|---|
| Bering Canyon | 10 | 0 | 5 | 3 |
| Bering -Pribilof Canyon | 17 | 0 | 4 | 9 |
| Pribilof Canyon | 36 | 18 | 24 | 9 |
| Pribilof -Zhemchug Canyon | 68 | 12 | 29 | 31 |
| Zhemchug Canyon | 25 | 1 | 12 | 11 |
| Zhemchug -Pervenets Canyon | 15 | 0 | 11 | 7 |
| Pervenets Canyon | 12 | 0 | 2 | 4 |
| Outer Shelf | 67 | 1 | 26 | 31 |

Table 2. Summary of fishes observed during the eastern Bering Sea slope and outer shelf camera

survey.

| Species or group | Number observed |
| --- | --- |
| Eelpout (*Bothracara* sp., *Lycodes* sp., unid.) | 2155 |
| *Chionocetes* sp. | 2068 |
| Popeye grenadier (*Coryphaenoides cinereus*) | 1481 |
| Pacific ocean perch (*Sebastes alutus*) | 1225 |
| Sculpin unid. (Cottidae) | 924 |
| Golden king crab (*Lithodes aequispina*) | 746 |
| Snailfish unid. (Liparidinae) | 613 |
| Other decapods (*Hyas* sp., *Oregonia* sp., Paguridae, etc.) | 601 |
| Poacher unid. (Agonidae) | 600 |
| Flatfish unid. (Pleuronectidae) | 505 |
| Roundfish unid. | 404 |
| Giant grenadier (*Albatrossia pectoralis*) | 370 |
| Shortspine thornyhead (*Sebastolobus alascanus*) | 281 |
| Northern rockfish (*Sebastes polyspinis*) | 226 |
| Grenadier sp. (Macrouridae) | 217 |
| *Sebastes* sp. | 213 |
| Searcher unid. (Bathymasteridae) | 154 |
| Skate unid. (Rajidae) | 148 |
| *Atheresthes* sp. | 123 |
| Deep sea sole (*Embassichthys bathybius*) | 76 |
| Walleye pollock (*Gadus chalcogramma*) | 72 |
| Rex sole (*Glyptocephalus zachirus*) | 69 |
| Prickleback unid. (Stichaeidae) | 67 |
| Shortraker rockfish (*Sebastes borealis*) | 61 |
| Octopus unid. (Octopodidae) | 56 |
| Flathead sole (*Hippoglossoides elassodon*) | 48 |
| Halibut (*Hippoglossoides stenolepis*) | 33 |
| Harlequin rockfish (*Sebastes variegatus*) | 31 |
| King crab unid. (Lithodidae) | 30 |
| Pacific cod (*Gadus macrocephalus*) | 27 |
| *Gadus* sp. | 15 |
| Blackspotted rockfish (*Sebastes melanostictus*) | 13 |
| Bigmouth sculpin (*Hemitripterus bolini*) | 12 |
| Darkfin sculpin (*Malacocottus zonerus*) | 11 |
| Greenland turbot (*Reinhardtius hippoglossoides*) | 10 |
| Sablefish (*Anoplopoma fimbria*) | 8 |
| Alaska skate (*Bathyraja parmifera*) | 5 |
| Whiteblotched skate (*Bathyraja maculata*) | 5 |
| Whitebrow skate (*Bathyraja minispinosa*) | 5 |
| Aleutian skate (*Bathyraja aleutica*) | 4 |
| Rougheye rockfish (*Sebastes aleutianus*) | 4 |
| Scarlet king crab (*Lithodes couesi*) | 4 |
| Starry flounder (*Platichthys stellatus*) | 2 |
| Atka mackerel (*Pleurogrammus monopterygius*) | 2 |
| Dusky rockfish (*Sebastes variabilis*) | 2 |
| Herring (Clupeidae) | 1 |
| Prowfish (*Zaprora silenus*) | 1 |
| Dover sole (*Microstomus pacificus*) | 1 |
| Greenling sp. (*Hexagrammos* sp.) | 1 |
| Spinyhead sculpin (*Dasycottus setiger*) | 1 |
| Commander skate (*Bathyraja lindbergi*) | 1 |
| Tubeshoulder unid. (Platytroctidae) | 1 |

Table 3. Summary of structure-forming invertebrate taxonomic groupings that were observed during the 2014 camera survey on the eastern Bering Sea outer shelf and slope. Also given are the mean, minimum, and maximum depths at which each taxa was observed.

| Taxonomic grouping | Number observed | Mean depth (m) | Minimum depth (m) | Maximum depth (m) |
|---|---|---|---|---|
| Demosponges | 37682 | 352 | 110 | 770 |
| *Halipteris* sp. | 29435 | 304 | 91 | 760 |
| Hexactinellid sponges | 1952 | 395 | 110 | 770 |
| *Plumerella* sp. | 775 | 555 | 349 | 761 |
| *Swiftia* sp. | 537 | 546 | 264 | 770 |
| Isididae | 69 | 562 | 349 | 760 |
| Primnoidae | 38 | 492 | 212 | 760 |
| *Plumerella aleutiana* | 36 | 555 | 349 | 761 |
| Calcareous sponges | 31 | 428 | 215 | 532 |
| Unidentified sponges | 27 | 553 | 150 | 761 |
| Plexauridae | 8 | 631 | 455 | 759 |
| Unidentified corals | 2 | 695 | -- | -- |

Table 4. Summary of model fits and AUC for model validation (trawl model vs. camera observations and camera model vs. trawl observations).

| Taxonomic group | Observations | Bottom trawl survey model | | | | | Camera survey model | | | | | Average model | | | | |
|---|---|---|---|---|---|---|---|---|---|---|---|---|---|---|---|---|
| | | AUC | Correlation | Percent correct | Threshold | Kappa | AUC | Correlation | Percent correct | Threshold | Kappa | AUC | Correlation | Percent correct | Threshold | Kappa |
| Corals | Bottom trawl data | 0.92 (0.01) | 0.53 | 0.8 | 0.08 | 0.27 (0.03) | 0.73 (0.04) | 0.27 | 0.78 | 0.01 | 0.19 (0.03) | 0.85 (0.03) | 0.48 | 0.8 | 0.01 | 0.22 (.03) |
| | Camera data | 0.73 (0.05) | 0.28 | 0.72 | 0.19 | 0.26 (0.06) | 0.95 (0.01) | 0.67 | 0.87 | 0.21 | 0.57 (0.07) | 0.90 (0.02) | 0.54 | 0.82 | 0.11 | 0.43 (0.07) |
| Sponges | Bottom trawl data | 0.83 (0.01) | 0.56 | 0.74 | 0.53 | 0.48 (0.02) | 0.54 (0.02) | -0.07 | 0.5 | 0.56 | -0.01 (0.03) | 0.71 (0.01) | 0.46 | 0.7 | 0.59 | 0.41 (0.01) |
| | Camera data | 0.63 (0.04) | 0.21 | 0.59 | 0.7 | 0.17 (0.06) | 0.80 (0.03) | 0.52 | 0.73 | 0.44 | 0.45 (0.06) | 0.76 (0.03) | 0.44 | 0.71 | 0.6 | 0.41 (0.06) |
| Sea whips | Bottom trawl data | 0.89 (0.01) | 0.58 | 0.8 | 0.13 | 0.37 (0.03) | 0.57 (0.02) | 0.12 | 0.55 | 0.72 | 0.04 (0.02) | 0.82 (0.02) | 0.37 | 0.72 | 0.4 | 0.24 (0.03) |
| | Camera data | 0.69 (0.03) | 0.3 | 0.65 | 0.06 | 0.29 (0.06) | 0.83 (0.03) | 0.56 | 0.76 | 0.44 | 0.51 (0.05) | 0.74 (0.03) | 0.41 | 0.7 | 0.155 | 0.40 (0.06) |

Table 5. Best-fitting models predicting presence or absence, density and height of corals, sponges and sea whips using data from the 2014 camera survey of the eastern Bering Sea slope and outer shelf.  Model terms are listed in order of importance in the models, estimated degrees of freedom (edf) for each of the variables are also given.

| Response variable | Model | Deviance explained | edf | $R^2$ |
|---|---|---|---|---|
| Coral presence or absence | s(depth)+s(latitude)+s(tidal current)+s(sediment sorting) | 51% | 2.9; 2.3; 2.3 ; 1.9 | 0.43 |
| Sponge presence or absence | s(slope)+s(sediment sorting)+s(depth)+s(latitude)+s(grain size)+s(temperature)+s(ocean color) | 16% | 2.9; 1.0; 2.8; 2.9; 2.0; 2.8; 2.2 | 0.22 |
| Sea whip presence or absence | s(grain size)+s(temperature)+s(depth)+s(tidal current)+s(current speed)+s(latitude)+s(slope) | 26% | 2.5; 2.6; 2.7; 2.8; 1.0; 2.3; 2.2 | 0.26 |
| Coral density | s(slope)+s(depth) | 70% | 2.3; 2.7 | 0.62 |
| Sponge density | s(latitude)+s(grain size)+s(current speed) | 20% | 2.3; 2.9; 1.0 | 0.13 |
| Sea whip density | s(depth)+s(slope) | 33% | 2.9; 2.6 | 0.28 |
| Coral height | s(latitude)+s(tidal current)+s(slope)+s(grain size)+s(temperature)+s(current speed) | 93% | 3.0; 1.0; 1.2; 1.8; 2.1; 2.6 | 0.86 |
| Sponge height | s(temperature)+s(slope)+s(grain size) | 41% | 2.0; 2.0; 2.6 | 0.36 |
| Sea whip height | s(depth)+s(temperature)+s(latitude)+s(current speed)+s(grain size) | 60% | 2.4; 2.7; 1.9; 1.0; 1.0 | 0.55 |

Table 6.  Average heights for invertebrate taxa measured during the eastern Bering Sea slope and outer shelf camera survey. The number measured (n), mean, standard deviation (SD), minimum (Min) and maximum (Max) heights are given in centimeters.

| Species | n | Mean | SD | Min | Max |
|---|---|---|---|---|---|
| Gorgonacea | 2 | 21 | 9.2 | 15 | 28 |
| Isididae | 31 | 48 | 28.4 | 10 | 116 |
| Plexauridae | 1 | 16 | | 16 | 16 |
| *Plumerella aleutiana* | 4 | 12 | 7.2 | 6 | 22 |
| *Plumerella* sp. | 265 | 16 | 9.4 | 4 | 53 |
| Primnoidae | 19 | 11 | 8.3 | 4 | 33 |
| *Swiftia* sp. | 41 | 10 | 4.2 | 2 | 24 |
| | | | | | |
| Porifera | 3 | 17 | 4.4 | 13 | 22 |
| Upright calcarea | 12 | 13 | 2.0 | 10 | 18 |
| Upright demosponge | 1972 | 18 | 8.3 | 10 | 135 |
| Upright hexactinellid | 569 | 25 | 18.5 | 10 | 204 |
| | | | | | |
| *Halipteris* sp. | 3496 | 62 | 54.2 | 2 | 266 |

Table 7. Summary table of analyses of covariance of fish density and structure-forming invertebrates (and depth). The table presents where there was a significant effect (meaning fish density was significantly higher or lower) of the presence of invertebrates by taxa. The interaction terms refer to the interaction between the factors (invertebrate presence or absence) and depth. "ns" indicates the relationship was non-significant, "sig" indicates a significant depth relationship, "sig +" indicates a positive effect of presence on density and "sig –" indicates a negative effect of presence on density.

| Species/group | Main | | | | Interaction | | |
| --- | --- | --- | --- | --- | --- | --- | --- |
| | Sponge | Coral | Whips | Depth | Sponge | Coral | Whips |
| Rockfish (all *Sebastes*) | sig + | sig - | ns | sig | sig | sig | ns |
| POP | sig + | ns | ns | sig | sig | sig | ns |
| Shortraker | ns | sig + | ns | ns | ns | ns | ns |
| SST | ns | ns | sig - | sig | ns | ns | sig |
| Cod | ns | ns | sig - | sig | ns | ns | ns |
| Sculpins | ns | ns | ns | sig | ns | ns | ns |
| Grenadier | sig - | sig - | sig - | sig | ns | ns | sig |
| Flatfish | ns | ns | sig + | sig | ns | ns | sig |
| Pollock | ns | ns | ns | sig | ns | ns | ns |
| Chionoecetes | sig - | sig - | ns | sig | ns | sig | ns |
| King crabs | sig + | sig + | ns | sig | ns | ns | ns |
| Skates | ns | ns | ns | sig | ns | ns | ns |
| Northern rockfish | ns | ns | ns | ns | sig | ns | ns |
| Rougheye/blackspotted | ns | sig + | ns | ns | ns | sig | ns |
| Sablefish | ns | ns | ns | ns | ns | ns | ns |

Table 8. The number and proportion of transects with damaged coral, sponge, or sea whip or evidence of fishing (e.g., lost gear). Only the 3 taxa listed were found damaged. The other observed taxa were Gorgonacea, *Plumarella aleutiana*, *Plumarella* sp., Primnoidae, *Swiftia* sp., Porifera, Calcarea, and Hexactinellid, but none were found damaged. The total sample size was 250 transects.

| Classification | Number of transects | Proportion of transects |
|---|---|---|
| Damaged Isididae | 2 | 0.008 |
| Damaged Demosponge | 7 | 0.028 |
| Damaged Halipteris | 60 | 0.240 |
| **Damaged taxa subtotal** | **68** | **0.272** |
| Longline or crab gear | 11 | 0.044 |
| Trawl net | 2 | 0.008 |
| Trawl tracks | 19 | 0.076 |
| **Evidence of fishing  subtotal** | **32** | **0.128** |
| **Damaged taxa or evidence of fishing total** | **92** | **0.368** |
| **Damaged taxa and evidence of fishing total** | **8** | **0.032** |

Table 9. The number and proportion of transects with damaged coral, sponge, or sea whip. Only the 3 taxa listed were found damaged. The other observed taxa were Gorgonacea, *Plumarella aleutiana*, *Plumarella* sp., Primnoidae, *Swiftia* sp., Porifera, Calcarea, and Hexactinellid, but none were found damaged. The total sample size was 250 transects.

| Taxa | Damaged | | Total | | Proportion of transects with damage |
|---|---|---|---|---|---|
| | Number of transects | Proportion of transects | Number of transects | Proportion of transects | |
| Isididae | 2 | 0.008 | 7 | 0.028 | 0.286 |
| Gorgonacea | 0 | 0 | 1 | 0.004 | 0.000 |
| Plexauridae | 0 | 0 | 5 | 0.020 | 0.000 |
| *Plumarella aleutiana* | 0 | 0 | 2 | 0.008 | 0.000 |
| *Plumarella* sp. | 0 | 0 | 22 | 0.088 | 0.000 |
| Primnoidae | 0 | 0 | 6 | 0.024 | 0.000 |
| *Swiftia* sp. | 0 | 0 | 19 | 0.076 | 0.000 |
| *Halipteris* sp. | 60 | 0.240 | 105 | 0.420 | 0.571 |
| Demosponge | 7 | 0.028 | 106 | 0.424 | 0.066 |
| Porifera | 0 | 0 | 9 | 0.036 | 0.000 |
| Calcarea | 0 | 0 | 4 | 0.016 | 0.000 |
| Hexactinellid | 0 | 0 | 56 | 0.224 | 0.000 |

Table 10. The number and proportion of individual coral, sponge, or sea whip that were damaged. Only the 3 taxa listed were found damaged. The other observed taxa were Gorgonacea, *Plumarella aleutiana*, *Plumarella* sp., Primnoidae, *Swiftia* sp., Porifera, Calcarea, and Hexactinellid, but none were found damaged.

| Taxa | Damaged | Undamaged | Total | Proportion damaged |
|---|---|---|---|---|
| Isididae | 2 | 67 | 69 | 0.029 |
| Gorgonacea | - | 2 | 2 | 0.000 |
| Plexauridae | - | 8 | 8 | 0.000 |
| *Plumarella aleutiana* | - | 36 | 36 | 0.000 |
| *Plumarella* sp. | - | 775 | 775 | 0.000 |
| Primnoidae | - | 38 | 38 | 0.000 |
| *Swiftia* sp. | - | 537 | 537 | 0.000 |
| *Halipteris* sp. | 2,653 | 26,782 | 29,435 | 0.090 |
| Demosponge | 115 | 37,567 | 37,682 | 0.003 |
| Porifera | - | 27 | 27 | 0.000 |
| Calcarea | - | 31 | 31 | 0.000 |
| Hexactinellid | - | 1,952 | 1,952 | 0.000 |

**9. Figures**
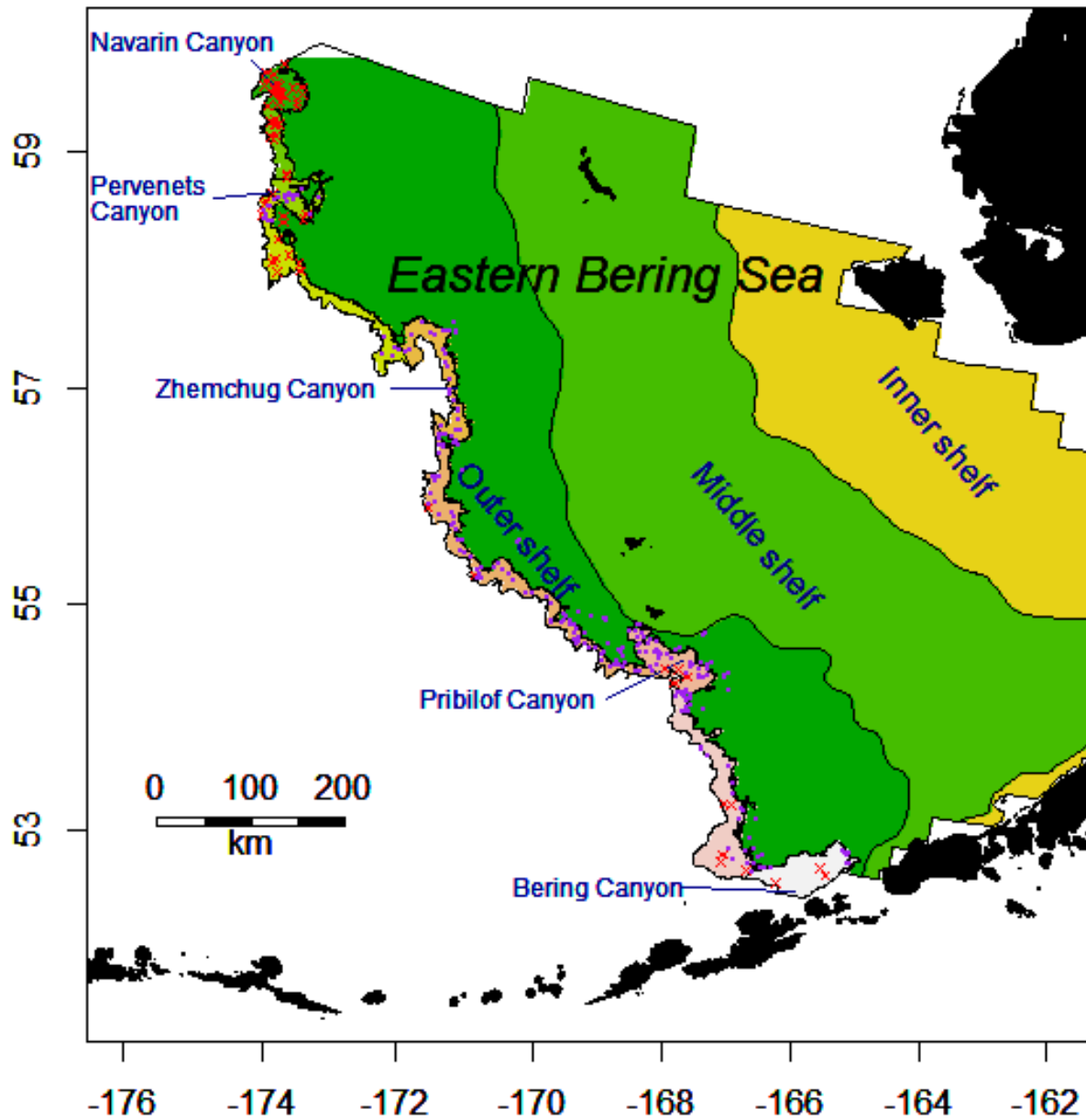


Figure 1. Eastern Bering Sea shelf and slope divided into the three major shelf domains. The map includes locations of the five major canyons and the intercanyon areas. Randomly selected sample sites are indicated by purple dots (occupied sites) and red crosses (sites that were not sampled due to time or depth constraints).
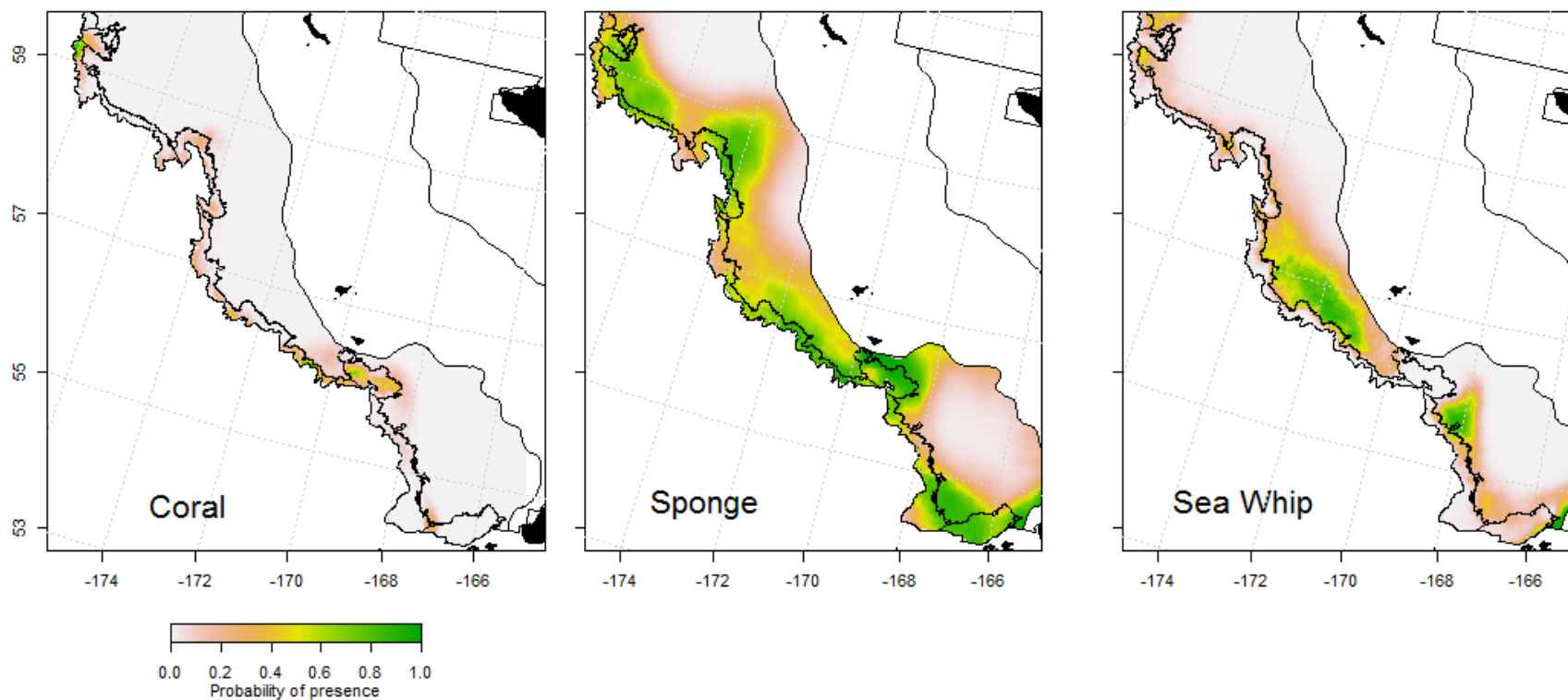
Figure 2. Predicted probability of structure-forming invertebrate presence predicted from the best fitting GAM model of presence or absence in the bottom trawl survey data.
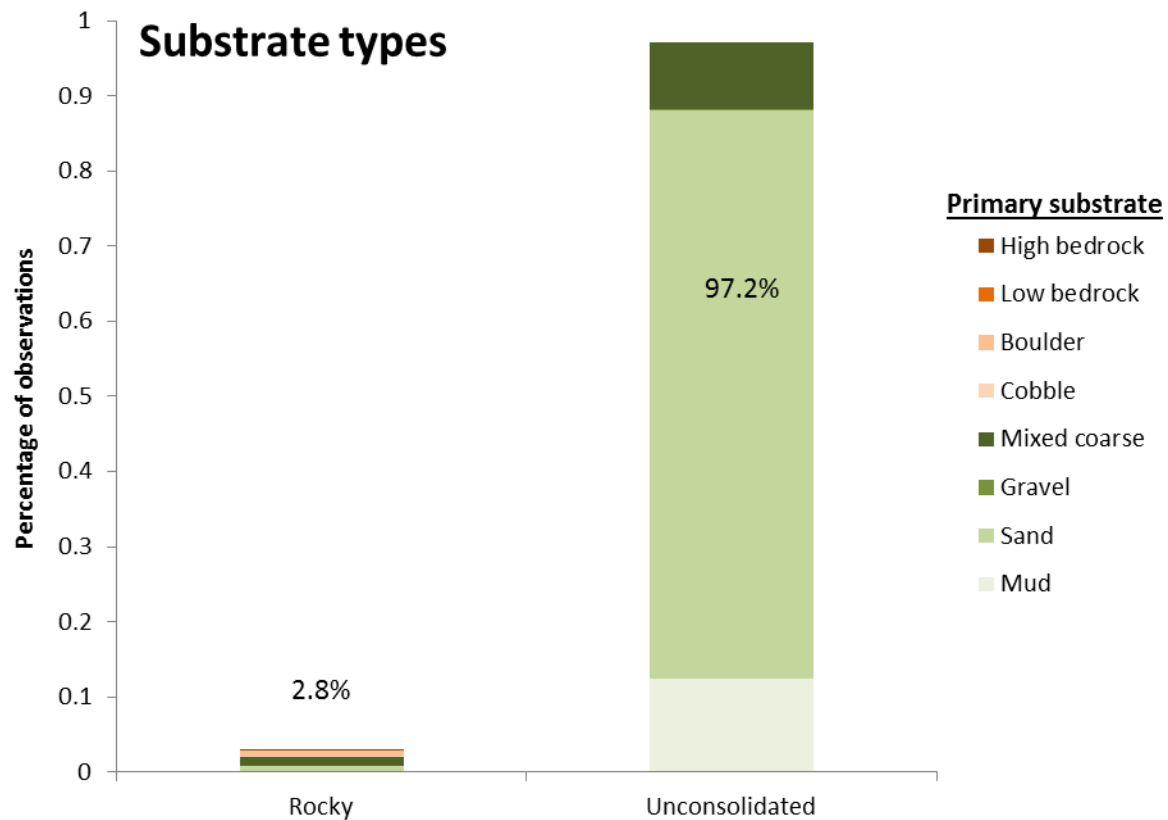
Figure 3. The proportions of seafloor substrates observed during the 2014 camera survey. Substrates were divided into purely unconsolidated (containing only mud, sand, gravel or mixed coarse substrates) and rocky substrates (those containing any type of cobble, boulder, or exposed bedrock). Colors indicate the primary substrate that was observed.
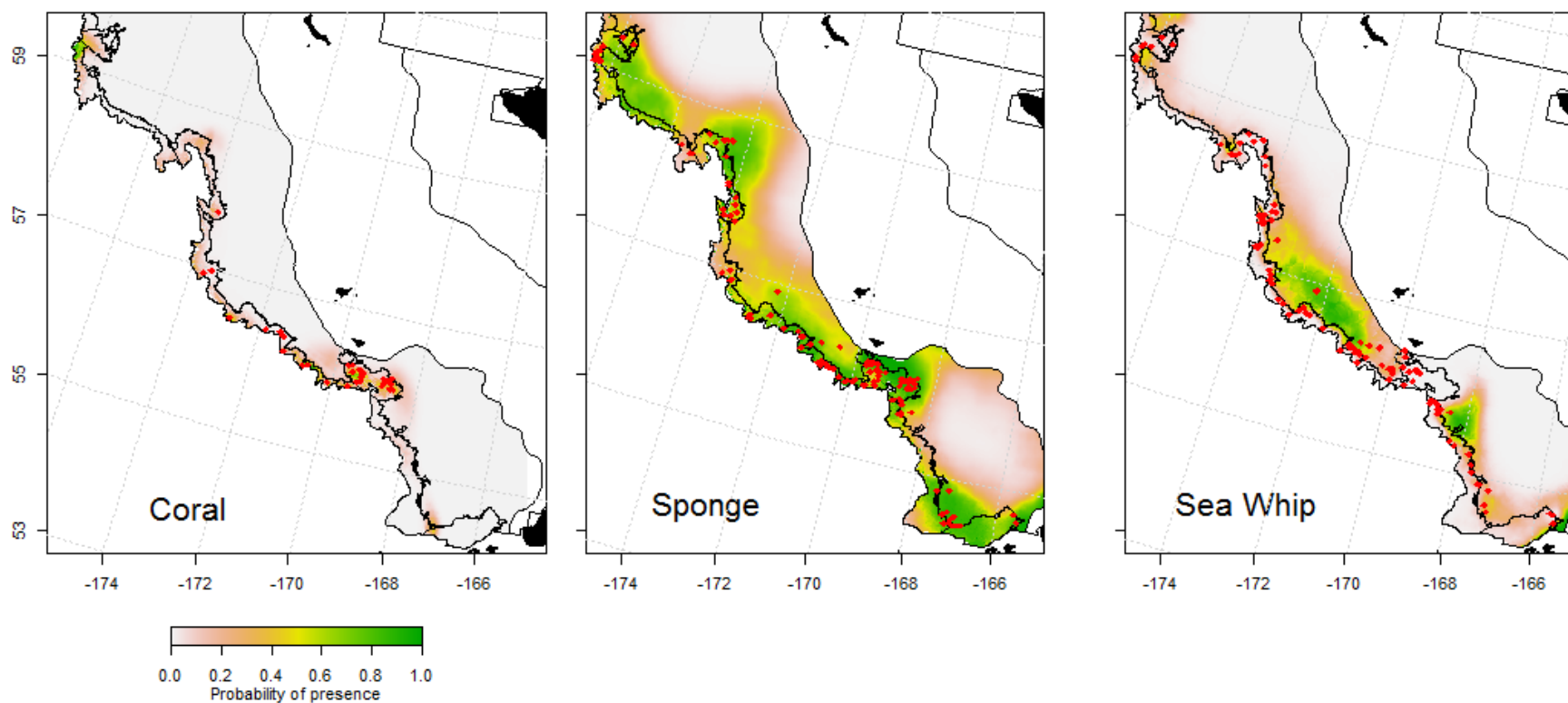
Figure 4. Predicted probability of presence for each taxa of structure-forming invertebrates with the points where each taxonomic group was observed during the 2014 stereo camera survey indicated in red.
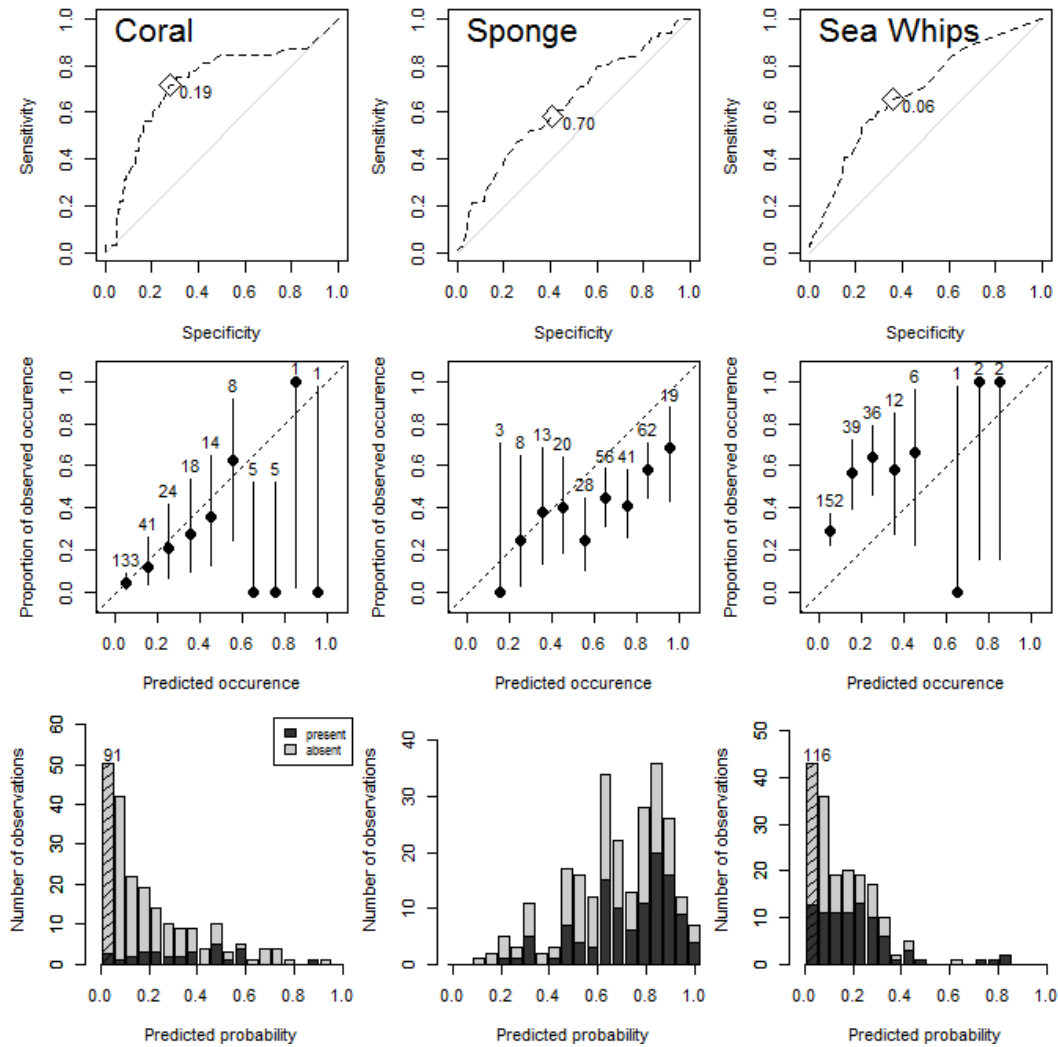
Figure 5. Diagnostic plots for the coral, sponge, and sea whip presence or absence observations from the camera survey tested against the models based on the bottom trawl survey data. The top row shows the area under the receiver operating curve (AUC) plot with a point indicating the threshold probability where sensitivity (true positive rate) is plotted against specificity (the false positive rate). The middle row of plots shows the shows the goodness-of-fit plots of observed versus predicted values within probability bins (i.e. based on the threshold probability from the figure above, what proportion of observations were predicted present in each bin). The bottom row of plots shows the histogram of observed presence or absence plotted against the predicted probability.
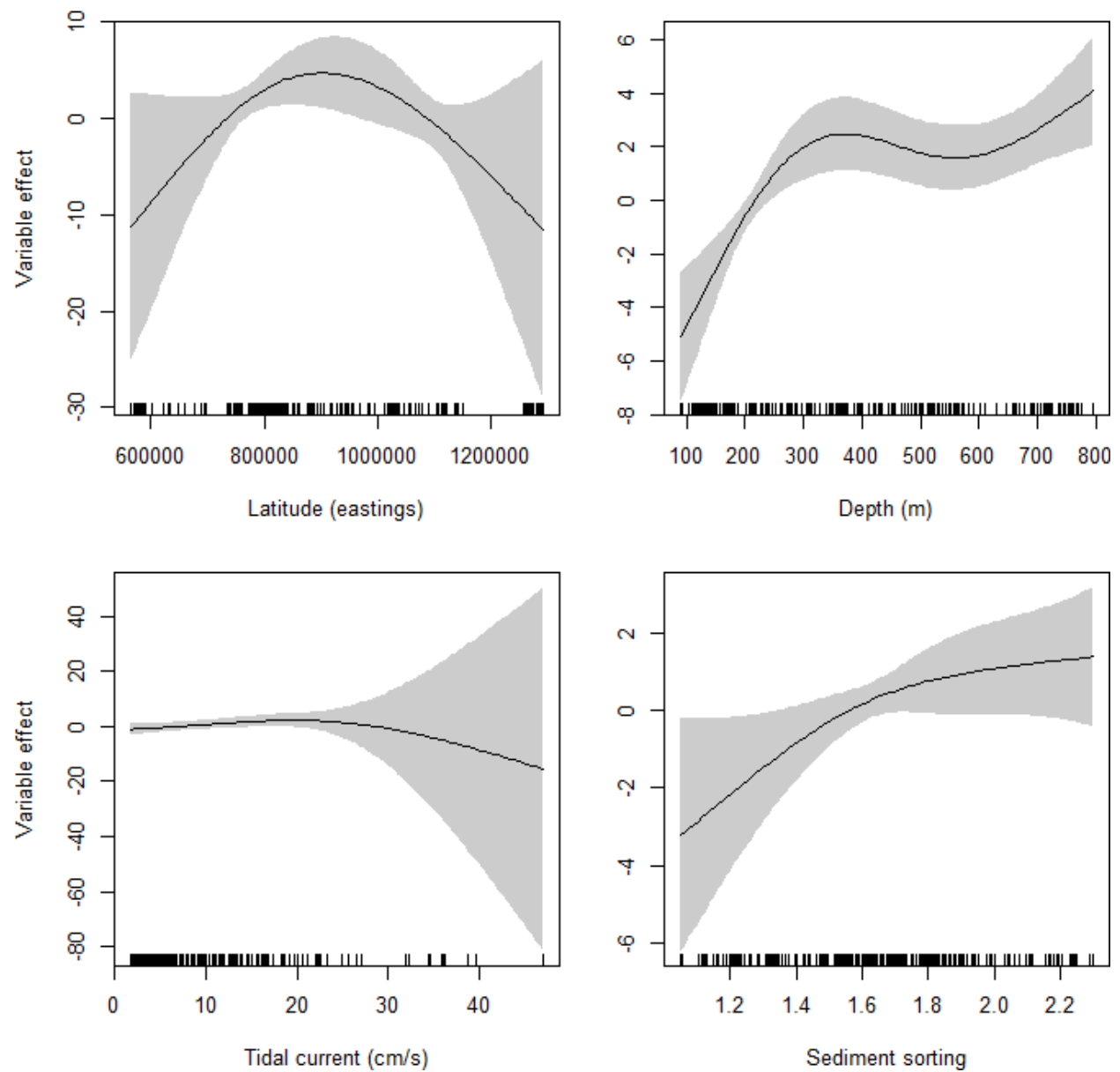
Figure 6. Smoothed relationships from the best-fitting GAM model between explanatory variables and the presence or absence of corals observed in the camera survey. Only significant variables are shown.
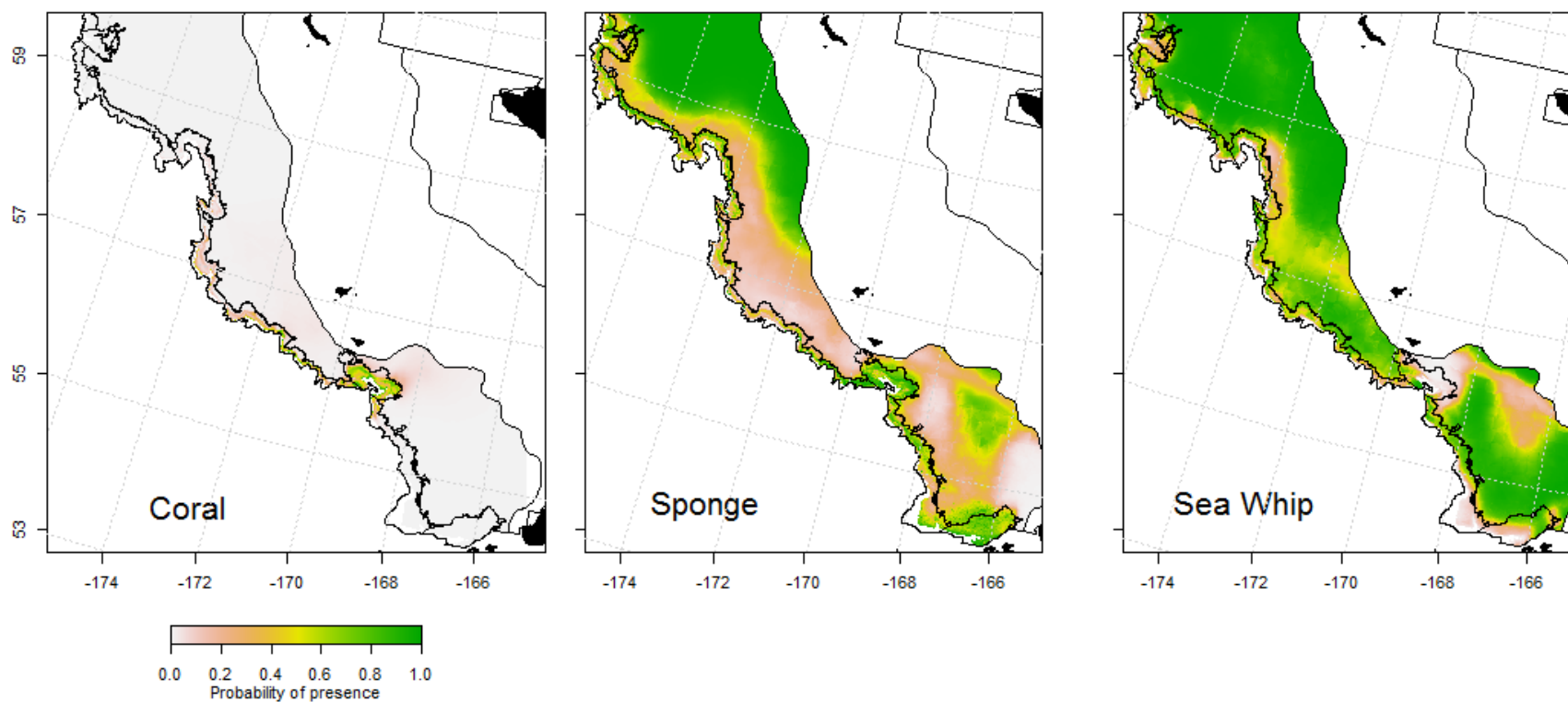
Figure 7. Predicted probability of structure-forming invertebrate presence predicted from the best fitting GAM model of presence or absence in the camera survey data. Panels represent coral, sponge and sea whips, predictions are made on a 100 m by 100 m grid.
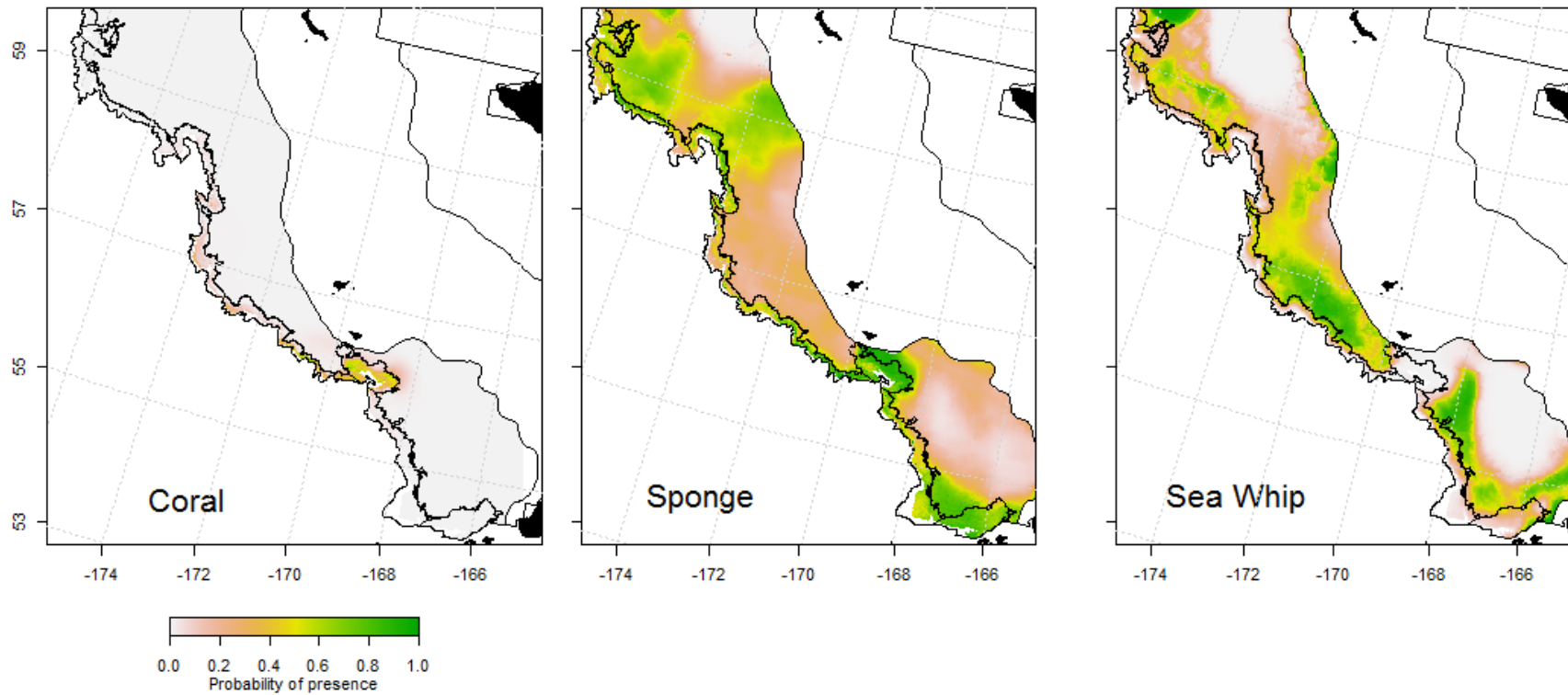
Figure 8. Predicted probability of structure-forming invertebrate presence predicted from the average of the best-fitting GAM models of presence or absence from the trawl survey data and camera survey data. The predictions were averaged by weighting with the inverse of the prediction error. Panels represent coral, sponge, and sea whip predictions on a 100 m by 100 m grid.
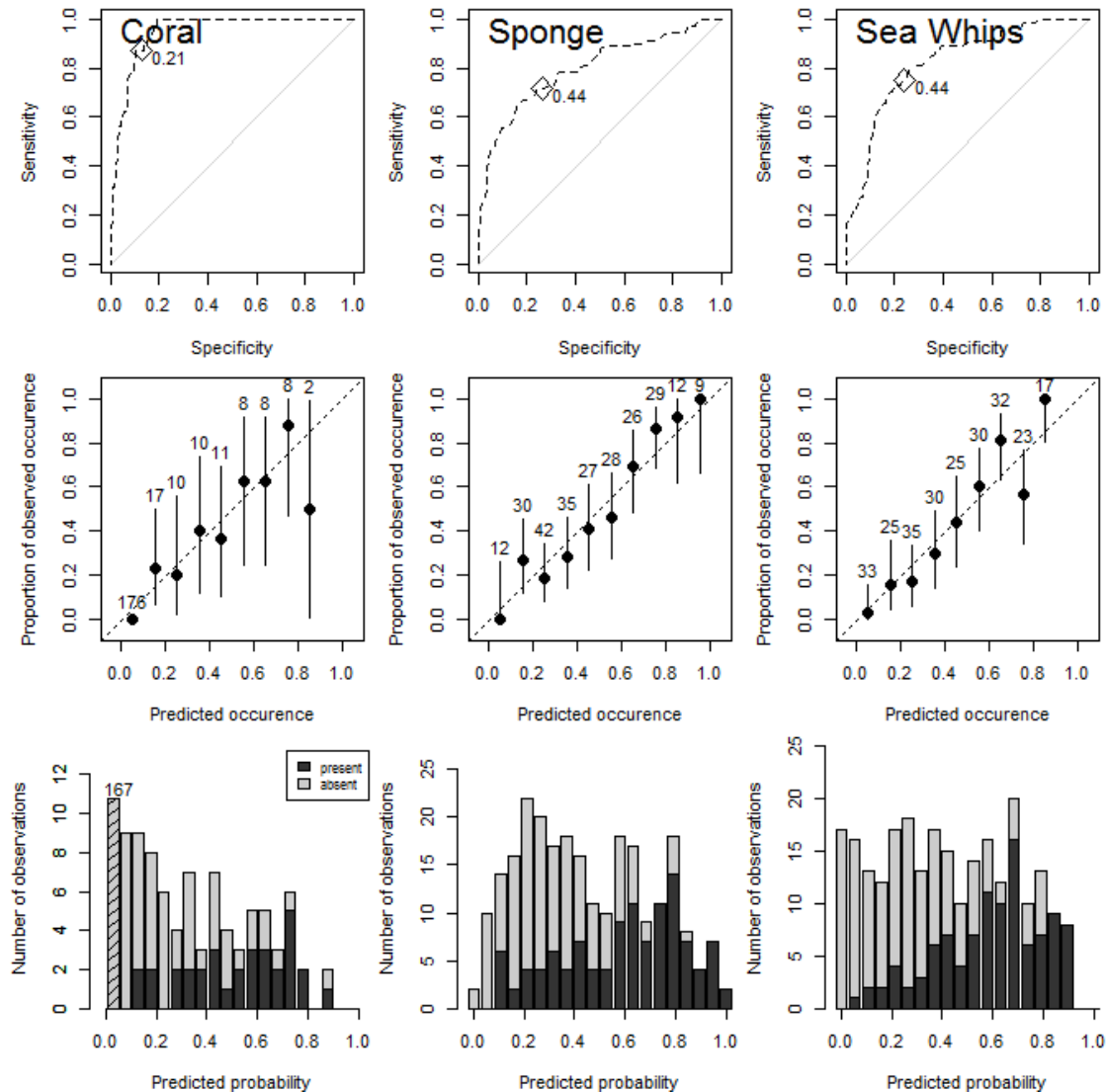
Figure 9. Diagnostic plots for the coral, sponge, and sea whip presence or absence observations from the camera survey tested against the model based on the camera survey data. The top row shows the area under the receiver operating curve (AUC) where sensitivity (true positive rate) is plotted against specificity (the false positive rate). The points indicate the threshold probability for presence. The middle plots show the goodness-of-fit of observed versus predicted values within probability bins (i.e. based on the threshold probability from the figure above, what proportion of observations were predicted present in each bin). The bottom row of plots shows the histogram of observed presence or absence plotted against the predicted probability.
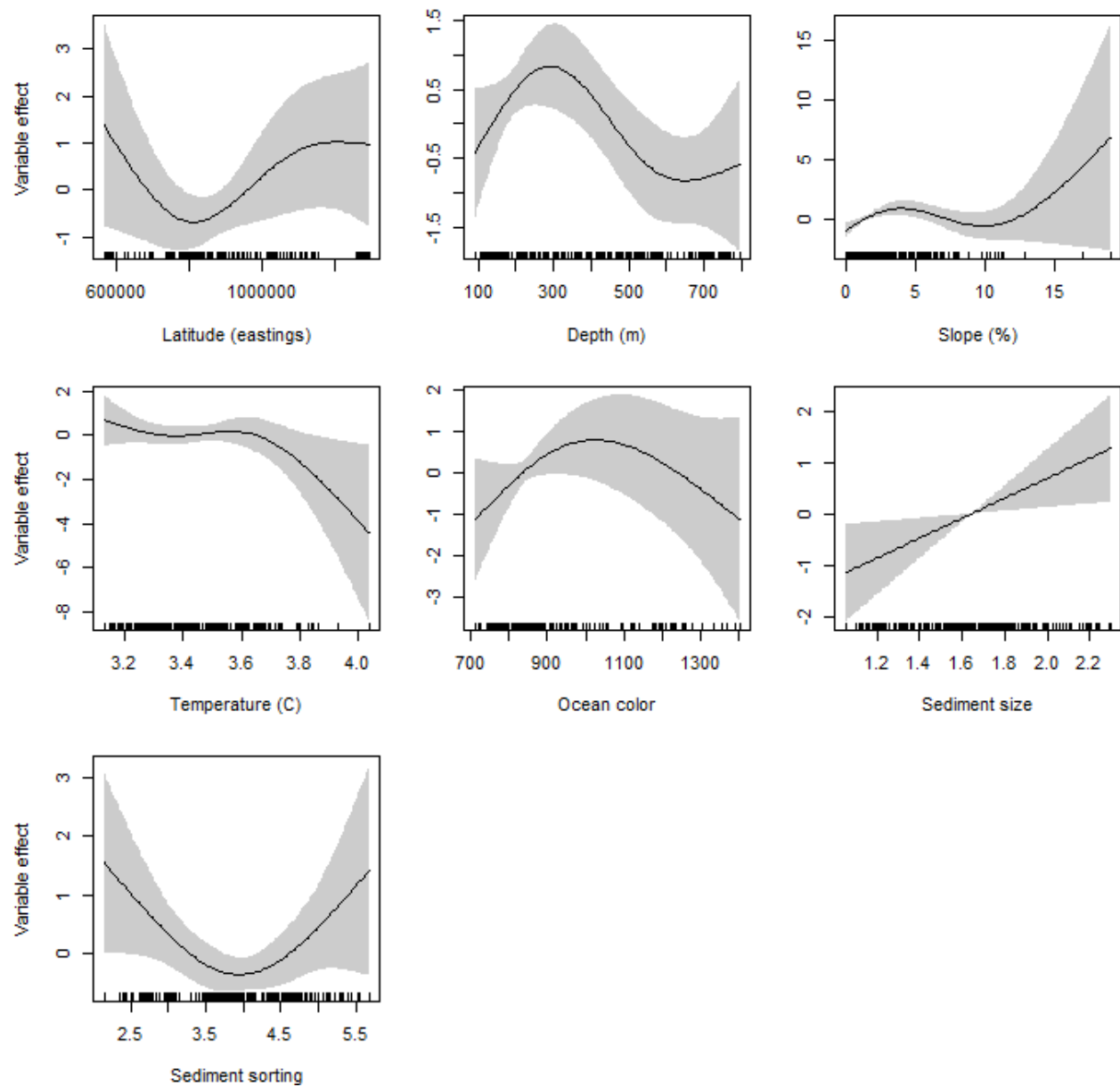
Figure 10. Smoothed relationships from the best-fitting GAM model between explanatory variables and the presence or absence of sponges observed in the camera survey. Only significant variables are shown.
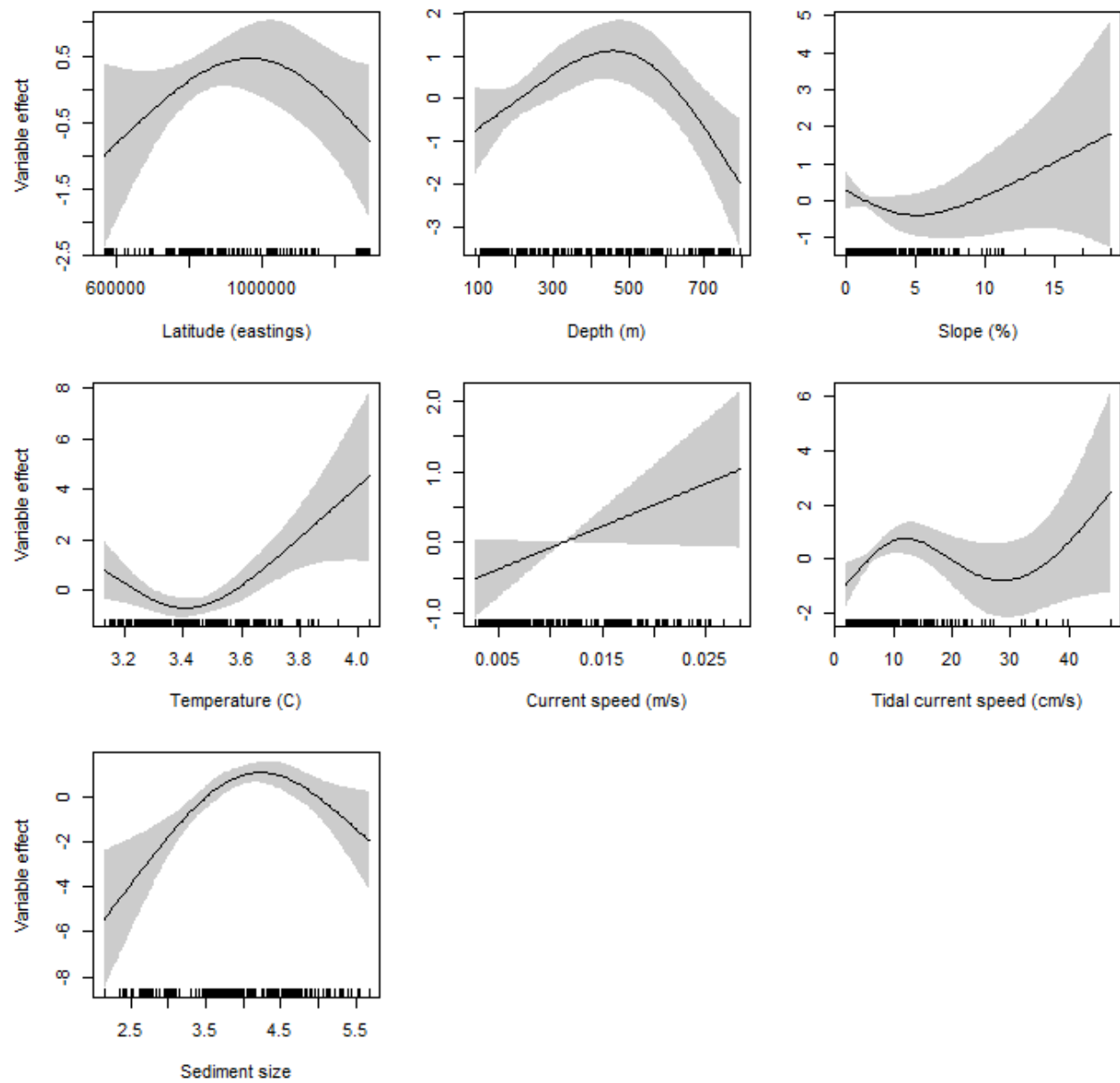
Figure 11. Smoothed relationships from the best-fitting GAM model between explanatory variables and the presence or absence of sea whips observed in the camera survey. Only significant variables are shown.
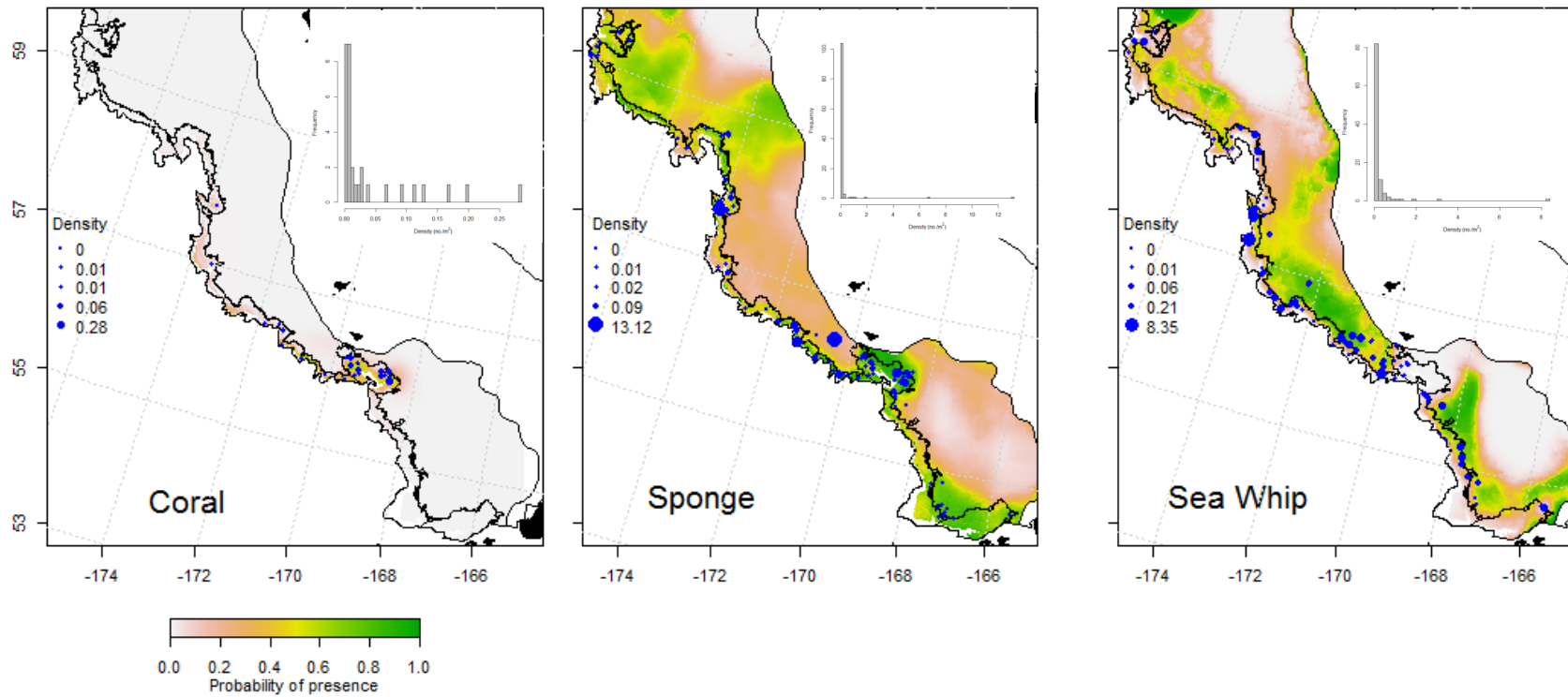
Figure 12. Observed structure-forming invertebrate densities (separated into quantiles) from the camera survey. The background shows the average presence absence model from Figure 8. The inset bar charts show the frequency histogram of observed density for stations where the invertebrate taxon was observed.
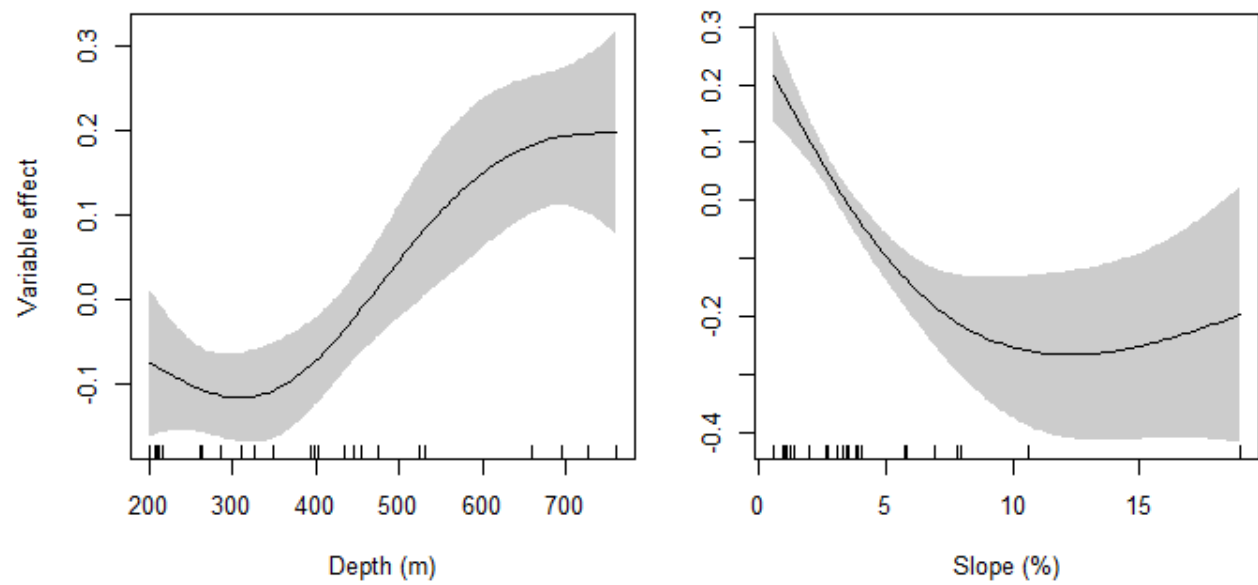
Figure 13. Smoothed relationships from the best-fitting GAM model between explanatory variables and density of corals (no.*m$^{-2}$) observed in the camera survey. Only significant variables are shown.
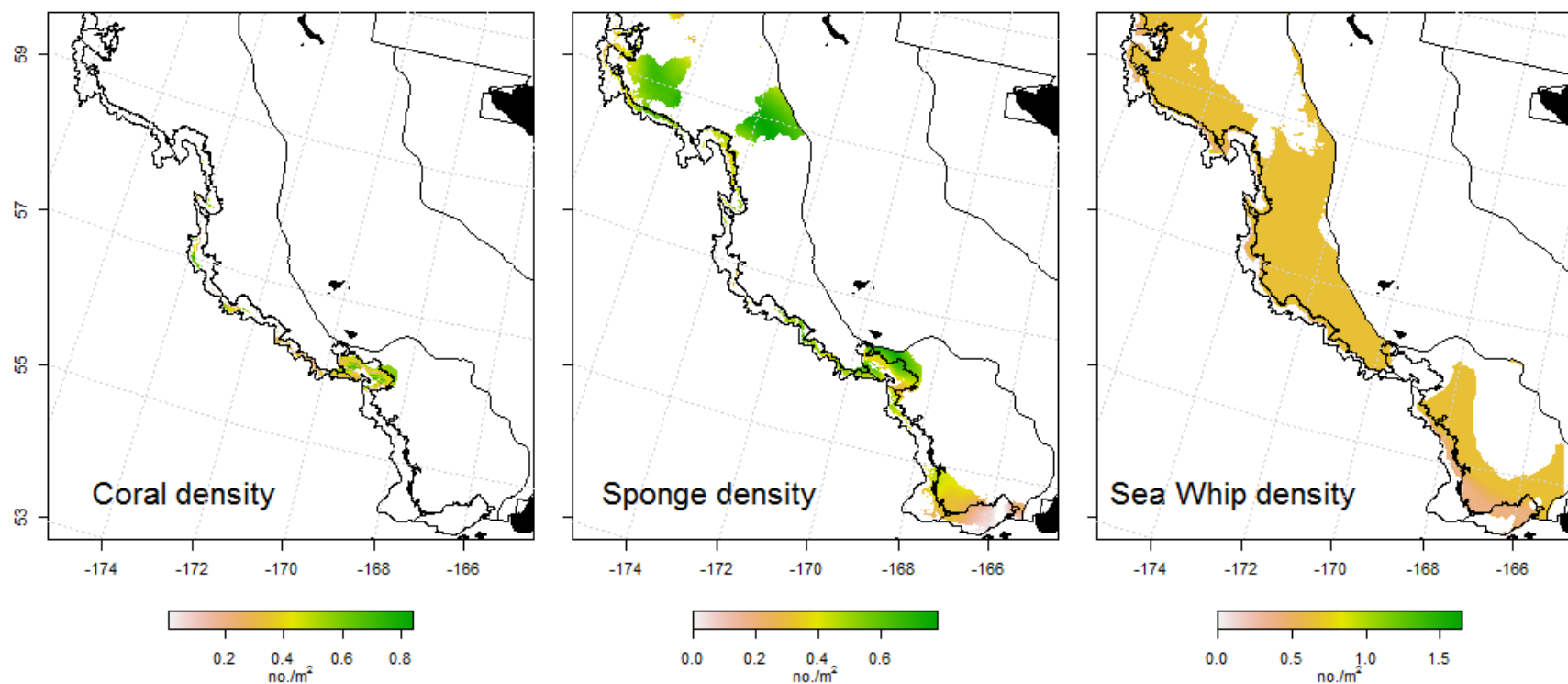
Figure 14. Predicted fourth-root transformed density (no.*m$^{-2}$) of corals, sponges, and sea whips based on GAM models of camera survey density data. Predictions are shown for only those grid cells where the average presence-absence model indicated that the invertebrate taxa would be present.
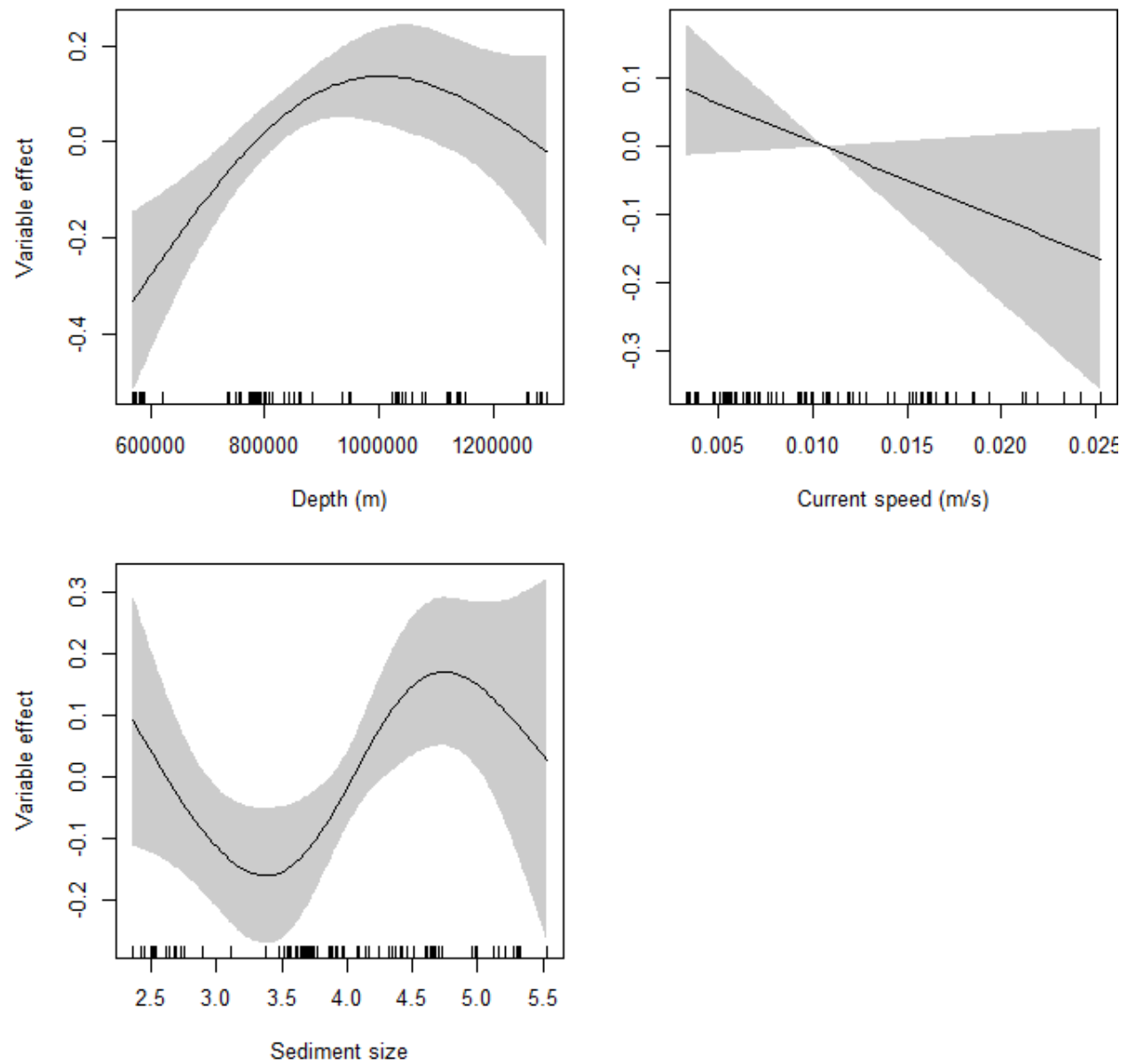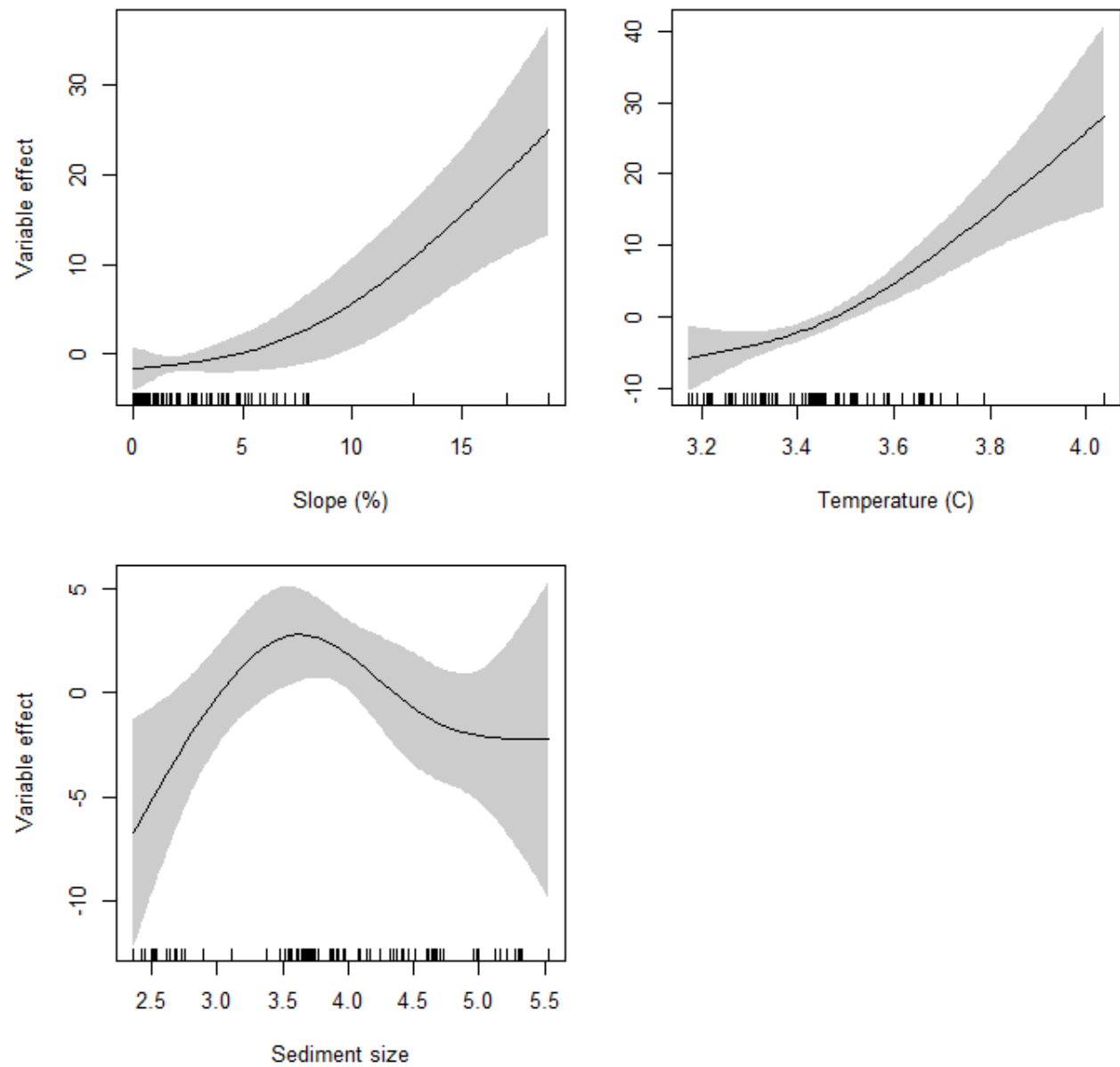
Figure 15. Smoothed relationships from the best-fitting GAM model between explanatory variables and density of sponges (no.*m$^{-2}$) observed in the camera survey. Only significant variables are shown.
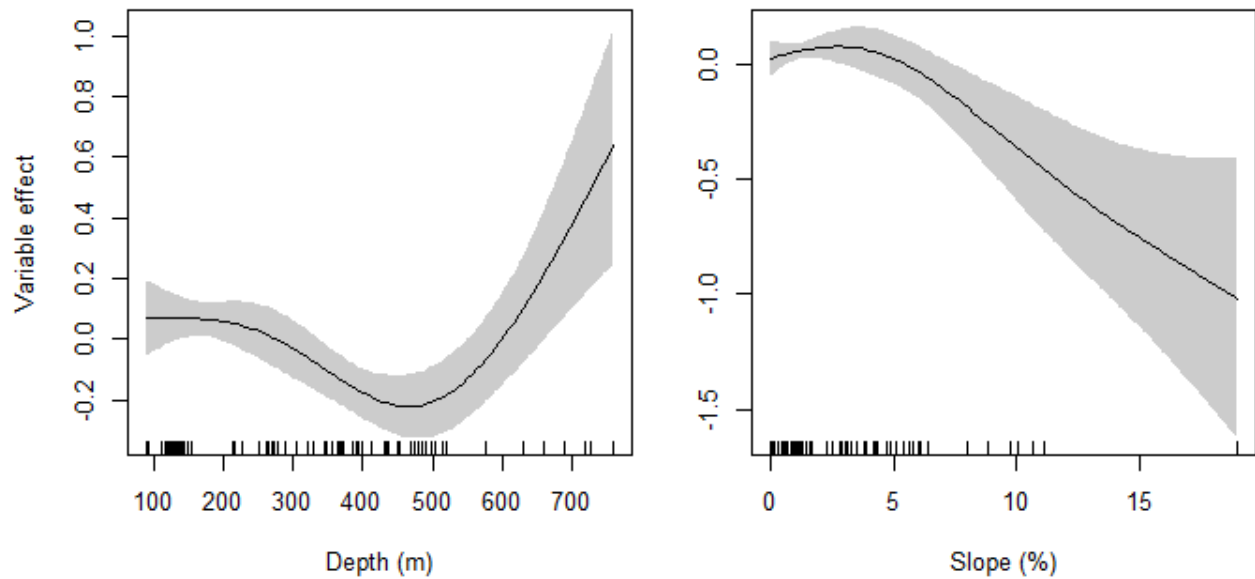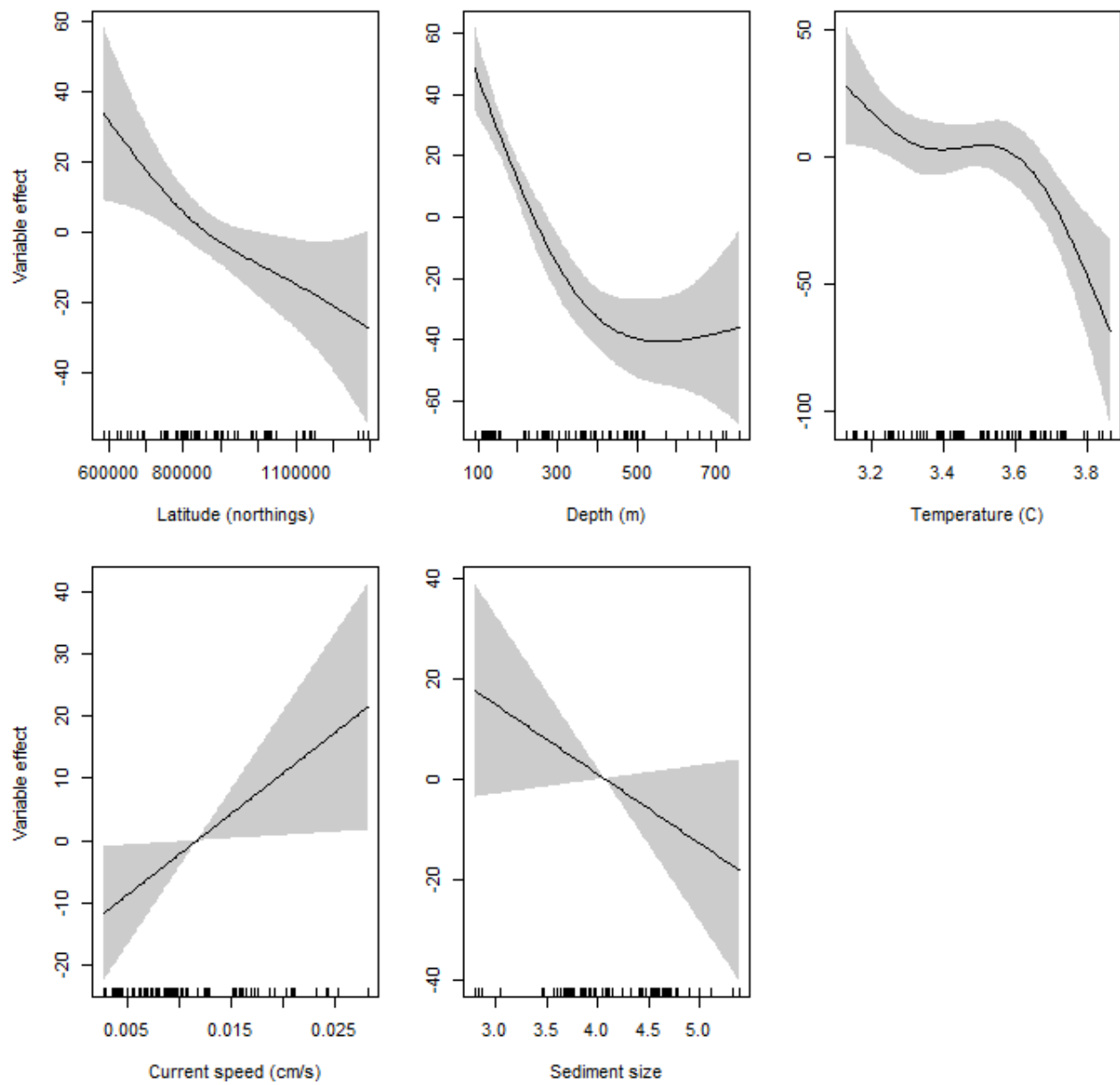
Figure 16. . Smoothed relationships from the best-fitting GAM model between explanatory variables and density of sea whips (no.*m$^{-2}$) observed in the camera survey. Only significant variables are shown.
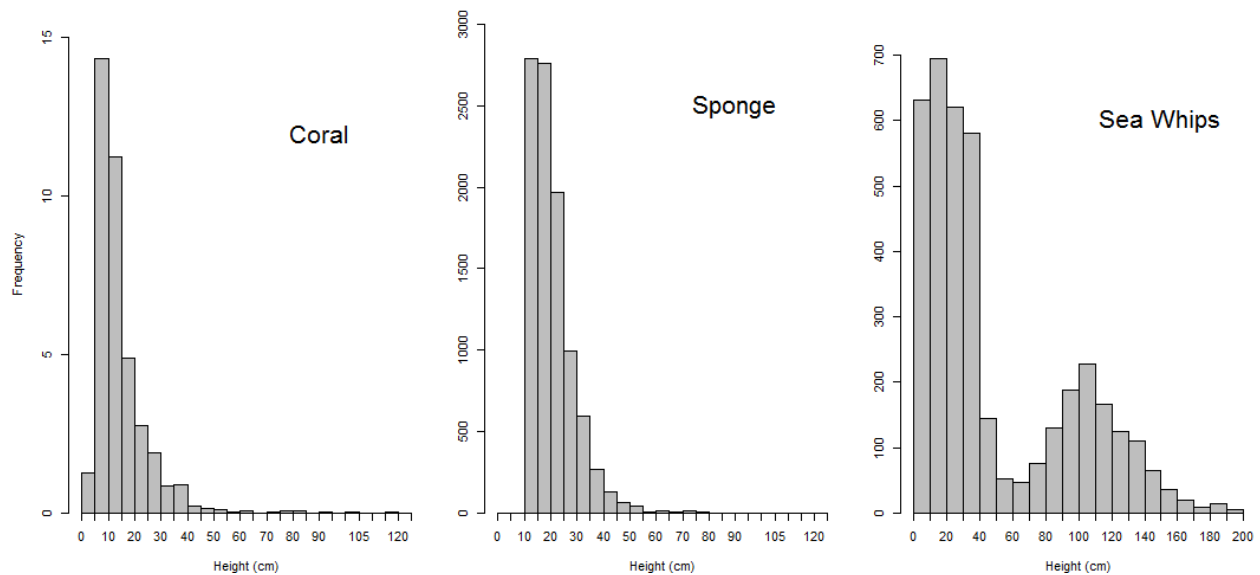


Figure 17. Height frequencies measured by the stereo camera for invertebrate taxa; corals, sponges and sea whips.
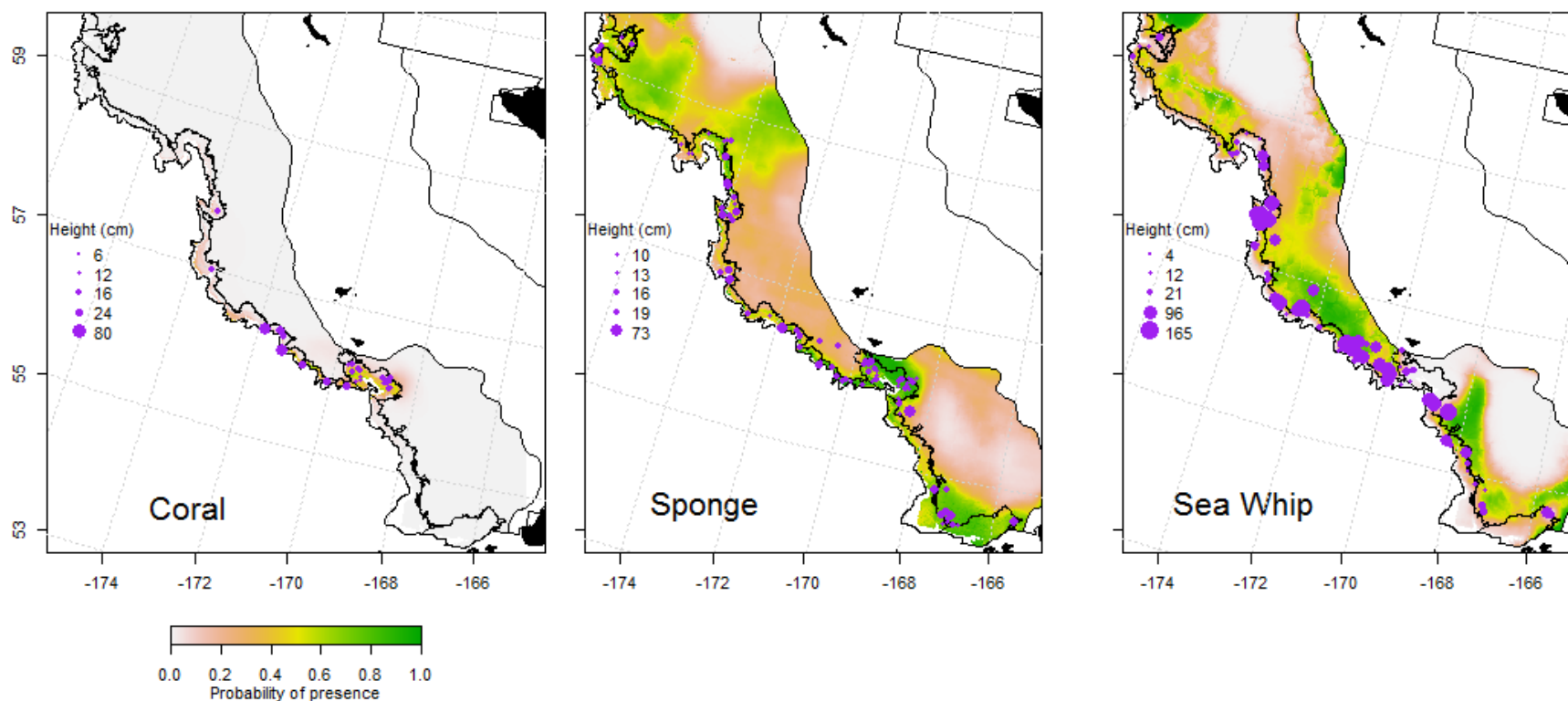
Figure 18. Observed structure-forming invertebrate average heights (separated into quantiles) from the camera survey. The background shows the average presence absence model from Figure 8.
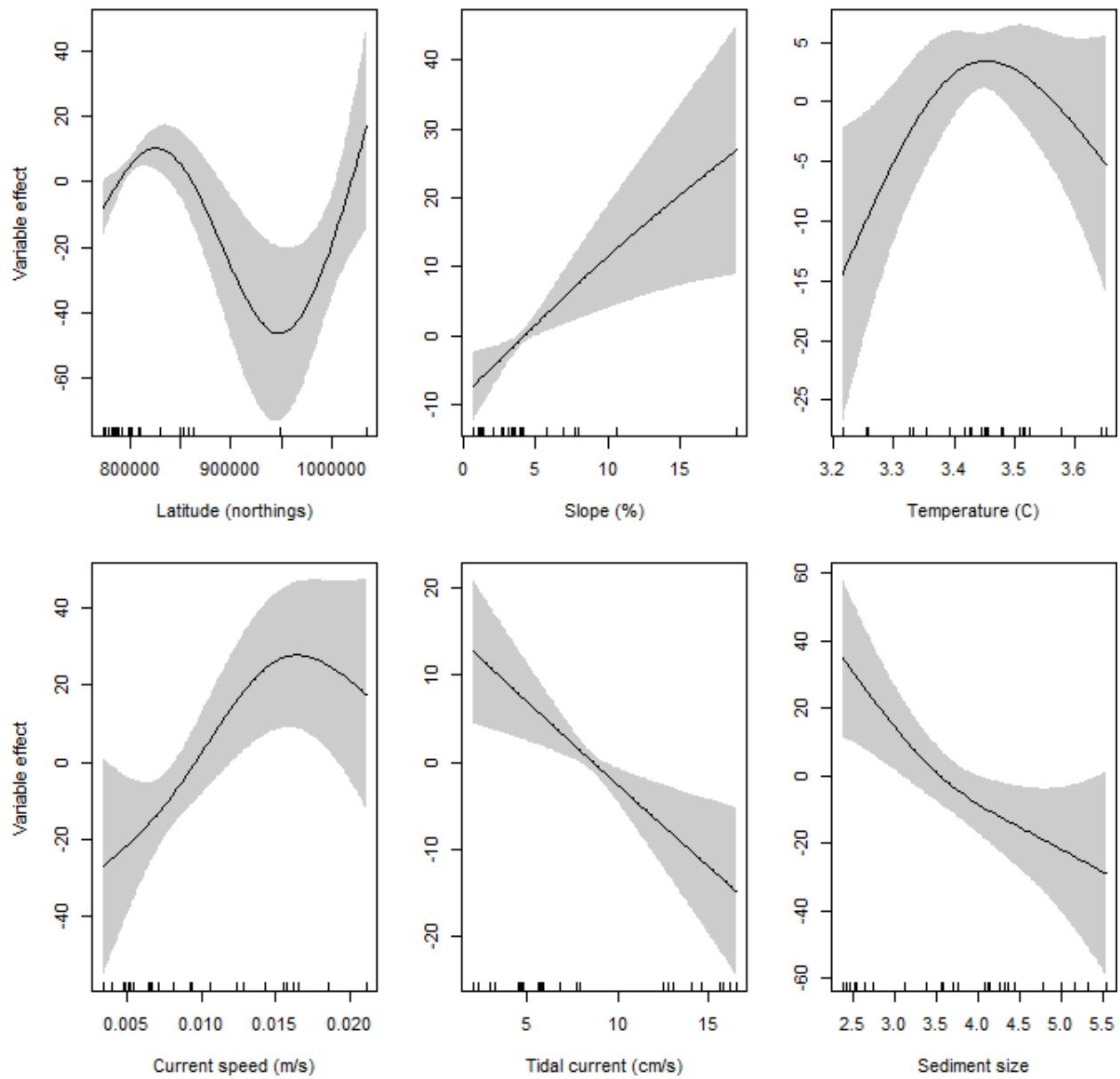
Figure 19. Smoothed relationships from the best-fitting GAM model between explanatory variables and height of coral (cm) observed in the camera survey. Only significant variables are shown.
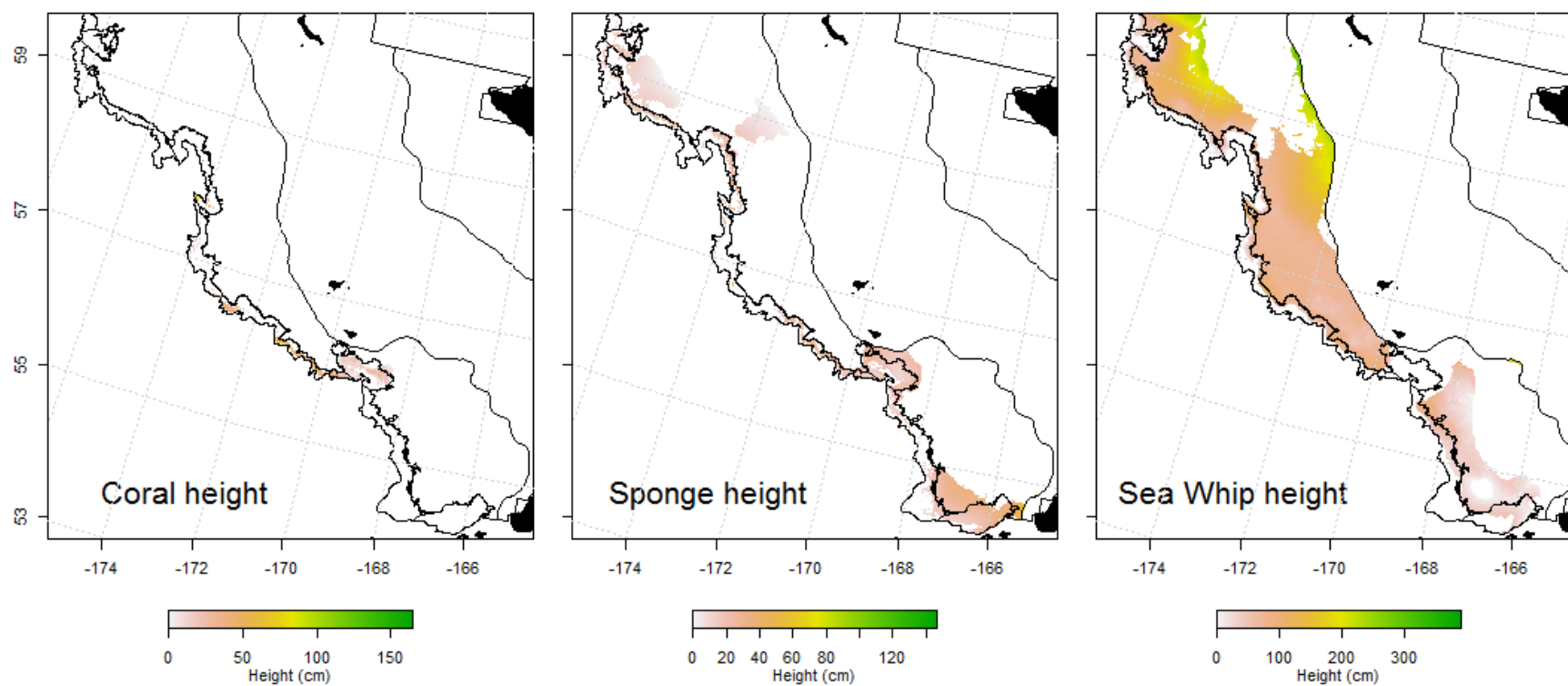
Figure 20. Predicted heights of corals, sponges, and sea whips based on GAM models of camera survey density data. Predictions are shown for only those grid cells where the average presence-absence model indicated that the invertebrate taxa would be present.

Figure 21. Smoothed relationships from the best-fitting GAM model between explanatory variables and height of sponges (cm) observed in the camera survey. Only significant variables are shown.

Figure 22. Smoothed relationships from the best-fitting GAM model between explanatory variables and height of sea whips (cm) observed in the camera survey. Only significant variables are shown.
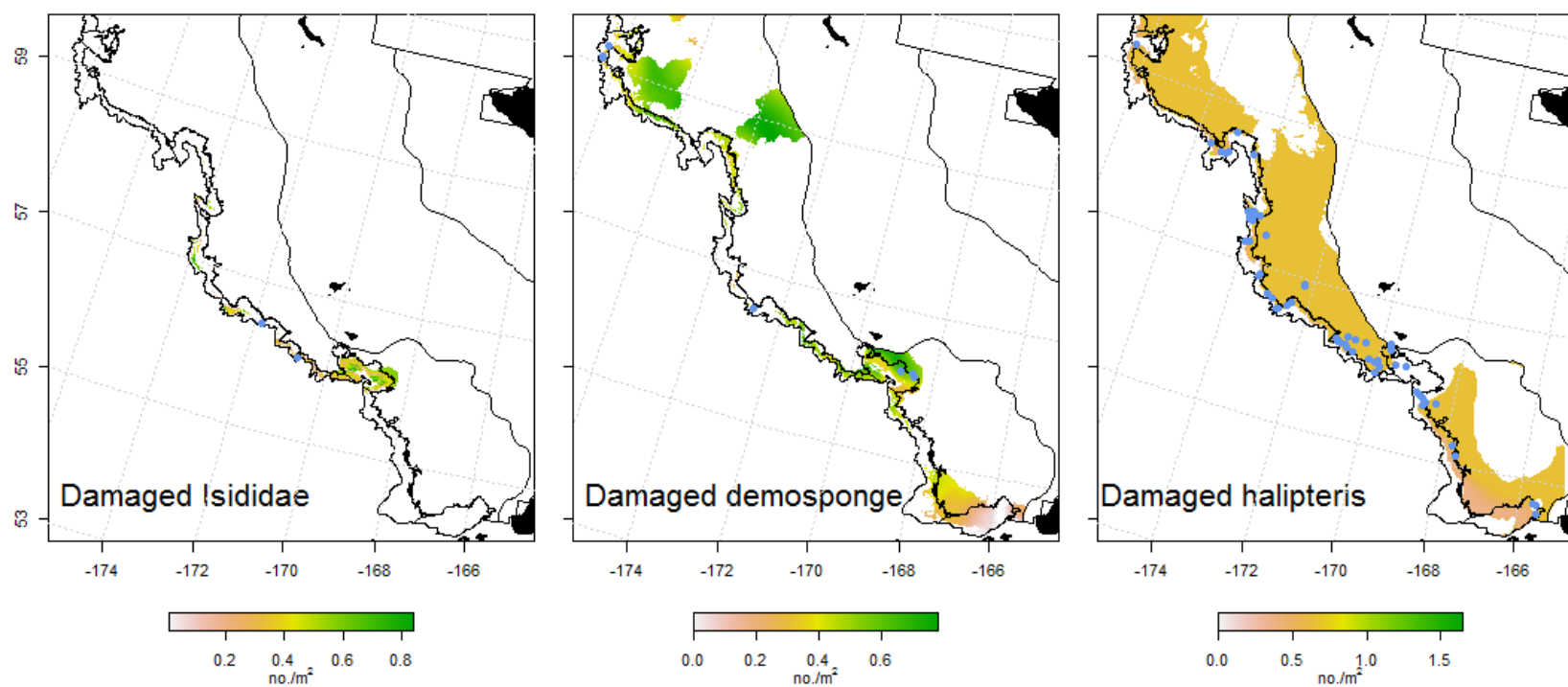
Figure 23. The location of transects with damaged coral, sponge, or sea whip indicated by blue dots. The dots are overlaid on predicted density for the coral, sponge, and sea whip models.
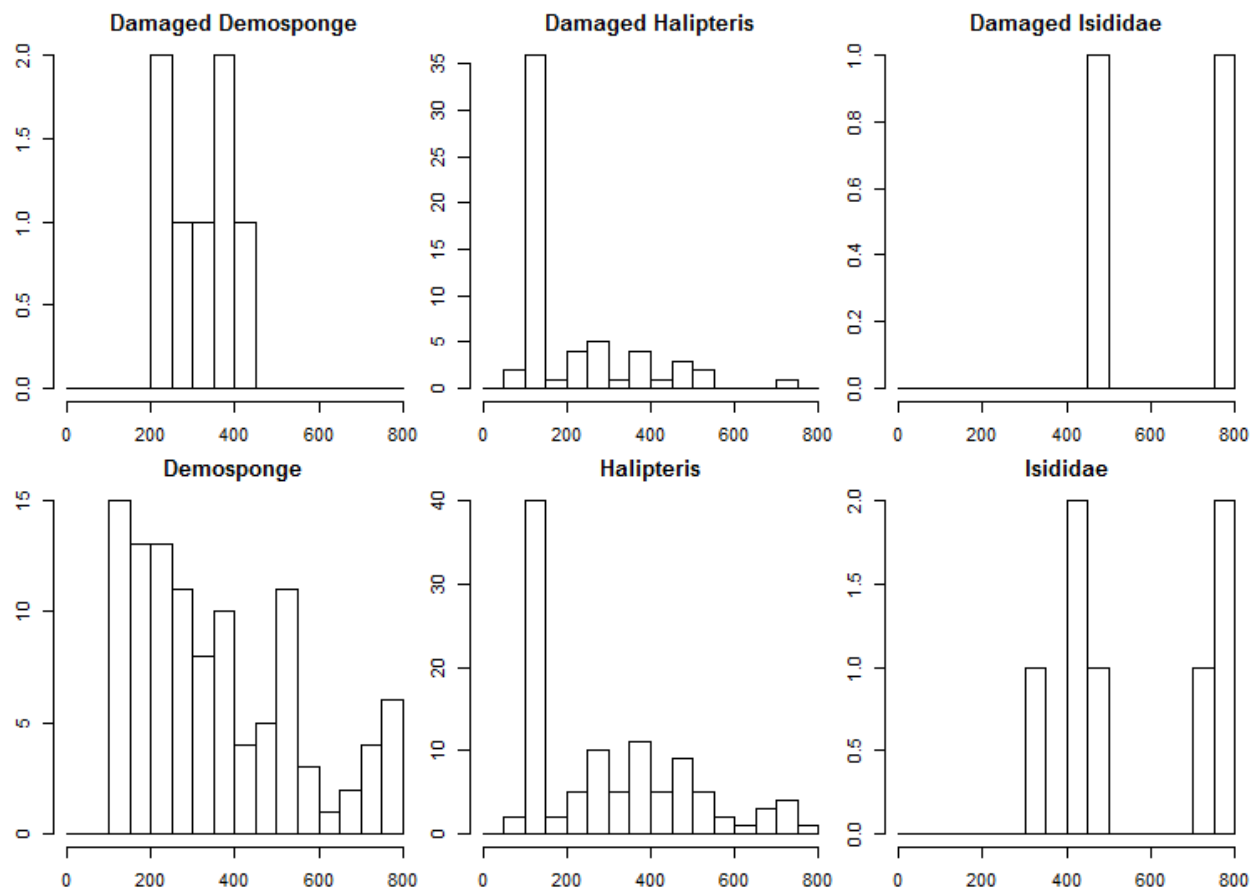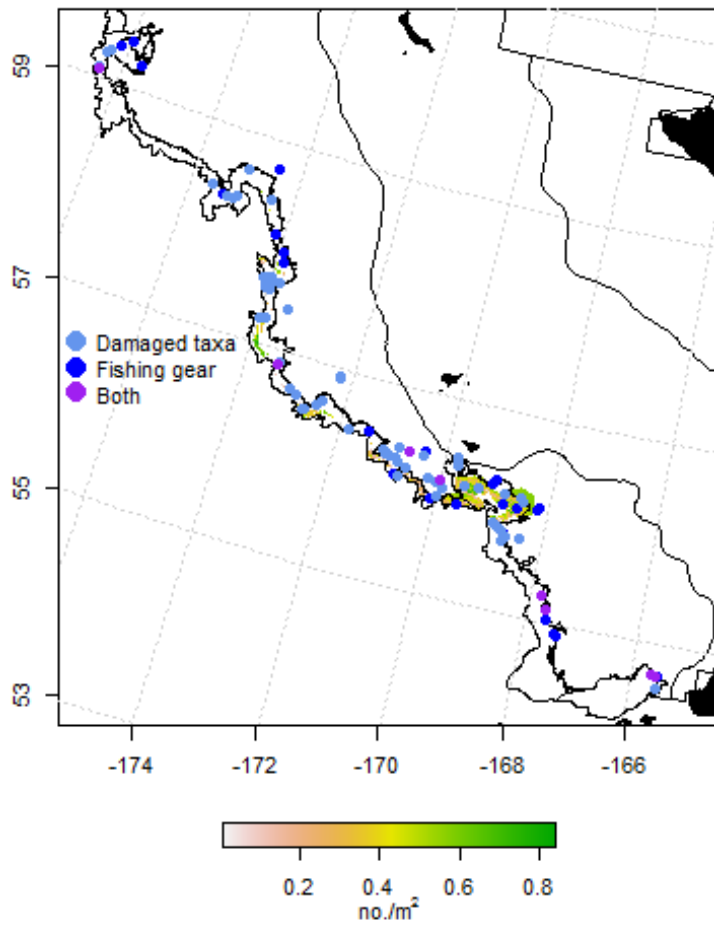
Figure 24. The depth of transects with damaged (upper) or present (lower) Demosponge,

*Halipteris* sp., or Isididae
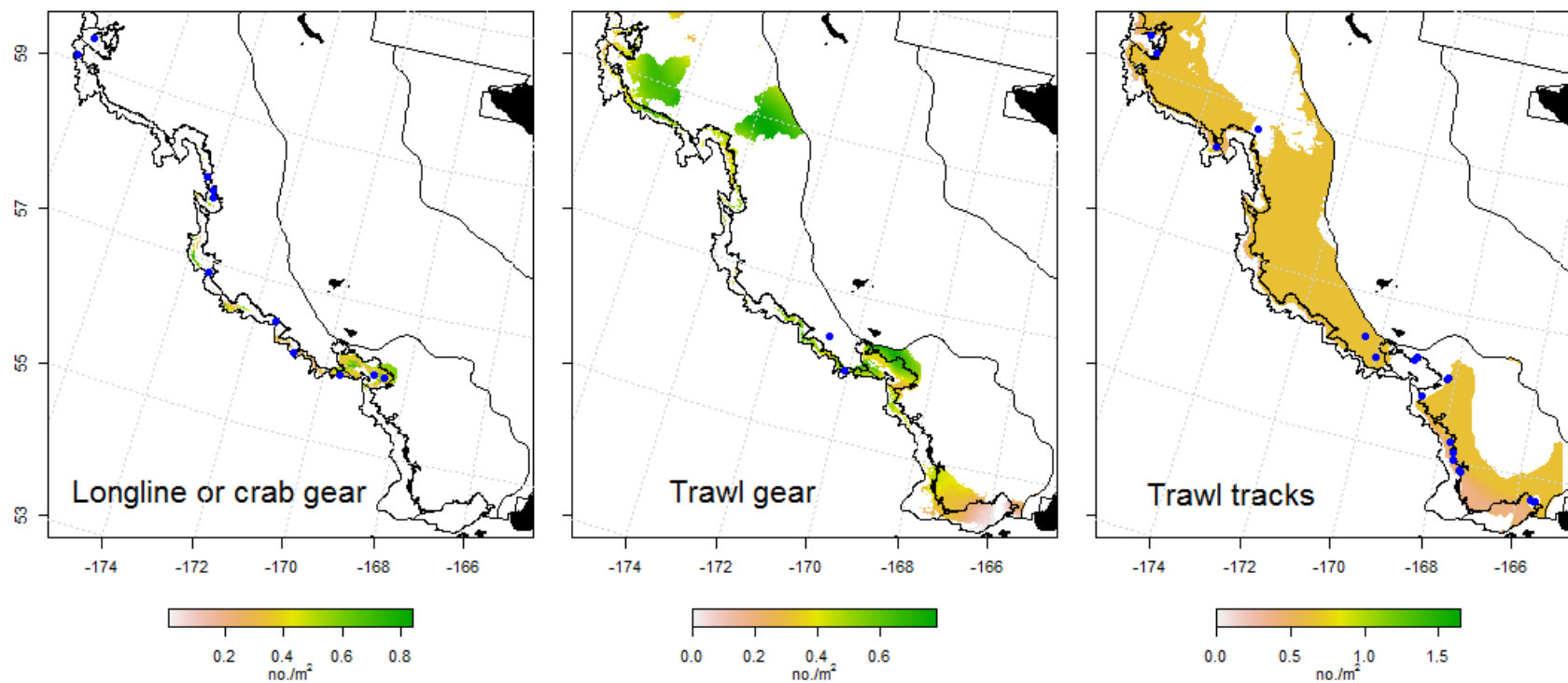
Figure 25. The location of transects with evidence of fishing (e.g., lost gear) indicated by blue dots. The dots are overlaid on predicted density for the coral, sponge and sea whip models (from left to right).

Figure 26. The location of transects with damaged coral, sponge, or sea whip or evidence of fishing (e.g., lost gear). The dots are overlaid on predicted density for the coral model.
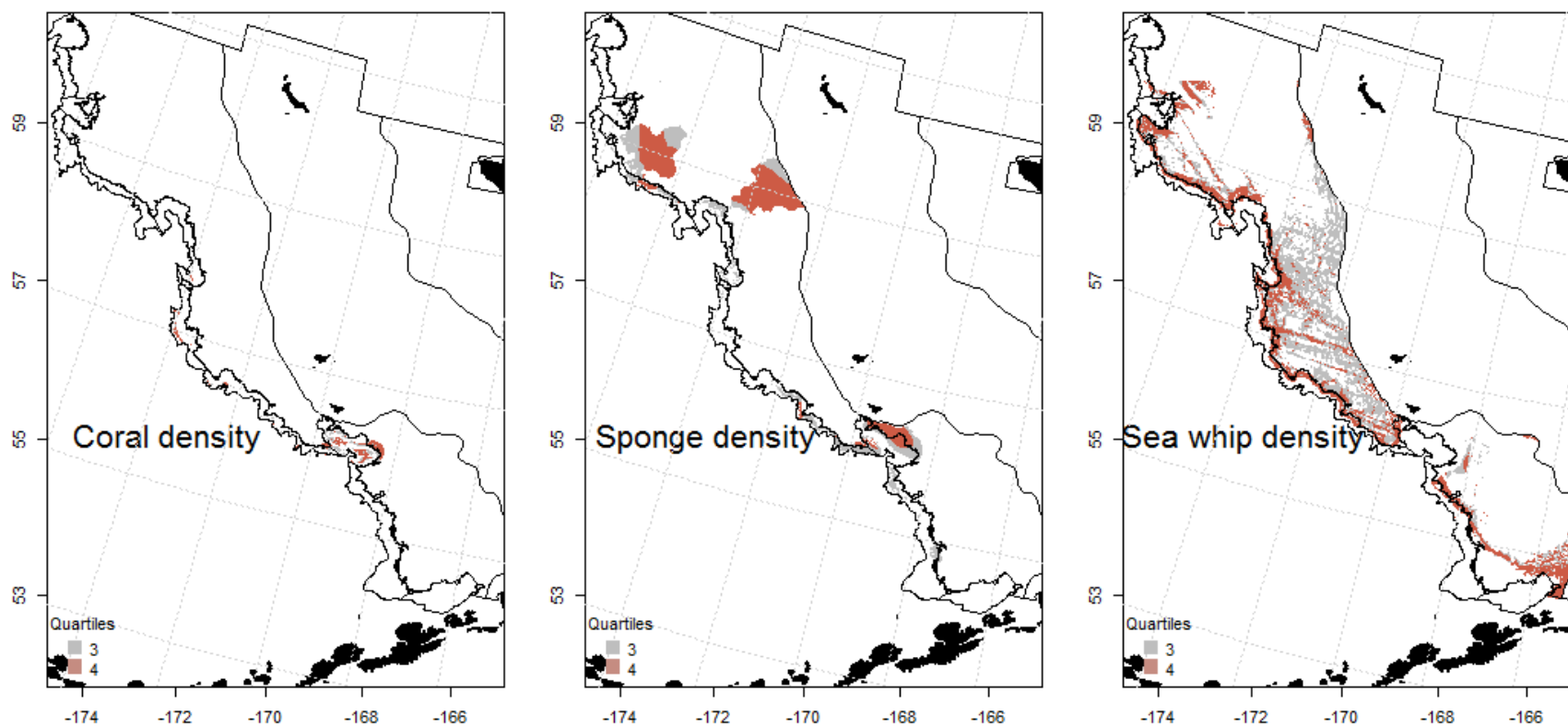
Figure 27. Plots of the upper two quantiles of predicted density for structure-forming invertebrates based on the density model for the eastern Bering Sea slope and outer shelf.
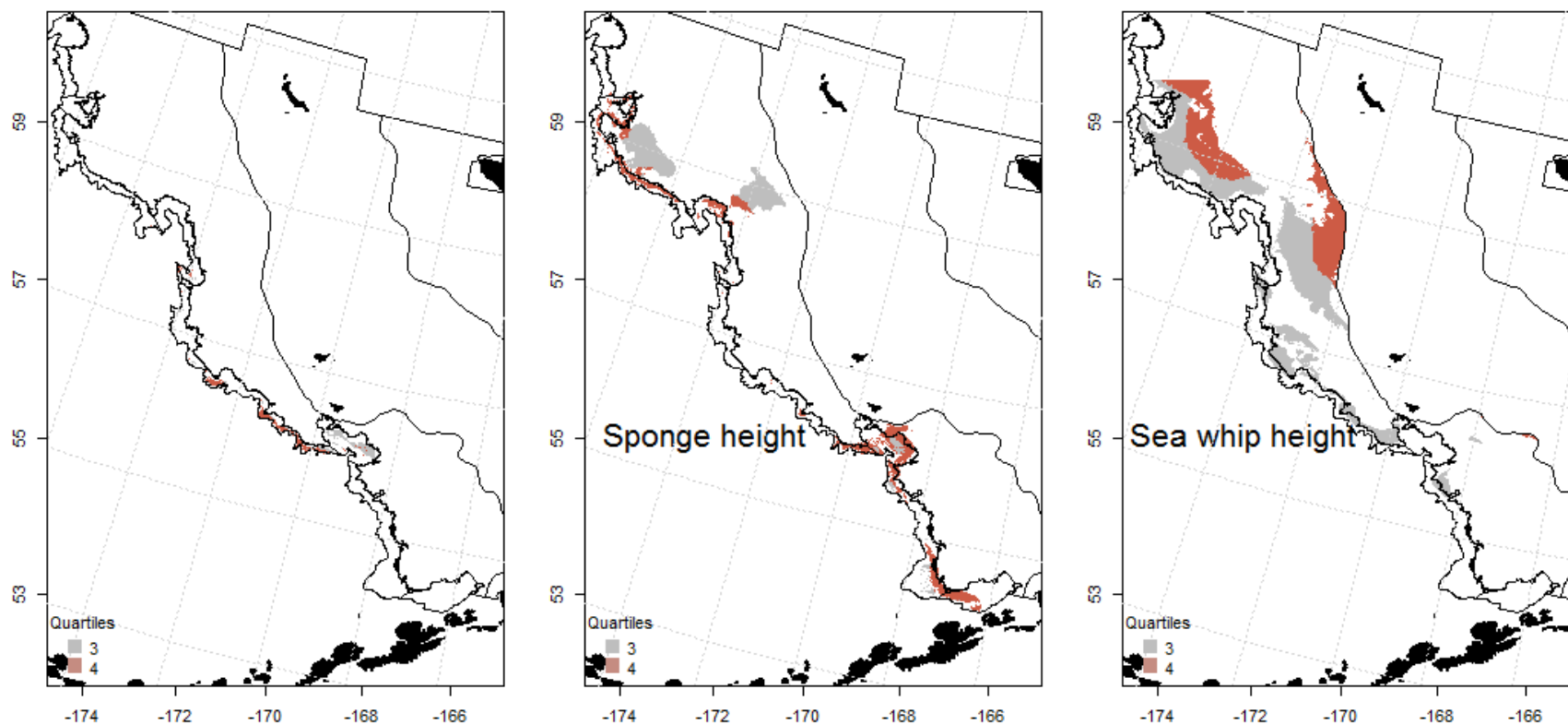
Figure 28. Plots of the upper two quartiles of predicted height for structure-forming invertebrates based on the height model for the eastern Bering Sea slope and outer shelf.
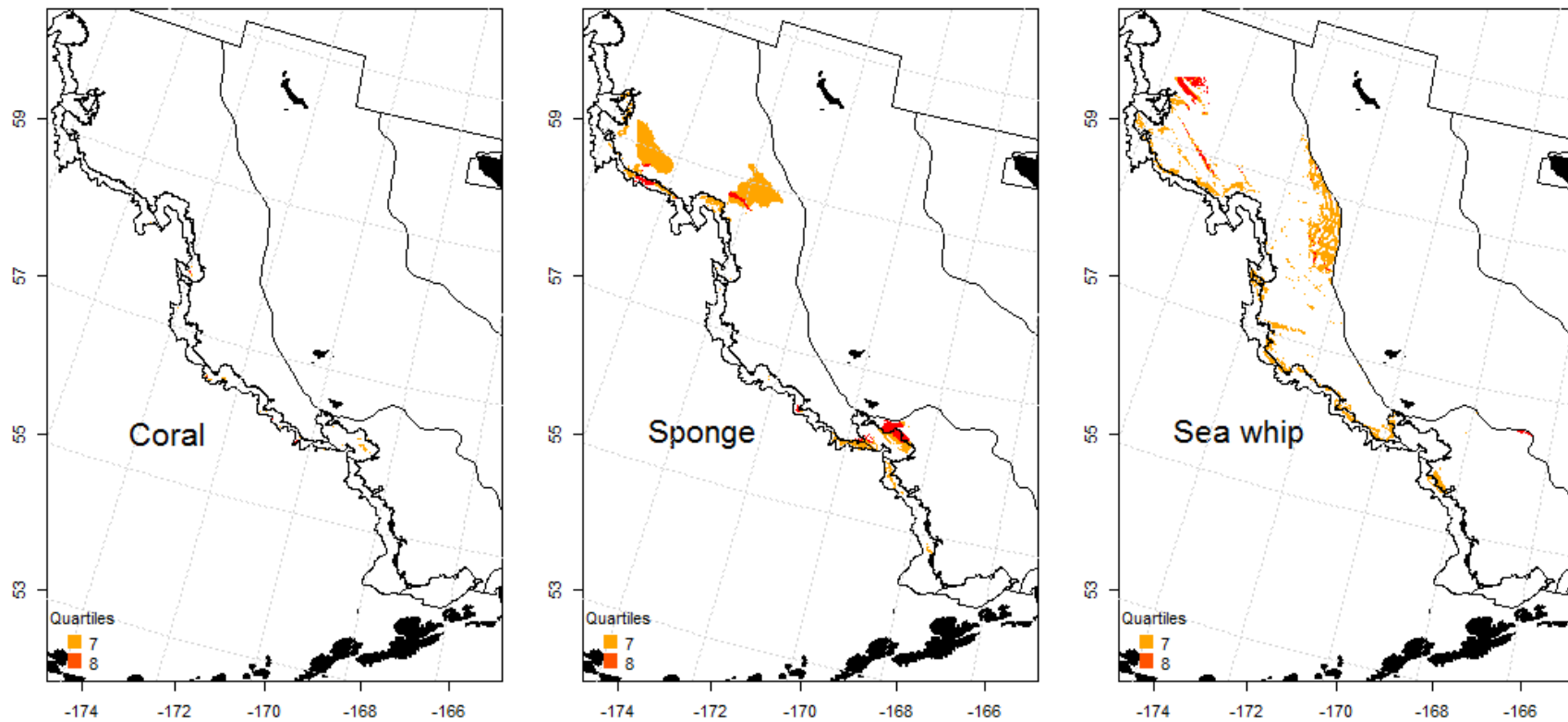
Figure 29. Plots of the upper two quartiles of predicted height for structure-forming invertebrates based on the height model for the eastern Bering Sea slope and outer shelf.
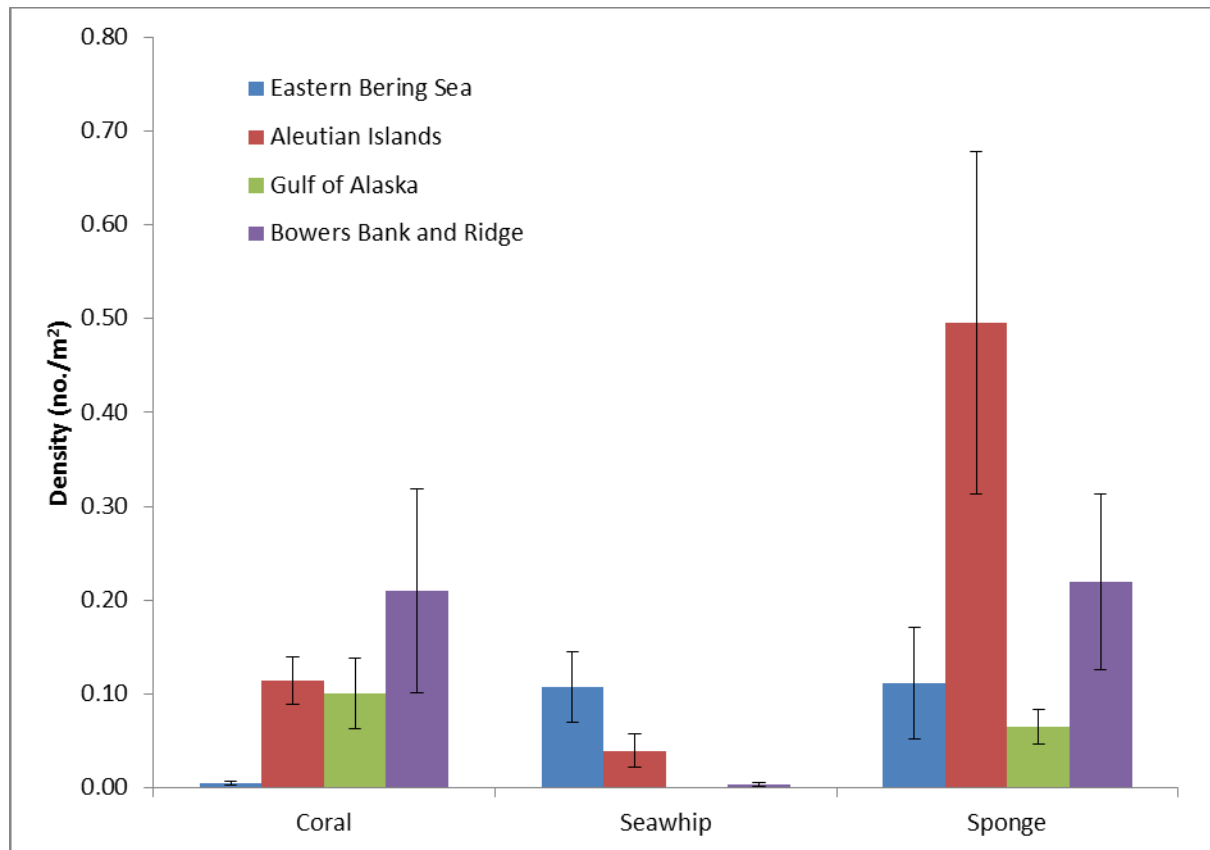
Figure 30. Densities (SE bars) of structure-forming invertebrates from four areas where the same type of study was conducted using randomly selected camera transects.